

UC Riverside

UC Riverside Electronic Theses and Dissertations

Title

Genetic and Environmental Causes of Infertility

Permalink

<https://escholarship.org/uc/item/0t6296n1>

Author

Villa, Pedro A

Publication Date

2024

Copyright Information

This work is made available under the terms of a Creative Commons Attribution License, available at <https://creativecommons.org/licenses/by/4.0/>

Peer reviewed|Thesis/dissertation

UNIVERSITY OF CALIFORNIA
RIVERSIDE

Genetic and Environmental Causes of Infertility

A Dissertation submitted in partial satisfaction
of the requirements for the degree of

Doctor of Philosophy

in

Biomedical Sciences

by

Pedro A. Villa

March 2024

Dissertation Committee:

Dr. Djurdjica Coss, Chairperson

Dr. Iryna Ethell

Dr. Ameae M. Walker

Copyright by
Pedro A. Villa
2024

The Dissertation of Pedro A. Villa is approved:

Committee Chairperson

University of California, Riverside

ACKNOWLEDGEMENTS

To my advisor, Dr. Djurdjica Coss, I am grateful for your unwavering support and guidance throughout my academic journey. You have always believed in my abilities, even when I doubted myself, and pushed me to reach my full potential. I am genuinely grateful for the invaluable knowledge and skills you have imparted, which have equipped me to face future challenges confidently. Without your mentorship and encouragement, I would not have become the scientist I am today. Thank you for everything.

To my dissertation committee members, Dr. Iryna Ethell and Dr. Vijayalakshmi Santhakumar, I am grateful for all your guidance, encouragement, and support throughout my academic journey. Your invaluable advice, insightful feedback, and challenging questions have been instrumental in shaping me into a better scientist. Thank you for being such amazing mentors.

To Dr. Ameae M. Walker, I express my deepest gratitude for welcoming me to your lab as an undergraduate and supporting me on my journey to becoming a scientist. I vividly recall the day I conducted my first experiment and ran to your office excitedly to show you my results. That day ignited my interest in research, and I am forever grateful to you for that. Thank you once again for providing me with such an incredible opportunity.

I would like to express my gratitude to my colleagues who have contributed to the success and experiments documented in this dissertation. I want to extend my heartfelt thanks to Dr. Rebecca Ruggiero-Ruff, Dr. Nancy Lainez, Sarah Berlin, Lina Morales,

Andrew Gomez, and Manolia Ghouli. I am also grateful to my friends and fellow cohort members, Dr. Kathy Pham, Rogelio Nunez-Flores, Dr. Shyleen Frost, Andrew Huang, and Andy Lei, and Dr. Parima Udompholkul for their scientific advice, discussion, and support that helped in the success of the experiments in this dissertation.

I would like to express my gratitude to my qualifying exam and guidance committee members, namely Dr. Ameae Walker, Dr. Iryna Ethell, Dr. Martin Garcia-Castro, Dr. Marcus Kaul, and Dr. Polly Campbell. I would also like to thank Dr. Meera Nair and Dr. Emma Wilson, additional mentors in my PhD training. Over the years, I have learned so much from all of you, and your support and guidance have greatly contributed to my growth and development as a scientist.

Acknowledgments of previous publications.

The text of this dissertation, in part, is a reprint of published material as it appears in:

1. Chapter Two

Altered GnRH neurons and ovarian innervation characterize reproductive dysfunction linked to the Fragile X Messenger ribonucleoprotein (Fmr1) gene mutation.

Frontiers in endocrinology vol. 14 1129534. 22 Feb. 2023

DEDICATION

I dedicate this to my mother who has supported me through so much struggle to get me and my siblings to a better place.

ABSTRACT OF THE DISSERTATION

Genetic and Environmental Causes of Infertility

by

Pedro A. Villa

Doctor of Philosophy, Graduate Program in Biomedical Sciences
University of California, Riverside, March 2024
Dr. Djurdjica Coss, Chairperson

Infertility, affecting 1 in 8 couples globally, is influenced by various factors such as delayed motherhood, poor dietary habits, genetic disorders, environmental endocrine disruptors, and obesity. Reproduction, orchestrated by gonadotropin-releasing hormone (GnRH) neurons from the hypothalamus, involves the pulsatile secretion of luteinizing hormone (LH) and follicle-stimulating hormone (FSH) from the pituitary, stimulating steroidogenesis and gametogenesis in the gonads. GnRH neuron pulsatile secretion requires regulation by afferent neurons, primarily kisspeptin, and potentially GABAergic signals that activate GnRH neurons.

Genetic factors, specifically mutations in the Fragile X messenger ribonucleoprotein 1 gene (*FMRI*), contribute to fertility issues, particularly premature ovarian failure (POF) in women under 40. Using the *Fmr1*KO mouse model, we determined elevated gonadotropin hormone levels, increased GABAergic innervation of GnRH neurons, and higher sympathetic innervation in the ovaries of *Fmr1*KO mice. Since GABA is excitatory to GnRH neurons this may contribute to an increase in LH

pulse frequency. Ovariectomy experiments revealed that the hypothalamus drives high LH, while increased FSH, is dependent on the ovaries and possibly influenced by heightened innervation.

Diet-induced obesity (DIO), affecting a third of the global population, induces hypogonadism in obese men, characterized by low testosterone and sperm count. Studying reproductive dysfunction in mice using the DIO model with a high-fat diet demonstrated lower sperm numbers and testosterone levels, aligning with observations in humans. Investigation of pituitary responsiveness to GnRH revealed comparable LH secretion in control and obese males, suggesting an unaffected pituitary response. Control mice showed an expected increase in LH after chemogenetic activation of kisspeptin neurons. Unexpectedly, activation of kisspeptin neurons caused a higher LH fold change in obese males, indicating suppressed kisspeptin neurons in DIO. Kisspeptin neurons are activated by proopiomelanocortin (POMC) neurons through α -melanocyte-secreting hormone (α -MSH) and its receptor, melanocortin 4 receptor (MC4R), and their pulse generation is synchronized by glutamate. Investigation into these components revealed a lower LH fold change response in DIO, suggesting that DIO leads to kisspeptin neuron suppression due to dysregulation in the crosstalk between the feeding and reproductive circuit. These studies uncover a mechanism contributing to reproductive dysregulation in women with *FMRI* mutations and obesity-mediated hypogonadism in males.

TABLE OF CONTENTS

ACKNOWLEDGEMENTS	iv
DEDICATION	vi
ABSTRACT	vii
LIST OF FIGURES AND TABLES	ix
CHAPTER ONE: Genetic and environmental causes of infertility	1
1.1 Infertility is becoming a global issue	2
1.2 The Hypothalamic-Pituitary-Gonadal (HPG) axis	3
1.3 The GnRH network	4
1.4 Kisspeptin neurons	6
1.5 GABA regulation of GnRH network	8
1.6 Glutamate regulation of GnRH network	9
1.7 Mutations in the GnRH network negatively affect reproductive function	11
1.8 FMR1 mutations have adverse effects on fertility	13
1.9 FMR1 mutation associated premature ovarian failure	14
1.10 FMR1 mutations affect GABAergic and glutamatergic innervation	15
1.11 Feeding circuit involved in the GnRH network	16
1.12 POMC neurons	17
1.13 AgRP/NPY neurons	18
1.14 Obesity an environmental factor altering GnRH network	19
1.15 Obesity leads to synaptic changes in the GnRH neurons	20
References	22

CHAPTER TWO:	35
2.1 Abstract	36
2.2 Rationale for elucidating the role of FMR1 gene in female reproduction	37
2.3 Materials and Methods	40
2.4 Results	48
2.5 Discussion	60
References	79
CHAPTER THREE:	91
3.1 Abstract	92
3.2 Rationale for elucidating mechanisms driving hypogonadism in obese males	93
3.3 Materials and Methods	96
3.4 Results	104
3.5 Discussion	113
References	125
CHAPTER FOUR CONCLUSION:	133
References	135

LIST OF FIGURES AND TABLES:

Fig 2.1 <i>Fmr1</i> knockout (KO) females stop reproducing early.	66
Fig 2.2 Ovarian histology demonstrates more corpora lutea in young <i>Fmr1</i> KO mice.	67
Fig 2.3 <i>Fmr1</i> KO mice have higher LH and FSH.	68
Fig 2.4 Ovariectomized <i>Fmr1</i> KO mice have higher LH.	69
Fig 2.5 <i>Fmr1</i> KO have increased corpus luteum vascularization.	70
Fig 2.6. <i>Fmr1</i> KO have higher innervation of growing follicles.	71
Fig 2.7 Nanostring analysis demonstrates significant changes in hypothalamic gene expression in <i>Fmr1</i> KO mice.	72
Fig 2.8 <i>Fmr1</i> KO females have higher levels of the obligatory GABA _A receptor subunit in hypothalami.	73
Fig 2.9 GnRH neurons of <i>Fmr1</i> KO females have more GABA _A receptors.	74
Fig 2.10 GnRH neurons of <i>Fmr1</i> KO females have more synaptic GABA _A receptors.	75
Fig 2.11 Higher LH / GnRH pulse frequency in <i>Fmr1</i> KO females before and after ovariectomy.	76
Supplemental	77
Fig 3.1 Male mice on a high fat diet experience lower LH pulse frequency	118
Fig 3.2 Kisspeptin treatment produces higher LH response in HFD mice than CTR	119

Fig 3.3 Chemogenetic activation of kisspeptin neurons also resulted in higher LH induction in HFD mice	120
Fig 3.4 LH induction by NMDA is decreased in HFD mice compared to CTR	121
Fig 3.5 Reduced glutamatergic innervation of kisspeptin neurons by HFD	122
Fig 3.6 HFD diminishes LH response to exogenous POMC activation and α MSH injection	123
Fig 3.7 Fewer active kisspeptin neurons in HFD mice compared to CTR	124

CHAPTER ONE

Genetic and Environmental Causes of Infertility

1.1 Infertility is becoming a global issue

Infertility has become a growing concern worldwide, with statistics revealing that approximately one in eight couples will experience infertility and require assisted reproductive technologies (ART) to conceive [1]. On average the cost for ART birth ranges from \$28,829 for a single birth and \$123,402 for twin births in the US [2]. In 2021, 3% of all live births required the use of ART, which constitutes 97,128 live births in the US alone [3]. A better understanding of the underlying causes of fertility disorders is needed to develop novel therapeutic treatments to improve the quality of life for couples struggling with infertility.

Infertility is a complex disease that stems from genetic and environmental contributions. Mutations in the GnRH network cause central dysregulation in reproductive function leading to hypogonadotropic hypogonadism. For example, mutations of anosmin 1 (*ANOS1*), fibroblast growth factor receptor 1 (*FGFR1*), fragile X messenger ribonucleoprotein 1 (*FMRI*) affect the GnRH network. Mutations in the *FMRI* gene affect fertility in both men and women. In men, *FMRI* mutations result in macroorchidism, and in females, mutations increase the risk for premature ovarian failure, which is the cessation of reproductive function before forty years of age.

On the other hand, environmental factors, such as poor diet, sedentary lifestyle, and endocrine disruptive chemicals also contribute to infertility. Obesity in particular is a significant contributor, caused by a long-term imbalance of calories consumed and calories expended [4]. Obesity rates show a steady rise, with current global estimates projecting an increase from the current 38% to 51% by 2035 [5]. Obesity is defined as

having a body mass index (BMI) of 30 kg/m² or higher. A multitude of adverse health outcomes are associated with obesity. Specifically, individuals affected by obesity are at an elevated risk of developing chronic conditions, including but not limited to cardiovascular disease, diabetes, osteoarthritis, certain cancers, and infertility in both men and women [6-9]. Understanding the mechanisms that drive infertility may help promote new therapies and treatments to ameliorate the global infertility issues we face today.

1.2 The Hypothalamic-Pituitary-Gonadal (HPG) axis

Reproductive function is regulated by the hypothalamic-pituitary-gonadal (HPG) axis. The hypothalamus is comprised of several neuronal populations that secrete neuropeptides and neurohormones to regulate many homeostatic systems, such as body weight, circadian rhythm, energy expenditure, thirst, food intake, metabolism, the stress response, and reproduction [10]. Hypothalamic nuclei, important in regulating reproduction, are in the medial septum near the organum vasculosum laminae terminalis (OVLT), anteroventral paraventricular nucleus (AVPV), and the arcuate nucleus (ARC), which is located above the median eminence (ME). Some of these regions, such as the OVLT and the ME, contain circumventricular organs with a leaky blood brain barrier. Neurons near these regions can sense peripheral cues from the circulation and neurons in the ME can also secrete neuropeptides into the portal circulation. The ARC contains nuclei that are involved in the regulation of feeding and satiety, and energy expenditure, as well as reproduction [11].

Gonadotropin releasing hormone (GnRH) is secreted by a neuronal population of about 1000 neurons scattered in the rostral preoptic area (POA), medial septum, and anterior hypothalamus. The GnRH neuropeptide is the final brain output regulating reproductive function [12-14]. GnRH neurons project to the ME where GnRH neuropeptide is secreted in a pulsatile manner [15, 16]. GnRH binds to its receptor in the anterior pituitary gonadotrope to stimulate the synthesis and secretion of luteinizing hormone (LH) and follicle stimulating hormone (FSH). Both LH and FSH stimulate the gonads to regulate steroidogenesis and gametogenesis. More specifically, LH acts on the Leydig cells in the testis and the theca cells in the ovary to stimulate testosterone and progesterone production. FSH acts on the Sertoli cells in the testis and the granulosa cells in the ovary to stimulate spermatogenesis and folliculogenesis, respectively. In females, the granulosa cells further convert testosterone produced by the theca cells into estrogen under the influence of FSH [16]. In addition to driving the development of physical sexual characteristics, testosterone and estrogen feedback to the hypothalamus to complete the endocrine loop.

1.3 The GnRH network

Central regulation of reproduction occurs in the hypothalamus through a very intricate network that regulates GnRH neuropeptide pulsatile activity [17]. It has been established in the field that every pulse in LH directly coincides with a pulse of GnRH secreted by GnRH neurons [15, 18]. GnRH neurons can have a unipolar or bipolar

morphology where they send long projections from the OVLT to the ME where they secrete GnRH. GnRH neurons are distinct, and they do not contain a classical axonal structure. Instead, GnRH neurons contain dendritic structures that conduct action potentials over many millimeters, branching and taking on an axonal structure when they enter the ME [19-21]. GnRH neuron distal projections contain the presence of functional GABA, glutamate, and kisspeptin receptors [20, 22]. The distinct morphology has been observed in mice and rats and may be a common feature in mammals [19, 20].

Since GnRH neurons are scattered in the hypothalamus, pulsatile secretion depends on afferent regulation. One of the main regulators of GnRH secretion is a small population of neurons that secrete kisspeptin located in the ARC. Kisspeptin is a 145 amino acid prepropeptide that is processed into four biologically active peptides that all contain an active c-terminal domain: kisspeptin 54, 14, 13, 10, all of which can bind and activate the kisspeptin receptor (Kiss1R) [23, 24]. Since kisspeptin 10 (Kp-10) is a small decapeptide, it is utilized for its ability to cross the blood brain barrier and stimulate LH release in rodents and humans [23]. GnRH neurons express the Kiss1R, and binding of kisspeptin to its receptor leads to the depolarization of GnRH neurons and the secretion of GnRH [25]. Kisspeptin neuropeptide secretion by the kisspeptin neurons robustly stimulates GnRH release. More specifically, kisspeptin stimulation of GnRH neurons occurs through the Kiss1R G-protein coupled receptor, by G alpha q, which leads to the influx of Ca^{2+} and promotes GnRH secretion [26]. Kisspeptin is important for the onset of puberty and the maintenance of reproductive function, and the loss of Kiss1R leads to hypogonadism in humans and rodents [27]. Both intracerebroventricular (icv) and

intraperitoneal (i.p) injections with Kp-10 induce strong LH secretion and promote precocious puberty in rats, suggesting kisspeptin is a key regulator of reproduction and puberty [28, 29]. Optogenetic activation of kisspeptin neurons in the ARC led to kisspeptin secretion, and patch clamp determined direct GnRH neuron activation [30].

1.4 Kisspeptin neurons

Kisspeptin neurons are located in two hypothalamic nuclei, the AVPV and the ARC. In rodents, females possess a larger population of kisspeptin neurons in the AVPV of the hypothalamus, which is necessary for the LH surge required to induce ovulation [31]. Estradiol plays an important role in stimulating kisspeptin neurons of the AVPV and is the site for positive feedback necessary for ovulation. High estrogen stimulates an increase in *Kiss1* mRNA in kisspeptin neurons of the AVPV [32]. While males have 1/5 of the number of kisspeptin neurons in the AVPV, similarly high testosterone increases *Kiss1* mRNA in this population [33]. Kisspeptin neurons in the AVPV project to GnRH neuron cell bodies, while the kisspeptin population in the ARC projects to GnRH terminals to regulate GnRH secretion.

The population of kisspeptin neurons in the ARC that regulate pulsatile secretion, does not differ between sexes. Kisspeptin neurons in the ARC respond to estrogen negative feedback in females and testosterone negative feedback in males, resulting in lower *Kiss1* mRNA [33, 34]. The kisspeptin neurons located in the ARC are known as KNDY neurons since they co-express kisspeptin, neurokinin B, and dynorphin [35]. Neurokinin B belongs to the tachykinin peptide family and is a potentiator of kisspeptin

neuron firing after binding to the tachykinin receptor 3 (TACR3) on KNDY neurons. Icv injections of neurokinin B agonist promotes LH secretion in humans, primates, mice, and sheep [36-39]. Mutations of the tachykinin 3 gene (*TAC3*) or its receptor result in dysfunctional GnRH release and reproductive dysfunction in humans and in mice [40-42]. On the other hand, dynorphin A, an endogenous opioid peptide that activates the κ -opioid receptor (KOR), suppresses kisspeptin neuron firing. Central treatment with a KOR antagonist norbinaltorphimine prevented the inhibitory effects of dynorphin A on LH secretion in rodents [43], [39], [44]. Recent studies revealed that kisspeptin pulse initiation and neuron synchronization occur through glutamate. Using genetically encoded calcium indicators (GCaMP) and gradient index (GRIN) lenses to observe in vivo kisspeptin burst firing, determined that kisspeptin pulse initiation and synchronization was mediated through glutamate as the gatekeeper for synchronized pulse initiation, which is potentiated by neurokinin B and pulse termination gated by dynorphin A [45]. Kisspeptin neurons express a variety of glutamatergic neurotransmitter receptors, and treatment with a cocktail of AMPA receptor and NMDA receptor antagonists in GCaMP fluorescence recordings resulted in an abrupt reduction in calcium events and termination of synchronized activation in both males and females [45, 46]. Together, the interconnected KNDY neurons regulate synchronous burst firing to promote the pulsatile firing pattern of kisspeptin neurons that regulate GnRH neuropeptide pulse secretion in mammals.

1.5 GABA regulation of GnRH network

Classical neurotransmission also plays a role in modulating the GnRH network. Gamma aminobutyric (GABA), which is the main inhibitory neurotransmitter in the central nervous system, is excitatory to GnRH neurons through the GABA_A receptor and inhibitory through the GABA_B receptor [47-51]. GABA_A receptors are ionotropic channels, while GABA_B receptors are heterodimers composed of R1 and R2 subunits forming transmembrane metabotropic G protein coupled receptors. Activation of GABA_B activates inwardly rectifying potassium channels, inactivating voltage-gated Ca²⁺ channels, and inhibition of adenylate cyclase, leading to hyperpolarization [52, 53]. The GABA_A receptor is a pentameric chloride ion channel comprised of a combination of two of six alpha subtypes α 1-6, two of three beta types, β 1-3, one of three gamma types, γ 1-3, and a δ subunit. It is necessary to have two alpha and two beta subunits to form a functioning chloride ion channel [54, 55]. Activation of the GABA_A receptor allows for the influx of chloride ions into the cell and causes hyperpolarization of the cell membrane [56, 57].

The GABA_A receptor, known throughout the brain as inhibitory, is excitatory to GnRH neurons due to their high internal chloride levels [58]. GnRH neurons express both GABA_A and GABA_B receptors. 90% of GnRH neurons respond to GABA activation at the level of the soma [48, 50, 59, 60] and greater than 80% of GnRH neurons respond to GABA at the terminals, when using a GABA_A agonist, muscimol. A majority express GABA_A receptors containing the γ 2 subunit, detected in 56% of all GnRH neurons in mice [61]. Mice in which the γ 2 subunit is conditionally knocked out in GnRH neurons

experience a diminished response to exogenous GABA activation, reduced by 90%, indicating that the $\gamma 2$ subunit is critical for normal GnRH neuron function [62]. Knocking out GABA_A receptors containing the $\gamma 2$ subunit had minor effects on fertility, however, the percent knockdown was not determined in this study. GABA_B is inhibitory to GnRH neurons and treatment with baclofen, a GABA_B agonist, inhibited 70% of GnRH neurons [47]. Furthermore, optogenetic activation of GABAergic populations in the ARC stimulates long lasting LH secretion; however, long term activation induced higher levels of testosterone in females and disrupted estrous cyclicity, suggesting that a balance in GABA regulation of the GnRH network is necessary for normal fertility [63].

1.6 Glutamate regulation of GnRH network

Glutamatergic neurotransmission also regulates the GnRH network. GnRH neurons have been shown to express excitatory ionotropic glutamate receptors, including N-methyl-D-Aspartate (NMDA) 2A, 2B, alpha-amino-3-hydroxy-5-methyl-4-isoxazolepropionic acid (AMPA) GluR1-4, and mainly receive input through the vesicular glutamate transporter 2 (VGLUT2) which is more prevalent in the hypothalamus [64-67]. While 90% of GnRH neurons respond to GABA_A receptor activation, only 30-50% of GnRH neurons respond to glutamate [68, 69]. Studies show that glutamate stimulation induces LH secretion, although GnRH neurons are not directly activated since glutamate injection does not show cFOS induction in GnRH neurons. Emerging evidence reveals that glutamatergic regulation of LH secretion occurs at the

level of kisspeptin neurons, a majority of which respond to glutamate. Specifically, glutamate plays a role in initiating a kisspeptin pulse. In addition, daily NMDA injections promoted precocious puberty in immature rats when stimulated with an agonist, and inhibition of NMDA receptors with an antagonist delays puberty [70]. I.p and icv injections of NMDA induce strong LH secretion in rats, mice, and rhesus monkeys [71-73]. Since only ~30% of GnRH neurons respond to NMDA, NMDA regulation of reproduction may occur through kisspeptin neurons, which express NMDA and AMPA receptors [74]. Peripheral i.p. injections of NMDA increased cFOS expression in a majority of ARC kisspeptin neurons but not GnRH neurons and stimulated a robust 10-fold change in LH secretion [72]. Electrophysiology reveals that 60% or higher GnRH neurons responded to AMPA stimulation [51, 75]. Central injection with 1 nmol of AMPA stimulated a 10-fold difference in LH secretion, however, whether central stimulation with AMPA is mediated through GnRH neuron activation or kisspeptin activation is not clear [76]. Recent studies show that AMPA is important in synchronizing the initiation of a pulse. In vivo studies in mice treated with an AMPA receptor antagonist suppressed kisspeptin neurons' ability to initiate a pulse in both males and females, suggesting a significant role of glutamate in the regulation of pulsatile activity in the GnRH neuronal network at the level of the kisspeptin neuron [45], [46].

1.7 Mutations in the GnRH network negatively affect reproductive function

Genetic mutations can have a profound impact on reproductive function. Various mutations can disrupt the normal function of genes involved in the HPG axis, leading to infertility or reproductive disorders. Among the genetic mutations affecting reproduction, those specifically targeting GnRH neurons can have severe consequences. GnRH neurons are crucial for the initiation and regulation of reproductive function. Mutations in genes related to GnRH production, secretion, or neuron migration can disrupt the normal development of these neurons. Mutations in GnRH neuron development led to a condition known as idiopathic hypogonadotropic hypogonadism (IHH), characterized by the absence or delayed onset of puberty and infertility. Reproduction relies on the intricate coordination of the hypothalamic-pituitary-gonadal axis. Genetic mutations can interfere with this complex system, adversely affecting reproductive function.

Understanding these genetic mutations and their effects on reproductive biology is crucial for diagnosing and treating individuals with fertility issues. Individuals with GnRH mutations may have underdeveloped or absent gonads and impaired production of sex hormones, making it difficult or impossible to conceive without medical intervention.

During prenatal development, at 32 days and stages E10 and E11 in humans and mice, respectively, GnRH neurons arise from the medial olfactory placode where they migrate to the preoptic area of the hypothalamus, establishing themselves by 20 weeks in humans and E15.5 in mice [77-79]. Any aberration in GnRH neuron development can have devastating effects on reproduction in addition to hyposmia, anosmia. These neurons undergo a complex migration process from their birthplace in the nasal

epithelium to the preoptic area in the hypothalamus, where they are ultimately established. This migration is crucial for the proper development and function of the reproductive system. Disruptions or abnormalities in GnRH neuron migration or development can significantly affect fertility. Mutations in genes such as anosmin 1 (*ANOS1*) and fibroblast growth factor receptor 1 (*FGFR1*) affect reproductive function by causing developmental dysregulation. *ANOS1* encodes for an extracellular membrane glycoprotein important in cell adhesion and migration of GnRH neurons during development [80]. *ANOS1* affects GnRH neuron development by affecting migration and establishment into the hypothalamus. *ANOS1* is also known as Kallman syndrome one sequence (KAL1) associated with Kallman syndrome, which involves symptoms of anosmia or lack of the ability to smell as well as hypogonadotropic hypogonadism and infertility. *ANOS1* mutations are a loss of function mutation, with a prevalence of Kallman syndrome 1:8000 in men and 1:40,000 in women [81], [82]. *FGFR1*, known as Kallman syndrome two sequence (KAL2), serves important functions, including migration proliferation and neuron differentiation [83]. Similar to mutations in *ANOS1*, *FGFR1* mutations also affect GnRH neuron migration during development, which leads to failure of the GnRH network establishment during development [80, 84]. Mutations in *FGFR1* are autosomal dominant and similar to what occurs in humans where GnRH neuron migration is disrupted; in mice, partial loss of the *Fgfr1* gene results in a 90% reduction in GnRH neurons [85]. Fibroblast growth factor 8 (FGF8), which acts through the FGFR1 receptor, is important in GnRH neuron differentiation and *GNRH1* gene expression. Treatment of the human pluripotent stem cell model of GnRH neurons with

FGF8 resulted in a strong dose dependent GNRH1 expression. In addition, FGF8 deficient mice did not develop GnRH neurons [85, 86]. Patients with *ANOS1* and *FGFR1* mutations have low serum gonadal hormone levels due to impaired GnRH neuron migration during development [87].

Mutations in *FMRI* gene leads to reproductive disorders in men and women. Macroorchidism in *FMRI* mutations in males stems from an increased Sertoli cell proliferation during testicular development [88]. Women experience premature reproductive senescence due to *FMRI* mutations. Although mutations of the *FMRI* gene cause neurodevelopmental disorders [89-93], it is not known if GnRH neuron development is impaired with *FMRI* mutations. It is possible that macroorchidism or enlarged testes stem from dysregulation of HPG development [94]. In females, however, emerging research is pointing to endocrine dysregulation rather than developmental dysfunction [95-97]. Future studies in our lab will address if *FMRI* is involved in GnRH neuron migration.

1.8 FMR1 mutations have adverse effects on fertility

The *FMRI* gene is located on the X-chromosome, and mutations of this gene more severely affect males. *FMRI* mutations exhibit X-linked dominant inheritance. Full mutation entails an expansion of CGG trinucleotide repeats in the 5' untranslated region of the *FMRI* gene to more than 200 repeats, which inhibits the expression of the Fragile X messenger ribonucleoprotein (FMRP) and causes FXS. *FMRI* mutations, with the

expansion of this region between 50-200 units, result in lower levels of FMRP and are known as permutations. Full mutation of the *FMR1* gene causes Fragile X syndrome (FXS), the most common cause of inherited autism or mental disability. *FMR1* permutations cause Fragile X-associated tremor/ataxia syndrome (FXTAS), which comprise neurological problems with movement and cognition disorders [98].

Females who are carriers for *FMR1* mutations have an increased infertility risk [95, 99, 100]. Significant effort has been made in understanding the effects of *FMR1* gene mutations on cortical brain function, which lead to neuronal impairments in FXS. Since the effects of mutation on the hypothalamus were completely unknown, our lab was the first to investigate the consequences on hypothalamic function [97, 101]. It is important to address this gap in our knowledge since mutations of this gene are also associated with reproductive disorders, such as enlarged testis in males and early cessation in reproductive function in females [102, 103]. Since reproduction is regulated by GnRH neurons in the hypothalamus, understanding the effects of *FMR1* mutations on GnRH neuron function can uncover new mechanisms by which *FMR1* mutations lead to reproductive dysfunction.

1.9 FMR1 mutation-associated premature ovarian failure

Premature ovarian failure (POF) is the early depletion of ovarian reserve before the age of 40 [104]. Fragile X carriers make up the bulk of individuals with known genetic causes of POF [95]. As a result of POF and early menopause, female carriers are at higher risk for osteoporosis and cardiovascular disease [105]. Most women don't know

they are carriers of *FMRI* mutations until they experience amenorrhea or infertility [106]. The risk for premature ovarian failure increases 30-fold in *FMRI* mutation carriers from the 1% risk in the general population [107-109]. The mechanisms that cause premature ovarian failure due to *FMRI* mutations are unknown. My data point to dysregulation of the GnRH network and neuronal dysregulation at the level of the ovary as potential mechanisms. These new discoveries shed light on the increased risk of premature ovarian failure, emphasizing the need for further research to elucidate the underlying mechanisms and explore potential therapeutic targets.

1.10 Fmr1 mutations affect GABAergic and glutamatergic innervation

Under normal conditions, FMRP functions as an mRNA binding protein, which is important in regulating protein translation. However, *FMRI* mutations lead to reduced FMRP levels [99, 110-112]. Lack of FMRP alters neurotransmitter receptor levels in the brain, due to the role of FMRP in the regulation of synaptic proteins [113-116]. A study by D'Hulst et al. determined a decrease in GABA_A receptor subunit mRNA, including $\gamma 1$ and $\gamma 2$, in the cortex of *Fmr1*KO mice [117]. At the protein level, the GABA_A receptor β subunit is reduced in the cortex, hippocampus, diencephalons, and brainstem of *Fmr1*KO mice, implicating a decrease in inhibitory signaling in the neuropathology of the disease [118]. Positron emission tomography quantification of GABA_A receptors observed a significant 17% decrease in the brain of FXS patients using a radioligand to the GABA_A receptor [119]. Glutamatergic receptor levels are also affected by *FMRI* mutations.

*Fmr1*KO mice have upregulated the NMDA receptor subunits NR2A and NR2B in the hippocampus, promoting an excitatory imbalance [120]. Glutamatergic AMPA receptor protein expression of the GluA1 and GluA2 subunits are also upregulated due to *Fmr1* mutations in mice, in addition to increased dendritic spine density in the hippocampus [121]. In the cortex there are changes in dendritic spine density due to an increase in NMDA and AMPA receptor synapses in *Fmr1*KO mice [122]. Neurotransmitter receptor changes have been studied in the areas of the brain important for cognition, and the role of *FMR1* mutations in areas of the brain important in reproductive function were not studied.

1.11 Feeding circuit involved in the GnRH network

Reproduction is an energy demanding process, and the GnRH network is modulated by the feeding circuitry. Neurons that regulate feeding and satiety are located in the hypothalamus, specifically in the ARC. The ARC contains a leaky blood-brain barrier that allows for the sensing of peripheral cues like leptin and insulin. Primary neurons that receive these cues are agouti-related protein/neuropeptide Y (AgRP/NPY) and pro-opiomelanocortin (POMC) neurons. Leptin is secreted from adipose tissue to signal the amount of stored energy to the central nervous system [123], and insulin is secreted in response to high glucose levels in the circulation due to food intake [124]. A fed state activates POMC neurons and inhibits AgRP/NPY neurons to promote satiety and energy expenditure. In contrast, starvation inhibits POMC neurons and activates AgRP/NPY neurons to promote feeding [125]. The reproductive axis is sensitive to

nutritional levels and both extremes of body weight negatively affect reproductive function. In mammals, a state of starvation, where energy is low, negatively affects reproduction. In children, it has been shown that 18% of body fat is necessary in order to initiate puberty [126]. In addition, female athletes experience amenorrhea due to low adipose tissue. At the other extreme, obese men experience low testosterone levels [127, 128]. In mice this balance between metabolism and reproduction is also observed; both female and male leptin knockout mice are infertile, and treatment with leptin rescues fertility, suggesting a critical connection between metabolism and reproduction [129, 130]. However, the involvement of POMC and AgRP/NPY neurons in regulating reproduction is still not well understood.

1.12 POMC neurons

POMC is a prohormone that is further processed into γ -MSH, α -MSH, β -MSH, and β -Endorphin to regulate food intake and energy expenditure. The role of these neuropeptides in regulating reproduction is not well understood [131]. α -MSH injection, which acts through the binding and activation of the MC4R receptor, leads to LH secretion [132, 133]. Icv injections with melanotan II (MT-II), an MC4R receptor agonist, induced LH secretion in rats [134]. GnRH neurons express the MC4R receptor and electrophysiology has demonstrated activation of GnRH neurons by α -MSH [135]. MT-II icv injections induced LH secretion in rats. Furthermore, chemogenetic suppression of kisspeptin neurons in conjunction with icv MT-II injection did not induce LH secretion, suggesting that MC4R regulation of LH is mediated through kisspeptin

neurons [134, 136]. Optogenetic activation of POMC neurons unveiled the direct activation of kisspeptin neurons determined by patch clamping onto kisspeptin neurons [137]. Direct POMC neuron fibers are colocalized with kisspeptin neuron perikarya, and kisspeptin immunoreactive axons are colocalized with POMC neurons, suggesting direct crosstalk between the feeding and reproductive circuits [134, 138]. Optogenetic activation of kisspeptin neurons determined that kisspeptin neurons can excite POMC neurons and inhibit AgRP/NPY neurons through glutamate [138]. In addition, knockout of the MC4R receptor in kisspeptin neurons alters LH pulsatility and estrous cyclicity in mice [139]. However, the role of POMC neuronal regulation through α -MSH in the crosstalk between the feeding and the reproductive circuit is not well understood.

1.13 AgRP/NPY neurons

Hunger activates AgRP/NPY neurons and suppresses reproductive function to ensure survival during situations of scarce resources [125]. This physiological adaptation prioritizes food seeking and suppresses energy demanding processes like reproduction until the organism has enough energy resources for survival. AgRP/NPY neurons secrete agouti-related protein (AgRP), a competitive antagonist to the MC4R receptor, suppressing satiety and promoting feeding [140]. AgRP neurons are mainly GABAergic and inhibit POMC neuron activity during hunger [141, 142]. Central injections of AgRP suppressed reproductive function by decreasing LH pulse frequency in rhesus monkeys [143]. Chemogenetic activation of AgRP/NPY neurons resulted in decreased fertility and

delayed estrous cyclicity in female mice [144]. In addition, there is evidence of direct inhibitory synaptic connections from AgRP/NPY neurons to kisspeptin neurons of the ARC and AVPV [144]. AgRP/NPY neuron activation by chemogenetics and optogenetics resulted in diminished LH pulse frequency [18]. The activation of AgRP/NPY neurons, triggered by a state of starvation, orchestrates a comprehensive physiological response by suppressing reproductive function and prioritizing energy acquisition, thereby ensuring the organism's survival.

1.14 Obesity an environmental factor altering GnRH network

Obesity, a state where there are high amounts of fat storage, also affects reproduction. Obesity promotes precocious puberty and reproductive dysfunction in adult men and women [7, 145].

Obesity leads to synaptic changes and affects neuron function [146], [147]. A dramatic reduction in POMC neuron function and activity was observed through a decrease in firing activity and impaired Ca^{2+} handling with obesity [146]. Obesity also promotes an increase in inhibitory synapses to POMC neurons, impeding POMC neuron activity, suggesting a dysregulation of the satiety signals necessary for metabolic and energy balance [148]. Another study investigated synaptic changes in the feeding circuit due to high fat diet and determined that both POMC and AgRP/NPY neurons are affected. Synaptic reorganization was observed where there was a loss of inhibitory contacts on the POMC neuron soma and a loss of excitatory contacts on AgRP/NPY

neurons [149]. The increase in excitatory synaptic contacts in POMC neurons were only promoted through a high fat diet, whereas a standard diet favored a more inhibitory tone. These synaptic changes were observed in POMC and AgRP/NPY neurons of the ARC, an area where kisspeptin neurons that regulate GnRH pulsatility reside; however, whether these changes negatively affect the crosstalk between the reproductive circuit and the feeding circuit is unknown.

1.15 Obesity leads to synaptic changes in the GnRH neurons

Consistent with synaptic changes in POMC and AgRP, we have shown that GnRH neurons also show synaptic changes. Chronic obesity leads to changes in synaptic plasticity in the hypothalamus that negatively affect reproductive function [7, 150-153]. Our group has determined that GnRH neurons themselves are affected by obesity [150]. Specifically, GnRH neurons in obese male mice exhibited a decrease in spine density proximal to the soma compared to control males, suggesting altered synaptic function and a potential decrease in the excitatory regulation of GnRH neurons. The decrease in GnRH neuron spine density may be contributing to the decrease in GnRH pulsatile activity. Synaptic molecule expression in the hypothalamus was also significantly decreased in the hypothalamus of obese males. Thus, low levels of post synaptic density 95 (PSD95), a scaffolding molecule important in clustering and arranging excitatory neurotransmitter receptors at the post synapse were observed in male mice, suggest a decrease in glutamatergic regulation in the hypothalamus [150]. However, another study determined

more cFOS positive GnRH neurons in obese males; this is attributed to chronic inflammation promoting cFOS activity that in turn decreases GnRH mRNA, suggesting central dysregulation due to obesity; however, whether these mechanisms affect GnRH neuron pulsatile activity is unknown [154]. The work to date demonstrates that obesity negatively affects the central regulation of reproduction by promoting synaptic remodeling and neuronal dysregulation.

References for Chapter One

1. Njagi, P., et al., *Financial costs of assisted reproductive technology for patients in low- and middle-income countries: a systematic review*. Hum Reprod Open, 2023. **2023**(2): p. hoad007.
2. Crawford, S., et al., *Costs of achieving live birth from assisted reproductive technology: a comparison of sequential single and double embryo transfer approaches*. Fertil Steril, 2016. **105**(2): p. 444-50.
3. Jain, M. and M. Singh, *Assisted Reproductive Technology (ART) Techniques*, in *StatPearls*. 2023, StatPearls Publishing

Copyright © 2023, StatPearls Publishing LLC.: Treasure Island (FL).
4. Beltrán-Carrillo, V.J., et al., *Elements behind sedentary lifestyles and unhealthy eating habits in individuals with severe obesity*. Int J Qual Stud Health Well-being, 2022. **17**(1): p. 2056967.
5. Koliaki, C., M. Dalamaga, and S. Liatis, *Update on the Obesity Epidemic: After the Sudden Rise, Is the Upward Trajectory Beginning to Flatten?* Curr Obes Rep, 2023. **12**(4): p. 514-527.
6. Organization, W.H. *Obesity and overweight*. 2021 [cited 2023 October 31]; Available from: <https://www.who.int/news-room/fact-sheets/detail/obesity-and-overweight>.
7. Lainez, N.M. and D. Coss, *Obesity, Neuroinflammation, and Reproductive Function*. Endocrinology, 2019. **160**(11): p. 2719-2736.
8. Chavarro, J.E., et al., *Body mass index and short-term weight change in relation to treatment outcomes in women undergoing assisted reproduction*. Fertil Steril, 2012. **98**(1): p. 109-16.
9. Sermondade, N., et al., *BMI in relation to sperm count: an updated systematic review and collaborative meta-analysis*. Hum Reprod Update, 2013. **19**(3): p. 221-31.
10. Shahid Z, A.E., Singh G. *Physiology, Hypothalamus*. 2023 [cited 2023 Jan]; Available from: <https://www.ncbi.nlm.nih.gov/books/NBK535380/>.
11. Naganawa, S., et al., *Appearance of the Organum Vasculosum of the Lamina Terminalis on Contrast-enhanced MR Imaging*. Magn Reson Med Sci, 2018. **17**(2): p. 132-137.

12. Navarro, V.M., *Metabolic regulation of kisspeptin - the link between energy balance and reproduction*. Nat Rev Endocrinol, 2020. **16**(8): p. 407-420.
13. Herbison, A.E., *Control of puberty onset and fertility by gonadotropin-releasing hormone neurons*. Nat Rev Endocrinol, 2016. **12**(8): p. 452-66.
14. Gill, J.C., et al., *The gonadotropin-releasing hormone (GnRH) neuronal population is normal in size and distribution in GnRH-deficient and GnRH receptor-mutant hypogonadal mice*. Endocrinology, 2008. **149**(9): p. 4596-604.
15. Skinner, D.C., et al., *Simultaneous measurement of gonadotropin-releasing hormone in the third ventricular cerebrospinal fluid and hypophyseal portal blood of the ewe*. Endocrinology, 1997. **138**(11): p. 4699-704.
16. Coss, D., *Regulation of reproduction via tight control of gonadotropin hormone levels*. Mol Cell Endocrinol, 2018. **463**: p. 116-130.
17. Herbison, A.E., *The Gonadotropin-Releasing Hormone Pulse Generator*. Endocrinology, 2018. **159**(11): p. 3723-3736.
18. Coutinho, E.A., et al., *Activation of a Classic Hunger Circuit Slows Luteinizing Hormone Pulsatility*. Neuroendocrinology, 2020. **110**(7-8): p. 671-687.
19. Herde, M.K., et al., *GnRH neurons elaborate a long-range projection with shared axonal and dendritic functions*. J Neurosci, 2013. **33**(31): p. 12689-97.
20. Moore, A.M., et al., *Synaptic Innervation of the GnRH Neuron Distal Dendron in Female Mice*. Endocrinology, 2018. **159**(9): p. 3200-3208.
21. Herde, M.K. and A.E. Herbison, *Morphological Characterization of the Action Potential Initiation Segment in GnRH Neuron Dendrites and Axons of Male Mice*. Endocrinology, 2015. **156**(11): p. 4174-86.
22. Iremonger, K.J., R. Porteous, and A.E. Herbison, *Spike and Neuropeptide-Dependent Mechanisms Control GnRH Neuron Nerve Terminal Ca(2+) over Diverse Time Scales*. J Neurosci, 2017. **37**(12): p. 3342-3351.
23. d'Anglemont de Tassigny, X., et al., *Mechanistic insights into the more potent effect of KP-54 compared to KP-10 in vivo*. PLoS One, 2017. **12**(5): p. e0176821.
24. Hu, K.L., et al., *Kisspeptin/Kisspeptin Receptor System in the Ovary*. Front Endocrinol (Lausanne), 2017. **8**: p. 365.
25. Dhillon, W.S., et al., *Kisspeptin-54 stimulates the hypothalamic-pituitary gonadal axis in human males*. J Clin Endocrinol Metab, 2005. **90**(12): p. 6609-15.

26. Messenger, S., et al., *Kisspeptin directly stimulates gonadotropin-releasing hormone release via G protein-coupled receptor 54*. Proc Natl Acad Sci U S A, 2005. **102**(5): p. 1761-6.
27. Seminara, S.B., et al., *The GPR54 gene as a regulator of puberty*. N Engl J Med, 2003. **349**(17): p. 1614-27.
28. Gottsch, M.L., et al., *A role for kisspeptins in the regulation of gonadotropin secretion in the mouse*. Endocrinology, 2004. **145**(9): p. 4073-7.
29. Navarro, V.M., et al., *Advanced vaginal opening and precocious activation of the reproductive axis by KiSS-1 peptide, the endogenous ligand of GPR54*. J Physiol, 2004. **561**(Pt 2): p. 379-86.
30. Qiu, J., et al., *High-frequency stimulation-induced peptide release synchronizes arcuate kisspeptin neurons and excites GnRH neurons*. Elife, 2016. **5**.
31. Zeydabadi Nejad, S., F. Ramezani Tehrani, and A. Zadeh-Vakili, *The Role of Kisspeptin in Female Reproduction*. Int J Endocrinol Metab, 2017. **15**(3): p. e44337.
32. Gottsch, M.L., et al., *Regulation of Kiss1 and dynorphin gene expression in the murine brain by classical and nonclassical estrogen receptor pathways*. J Neurosci, 2009. **29**(29): p. 9390-5.
33. Smith, J.T., et al., *Differential regulation of KiSS-1 mRNA expression by sex steroids in the brain of the male mouse*. Endocrinology, 2005. **146**(7): p. 2976-84.
34. Dungan, H.M., D.K. Clifton, and R.A. Steiner, *Minireview: kisspeptin neurons as central processors in the regulation of gonadotropin-releasing hormone secretion*. Endocrinology, 2006. **147**(3): p. 1154-8.
35. Goodman, R.L., et al., *Kisspeptin neurons in the arcuate nucleus of the ewe express both dynorphin A and neurokinin B*. Endocrinology, 2007. **148**(12): p. 5752-60.
36. Jayasena, C.N., et al., *Effects of neurokinin B administration on reproductive hormone secretion in healthy men and women*. J Clin Endocrinol Metab, 2014. **99**(1): p. E19-27.
37. Ramaswamy, S., et al., *Neurokinin B stimulates GnRH release in the male monkey (Macaca mulatta) and is colocalized with kisspeptin in the arcuate nucleus*. Endocrinology, 2010. **151**(9): p. 4494-503.

38. Billings, H.J., et al., *Neurokinin B acts via the neurokinin-3 receptor in the retrochiasmatic area to stimulate luteinizing hormone secretion in sheep*. Endocrinology, 2010. **151**(8): p. 3836-46.
39. Lehman, M.N., L.M. Coolen, and R.L. Goodman, *Minireview: kisspeptin/neurokinin B/dynorphin (KNDy) cells of the arcuate nucleus: a central node in the control of gonadotropin-releasing hormone secretion*. Endocrinology, 2010. **151**(8): p. 3479-89.
40. Topaloglu, A.K., et al., *TAC3 and TACR3 mutations in familial hypogonadotropic hypogonadism reveal a key role for Neurokinin B in the central control of reproduction*. Nat Genet, 2009. **41**(3): p. 354-358.
41. Guran, T., et al., *Hypogonadotropic hypogonadism due to a novel missense mutation in the first extracellular loop of the neurokinin B receptor*. J Clin Endocrinol Metab, 2009. **94**(10): p. 3633-3639.
42. Yang, J.J., et al., *Uncovering novel reproductive defects in neurokinin B receptor null mice: closing the gap between mice and men*. Endocrinology, 2012. **153**(3): p. 1498-508.
43. Uenoyama, Y., et al., *Role of KNDy Neurons Expressing Kisspeptin, Neurokinin B, and Dynorphin A as a GnRH Pulse Generator Controlling Mammalian Reproduction*. Front Endocrinol (Lausanne), 2021. **12**: p. 724632.
44. Liu, Y., et al., *Dynorphin and GABAA Receptor Signaling Contribute to Progesterone's Inhibition of the LH Surge in Female Mice*. Endocrinology, 2020. **161**(5).
45. Han, S.Y., et al., *Mechanism of kisspeptin neuron synchronization for pulsatile hormone secretion in male mice*. Cell Rep, 2023. **42**(1): p. 111914.
46. Morris, P.G. and A.E. Herbison, *Mechanism of Arcuate Kisspeptin Neuron Synchronization in Acute Brain Slices From Female Mice*. Endocrinology, 2023. **164**(12).
47. Liu, X., R. Porteous, and A.E. Herbison, *Robust GABAergic Regulation of the GnRH Neuron Distal Dendron*. Endocrinology, 2022. **164**(1).
48. Moenter, S.M. and R.A. DeFazio, *Endogenous gamma-aminobutyric acid can excite gonadotropin-releasing hormone neurons*. Endocrinology, 2005. **146**(12): p. 5374-9.

49. Sullivan, S.D. and S.M. Moenter, *Gamma-aminobutyric acid neurons integrate and rapidly transmit permissive and inhibitory metabolic cues to gonadotropin-releasing hormone neurons*. *Endocrinology*, 2004. **145**(3): p. 1194-202.
50. Constantin, S., et al., *Gamma-aminobutyric acid and glutamate differentially regulate intracellular calcium concentrations in mouse gonadotropin-releasing hormone neurons*. *Endocrinology*, 2010. **151**(1): p. 262-70.
51. Constantin, S., et al., *GnRH neuron firing and response to GABA in vitro depend on acute brain slice thickness and orientation*. *Endocrinology*, 2012. **153**(8): p. 3758-69.
52. Whiting, P.J., *GABA-A receptor subtypes in the brain: a paradigm for CNS drug discovery?* *Drug Discov Today*, 2003. **8**(10): p. 445-50.
53. Terunuma, M., *Diversity of structure and function of GABA(B) receptors: a complexity of GABA(B)-mediated signaling*. *Proc Jpn Acad Ser B Phys Biol Sci*, 2018. **94**(10): p. 390-411.
54. Nutt, D., *GABAA receptors: subtypes, regional distribution, and function*. *J Clin Sleep Med*, 2006. **2**(2): p. S7-11.
55. Connolly, C.N., et al., *Assembly and cell surface expression of heteromeric and homomeric gamma-aminobutyric acid type A receptors*. *J Biol Chem*, 1996. **271**(1): p. 89-96.
56. Sivilotti, L. and A. Nistri, *GABA receptor mechanisms in the central nervous system*. *Prog Neurobiol*, 1991. **36**(1): p. 35-92.
57. Chen, K., et al., *Role of GABAB receptors in GABA and baclofen-induced inhibition of adult rat cerebellar interpositus nucleus neurons in vitro*. *Brain Res Bull*, 2005. **67**(4): p. 310-8.
58. Watanabe, M., A. Fukuda, and J. Nabekura, *The role of GABA in the regulation of GnRH neurons*. *Front Neurosci*, 2014. **8**: p. 387.
59. Sullivan, S.D., R.A. DeFazio, and S.M. Moenter, *Metabolic regulation of fertility through presynaptic and postsynaptic signaling to gonadotropin-releasing hormone neurons*. *J Neurosci*, 2003. **23**(24): p. 8578-85.
60. Simonian, S.X., et al., *Role of the GABA(A) receptor gamma2 subunit in the development of gonadotropin-releasing hormone neurons in vivo*. *Eur J Neurosci*, 2000. **12**(10): p. 3488-96.

61. Sim, J.A., et al., *Late postnatal reorganization of GABA(A) receptor signalling in native GnRH neurons*. Eur J Neurosci, 2000. **12**(10): p. 3497-504.
62. Lee, K., et al., *Knockdown of GABA(A) receptor signaling in GnRH neurons has minimal effects upon fertility*. Endocrinology, 2010. **151**(9): p. 4428-36.
63. Silva, M.S.B., et al., *Activation of arcuate nucleus GABA neurons promotes luteinizing hormone secretion and reproductive dysfunction: Implications for polycystic ovary syndrome*. EBioMedicine, 2019. **44**: p. 582-596.
64. Kiss, J., et al., *Evidence for vesicular glutamate transporter synapses onto gonadotropin-releasing hormone and other neurons in the rat medial preoptic area*. Eur J Neurosci, 2003. **18**(12): p. 3267-78.
65. Bailey, J.D., A. Centers, and L. Jennes, *Expression of AMPA receptor subunits (GluR1-GluR4) in gonadotrophin-releasing hormone neurones of young and middle-aged persistently oestrous rats during the steroid-induced luteinising hormone surge*. J Neuroendocrinol, 2006. **18**(1): p. 1-12.
66. Eyigor, O. and L. Jennes, *Kainate receptor subunit-positive gonadotropin-releasing hormone neurons express c-Fos during the steroid-induced luteinizing hormone surge in the female rat*. Endocrinology, 2000. **141**(2): p. 779-86.
67. Abbud, R. and M.S. Smith, *Do GnRH neurons express the gene for the NMDA receptor?* Brain Res, 1995. **690**(1): p. 117-20.
68. Iremonger, K.J., et al., *Glutamate regulation of GnRH neuron excitability*. Brain Res, 2010. **1364**: p. 35-43.
69. Christian, C.A. and S.M. Moenter, *The neurobiology of preovulatory and estradiol-induced gonadotropin-releasing hormone surges*. Endocr Rev, 2010. **31**(4): p. 544-77.
70. Smyth, C. and M. Wilkinson, *A critical period for glutamate receptor-mediated induction of precocious puberty in female rats*. J Neuroendocrinol, 1994. **6**(3): p. 275-84.
71. Christian, C.A. and S.M. Moenter, *Estradiol induces diurnal shifts in GABA transmission to gonadotropin-releasing hormone neurons to provide a neural signal for ovulation*. J Neurosci, 2007. **27**(8): p. 1913-21.
72. d'Anglemon de Tassigny, X., et al., *Kisspeptin signaling is required for peripheral but not central stimulation of gonadotropin-releasing hormone neurons by NMDA*. J Neurosci, 2010. **30**(25): p. 8581-90.

73. Medhamurthy, R., V.L. Gay, and T.M. Plant, *Repetitive injections of L-glutamic acid, in contrast to those of N-methyl-D,L-aspartic acid, fail to elicit sustained hypothalamic GnRH release in the prepubertal male rhesus monkey (Macaca mulatta)*. Neuroendocrinology, 1992. **55**(6): p. 660-6.
74. Piet, R., et al., *Electrical properties of kisspeptin neurons and their regulation of GnRH neurons*. Front Neuroendocrinol, 2015. **36**: p. 15-27.
75. Constantin, S., K.J. Iremonger, and A.E. Herbison, *In vivo recordings of GnRH neuron firing reveal heterogeneity and dependence upon GABAA receptor signaling*. J Neurosci, 2013. **33**(22): p. 9394-401.
76. Ping, L., et al., *Regulation of gonadotropin-releasing hormone and luteinizing hormone secretion by AMPA receptors. Evidence for a physiological role of AMPA receptors in the steroid-induced luteinizing hormone surge*. Neuroendocrinology, 1997. **66**(4): p. 246-53.
77. Schwanzel-Fukuda, M. and D.W. Pfaff, *Origin of luteinizing hormone-releasing hormone neurons*. Nature, 1989. **338**(6211): p. 161-4.
78. Wray, S., P. Grant, and H. Gainer, *Evidence that cells expressing luteinizing hormone-releasing hormone mRNA in the mouse are derived from progenitor cells in the olfactory placode*. Proc Natl Acad Sci U S A, 1989. **86**(20): p. 8132-6.
79. Duittoz, A.H., Y. Tillet, and S. Geller, *The great migration: How glial cells could regulate GnRH neuron development and shape adult reproductive life*. J Chem Neuroanat, 2022. **125**: p. 102149.
80. de Castro, F., R. Seal, and R. Maggi, *ANOS1: a unified nomenclature for Kallmann syndrome 1 gene (KAL1) and anosmin-1*. Brief Funct Genomics, 2017. **16**(4): p. 205-210.
81. Nie, M., et al., *Analysis of genetic and clinical characteristics of a Chinese Kallmann syndrome cohort with ANOS1 mutations*. Eur J Endocrinol, 2017. **177**(4): p. 389-398.
82. Dodé, C. and J.P. Hardelin, *Kallmann syndrome*. Eur J Hum Genet, 2009. **17**(2): p. 139-46.
83. Xie, Y., et al., *FGF/FGFR signaling in health and disease*. Signal Transduct Target Ther, 2020. **5**(1): p. 181.
84. Cho, H.J., et al., *Nasal Placode Development, GnRH Neuronal Migration and Kallmann Syndrome*. Front Cell Dev Biol, 2019. **7**: p. 121.

85. Chung, W.C., S.S. Moyle, and P.S. Tsai, *Fibroblast growth factor 8 signaling through fibroblast growth factor receptor 1 is required for the emergence of gonadotropin-releasing hormone neurons*. *Endocrinology*, 2008. **149**(10): p. 4997-5003.
86. Yellapragada, V., et al., *FGF8-FGFR1 signaling regulates human GnRH neuron differentiation in a time- and dose-dependent manner*. *Dis Model Mech*, 2022. **15**(8).
87. MacColl, G., P. Bouloux, and R. Quinton, *Kallmann syndrome: adhesion, afferents, and anosmia*. *Neuron*, 2002. **34**(5): p. 675-8.
88. Slegtenhorst-Eegdeman, K.E., et al., *Macroorchidism in FMR1 knockout mice is caused by increased Sertoli cell proliferation during testicular development*. *Endocrinology*, 1998. **139**(1): p. 156-62.
89. Nguyen, A.O., et al., *Abnormal development of auditory responses in the inferior colliculus of a mouse model of Fragile X Syndrome*. *J Neurophysiol*, 2020. **123**(6): p. 2101-2121.
90. Shi, D., et al., *White Matter Alterations in Fmr1 Knockout Mice during Early Postnatal Brain Development*. *Dev Neurosci*, 2019. **41**(5-6): p. 274-289.
91. Kurosaki, T., et al., *NMD abnormalities during brain development in the Fmr1-knockout mouse model of fragile X syndrome*. *Genome Biol*, 2021. **22**(1): p. 317.
92. Rais, M., et al., *Functional consequences of postnatal interventions in a mouse model of Fragile X syndrome*. *Neurobiol Dis*, 2022. **162**: p. 105577.
93. Lovelace, J.W., et al., *Matrix metalloproteinase-9 deletion rescues auditory evoked potential habituation deficit in a mouse model of Fragile X Syndrome*. *Neurobiol Dis*, 2016. **89**: p. 126-35.
94. Berkovitz, G.D., et al., *Gonadal function in men with the Martin-Bell (fragile-X) syndrome*. *Am J Med Genet*, 1986. **23**(1-2): p. 227-39.
95. Allingham-Hawkins, D.J., et al., *Fragile X premutation is a significant risk factor for premature ovarian failure: the International Collaborative POF in Fragile X study--preliminary data*. *Am J Med Genet*, 1999. **83**(4): p. 322-5.
96. Wheeler, A.C., et al., *Health and reproductive experiences of women with an FMR1 premutation with and without fragile X premature ovarian insufficiency*. *Front Genet*, 2014. **5**: p. 300.

97. Villa, P.A., et al., *Altered GnRH neuron and ovarian innervation characterize reproductive dysfunction linked to the Fragile X messenger ribonucleoprotein (Fmr1) gene mutation*. Front Endocrinol (Lausanne), 2023. **14**: p. 1129534.
98. Leehey, M.A., *Fragile X-associated tremor/ataxia syndrome: clinical phenotype, diagnosis, and treatment*. J Investig Med, 2009. **57**(8): p. 830-6.
99. Wijetunge, L.S., et al., *Fragile X syndrome: from targets to treatments*. Neuropharmacology, 2013. **68**: p. 83-96.
100. Murray, A., *Premature ovarian failure and the FMR1 gene*. Semin Reprod Med, 2000. **18**(1): p. 59-66.
101. Ruggiero-Ruff, R.E., et al., *Increased body weight in mice with fragile X messenger ribonucleoprotein 1 (Fmr1) gene mutation is associated with hypothalamic dysfunction*. Sci Rep, 2023. **13**(1): p. 12666.
102. Lozano, R., et al., *Association between macroorchidism and intelligence in FMR1 premutation carriers*. Am J Med Genet A, 2014. **164a**(9): p. 2206-11.
103. Murray, A., et al., *Reproductive and menstrual history of females with fragile X expansions*. Eur J Hum Genet, 2000. **8**(4): p. 247-52.
104. Jankowska, K., *Premature ovarian failure*. Prz Menopauzalny, 2017. **16**(2): p. 51-56.
105. Eastell, R., *Management of osteoporosis due to ovarian failure*. Med Pediatr Oncol, 2003. **41**(3): p. 222-7.
106. Bretherick, K.L., M.R. Fluker, and W.P. Robinson, *FMR1 repeat sizes in the gray zone and high end of the normal range are associated with premature ovarian failure*. Hum Genet, 2005. **117**(4): p. 376-82.
107. Sullivan, A.K., et al., *Association of FMR1 repeat size with ovarian dysfunction*. Hum Reprod, 2005. **20**(2): p. 402-12.
108. Fu, Y.H., et al., *Variation of the CGG repeat at the fragile X site results in genetic instability: resolution of the Sherman paradox*. Cell, 1991. **67**(6): p. 1047-58.
109. Allen, E.G., et al., *Refining the risk for fragile X-associated primary ovarian insufficiency (FXPOI) by FMR1 CGG repeat size*. Genet Med, 2021. **23**(9): p. 1648-1655.
110. Feng, Y., et al., *Translational suppression by trinucleotide repeat expansion at FMR1*. Science, 1995. **268**(5211): p. 731-4.

111. Edbauer, D., et al., *Regulation of synaptic structure and function by FMRP-associated microRNAs miR-125b and miR-132*. *Neuron*, 2010. **65**(3): p. 373-84.
112. Bagni, C., et al., *Fragile X syndrome: causes, diagnosis, mechanisms, and therapeutics*. *J Clin Invest*, 2012. **122**(12): p. 4314-22.
113. Ascano, M., Jr., et al., *FMRP targets distinct mRNA sequence elements to regulate protein expression*. *Nature*, 2012. **492**(7429): p. 382-6.
114. Darnell, J.C., et al., *FMRP stalls ribosomal translocation on mRNAs linked to synaptic function and autism*. *Cell*, 2011. **146**(2): p. 247-61.
115. Korb, E., et al., *Excess Translation of Epigenetic Regulators Contributes to Fragile X Syndrome and Is Alleviated by Brd4 Inhibition*. *Cell*, 2017. **170**(6): p. 1209-1223.e20.
116. Hale, C.R., et al., *FMRP regulates mRNAs encoding distinct functions in the cell body and dendrites of CA1 pyramidal neurons*. *Elife*, 2021. **10**.
117. D'Hulst, C., et al., *Decreased expression of the GABAA receptor in fragile X syndrome*. *Brain Res*, 2006. **1121**(1): p. 238-45.
118. El Idrissi, A., et al., *Decreased GABA(A) receptor expression in the seizure-prone fragile X mouse*. *Neurosci Lett*, 2005. **377**(3): p. 141-6.
119. D'Hulst, C., et al., *Positron Emission Tomography (PET) Quantification of GABAA Receptors in the Brain of Fragile X Patients*. *PLoS One*, 2015. **10**(7): p. e0131486.
120. Toft, A.K., C.J. Lundbye, and T.G. Banke, *Dysregulated NMDA-Receptor Signaling Inhibits Long-Term Depression in a Mouse Model of Fragile X Syndrome*. *J Neurosci*, 2016. **36**(38): p. 9817-27.
121. Prieto, M., et al., *Missense mutation of Fmr1 results in impaired AMPAR-mediated plasticity and socio-cognitive deficits in mice*. *Nat Commun*, 2021. **12**(1): p. 1557.
122. Booker, S.A., et al., *Altered dendritic spine function and integration in a mouse model of fragile X syndrome*. *Nat Commun*, 2019. **10**(1): p. 4813.
123. Kelesidis, T., et al., *Narrative review: the role of leptin in human physiology: emerging clinical applications*. *Ann Intern Med*, 2010. **152**(2): p. 93-100.
124. Fu, Z., E.R. Gilbert, and D. Liu, *Regulation of insulin synthesis and secretion and pancreatic Beta-cell dysfunction in diabetes*. *Curr Diabetes Rev*, 2013. **9**(1): p. 25-53.

125. Andermann, M.L. and B.B. Lowell, *Toward a Wiring Diagram Understanding of Appetite Control*. *Neuron*, 2017. **95**(4): p. 757-778.
126. Huang, L., et al., *Critical body fat percentage required for puberty onset: the Taiwan Pubertal Longitudinal Study*. *J Endocrinol Invest*, 2023. **46**(6): p. 1177-1185.
127. Gimunová, M., et al., *The Prevalence of Menstrual Cycle Disorders in Female Athletes from Different Sports Disciplines: A Rapid Review*. *Int J Environ Res Public Health*, 2022. **19**(21).
128. Mancini, M., et al., *Obesity Is Strongly Associated With Low Testosterone and Reduced Penis Growth During Development*. *J Clin Endocrinol Metab*, 2021. **106**(11): p. 3151-3159.
129. Chehab, F.F., M.E. Lim, and R. Lu, *Correction of the sterility defect in homozygous obese female mice by treatment with the human recombinant leptin*. *Nat Genet*, 1996. **12**(3): p. 318-20.
130. Mounzih, K., R. Lu, and F.F. Chehab, *Leptin treatment rescues the sterility of genetically obese ob/ob males*. *Endocrinology*, 1997. **138**(3): p. 1190-3.
131. Harno, E., et al., *POMC: The Physiological Power of Hormone Processing*. *Physiol Rev*, 2018. **98**(4): p. 2381-2430.
132. Celis, M.E., *Release of LH in response to alpha-MSH administration*. *Acta Physiol Pharmacol Latinoam*, 1985. **35**(3): p. 281-90.
133. Berberian, V., et al., *Effect of alpha-melanotropin hormone on serum levels of luteinizing hormone and progesterone in experimental rat autoimmune oophoritis*. *Peptides*, 2006. **27**(9): p. 2295-9.
134. Manfredi-Lozano, M., et al., *Defining a novel leptin-melanocortin-kisspeptin pathway involved in the metabolic control of puberty*. *Mol Metab*, 2016. **5**(10): p. 844-857.
135. Roa, J. and A.E. Herbison, *Direct regulation of GnRH neuron excitability by arcuate nucleus POMC and NPY neuron neuropeptides in female mice*. *Endocrinology*, 2012. **153**(11): p. 5587-99.
136. Cravo, R.M., et al., *Characterization of Kiss1 neurons using transgenic mouse models*. *Neuroscience*, 2011. **173**: p. 37-56.
137. Stincic, T.L., et al., *Estradiol Drives the Anorexigenic Activity of Proopiomelanocortin Neurons in Female Mice*. *eNeuro*, 2018. **5**(4).

138. Fu, L.Y. and A.N. van den Pol, *Kisspeptin directly excites anorexigenic proopiomelanocortin neurons but inhibits orexigenic neuropeptide Y cells by an indirect synaptic mechanism*. J Neurosci, 2010. **30**(30): p. 10205-19.
139. Chen, X., et al., *Deficient melanocortin-4 receptor causes abnormal reproductive neuroendocrine profile in female mice*. Reproduction, 2017. **153**(3): p. 267-276.
140. Pritchard, L.E., et al., *Agouti-related protein (83-132) is a competitive antagonist at the human melanocortin-4 receptor: no evidence for differential interactions with pro-opiomelanocortin-derived ligands*. J Endocrinol, 2004. **180**(1): p. 183-91.
141. Deem, J.D., C.L. Faber, and G.J. Morton, *AgRP neurons: Regulators of feeding, energy expenditure, and behavior*. Febs j, 2022. **289**(8): p. 2362-2381.
142. Garfield, A.S., et al., *A neural basis for melanocortin-4 receptor-regulated appetite*. Nat Neurosci, 2015. **18**(6): p. 863-71.
143. Vulliémoz, N.R., et al., *Central infusion of agouti-related peptide suppresses pulsatile luteinizing hormone release in the ovariectomized rhesus monkey*. Endocrinology, 2005. **146**(2): p. 784-9.
144. Padilla, S.L., et al., *AgRP to Kiss1 neuron signaling links nutritional state and fertility*. Proc Natl Acad Sci U S A, 2017. **114**(9): p. 2413-2418.
145. Shi, L., Z. Jiang, and L. Zhang, *Childhood obesity and central precocious puberty*. Front Endocrinol (Lausanne), 2022. **13**: p. 1056871.
146. Paeger, L., et al., *Energy imbalance alters Ca(2+) handling and excitability of POMC neurons*. Elife, 2017. **6**.
147. Millington, G.W., *The role of proopiomelanocortin (POMC) neurones in feeding behaviour*. Nutr Metab (Lond), 2007. **4**: p. 18.
148. Newton, A.J., et al., *AgRP innervation onto POMC neurons increases with age and is accelerated with chronic high-fat feeding in male mice*. Endocrinology, 2013. **154**(1): p. 172-83.
149. Horvath, T.L., et al., *Synaptic input organization of the melanocortin system predicts diet-induced hypothalamic reactive gliosis and obesity*. Proc Natl Acad Sci U S A, 2010. **107**(33): p. 14875-80.
150. Lainez, N.M., et al., *Diet-Induced Obesity Elicits Macrophage Infiltration and Reduction in Spine Density in the Hypothalamus of Male but Not Female Mice*. Front Immunol, 2018. **9**: p. 1992.

151. Chen, K.E., N.M. Lainez, and D. Coss, *Sex Differences in Macrophage Responses to Obesity-Mediated Changes Determine Migratory and Inflammatory Traits*. *J Immunol*, 2021. **206**(1): p. 141-153.
152. Chen, K.E., et al., *Visceral adipose tissue imparts peripheral macrophage influx into the hypothalamus*. *J Neuroinflammation*, 2021. **18**(1): p. 140.
153. Jais, A. and J.C. Brüning, *Hypothalamic inflammation in obesity and metabolic disease*. *J Clin Invest*, 2017. **127**(1): p. 24-32.
154. Lainez, N.M. and D. Coss, *Leukemia Inhibitory Factor Represses GnRH Gene Expression via cFOS during Inflammation in Male Mice*. *Neuroendocrinology*, 2019. **108**(4): p. 291-307.

CHAPTER TWO

Altered GnRH Neuron and Ovarian Innervation Characterize Reproductive Dysfunction

Linked to the Fragile X Messenger Ribonucleoprotein (*Fmr1*) Gene Mutation

A version of this chapter was published in Pedro et al., *Frontiers in Endocrinology* 2023

2.1 Abstract

Mutations in the Fragile X Messenger Ribonucleoprotein 1 (*FMRI*) gene cause Fragile X Syndrome, the most common monogenic cause of intellectual disability. Mutations of *FMRI* are also associated with reproductive disorders, such as early cessation of reproductive function in females. While progress has been made in understanding the mechanisms of mental impairment, the causes of reproductive disorders are not clear. FMR1-associated reproductive disorders were studied exclusively from the endocrine perspective, while *FMRI* role in neurons that control reproduction was addressed. Here, we demonstrate that similar to women with *FMRI* mutations, female *Fmr1* null mice stop reproducing early. However, young null females display larger litters, more corpora lutea in the ovaries, increased inhibin, progesterone, testosterone, and gonadotropin hormones in circulation. Given elevated ovarian hormones, the increase in gonadotropins is not due to the lack of ovarian feedback, and ovariectomy reveals both a hypothalamic and an ovarian contribution to elevated gonadotropins. Increased vascularization of corpora lutea, higher sympathetic innervation of growing follicles in the ovaries of *Fmr1* nulls, and higher numbers of synaptic GABA_A receptors in GnRH neurons, which are excitatory for GnRH neurons, are also determined. Altered mRNA and protein levels of synaptic molecules in the hypothalamus are identified. Unmodified and ovariectomized *Fmr1* nulls have increased LH pulse frequency, suggesting that *Fmr1* nulls exhibit hyperactive GnRH neurons, regardless of ovarian feedback. These results reveal *Fmr1* function in the regulation of GnRH neuron

activity, and point to the role of GnRH neurons, in addition to the ovarian innervation, in the etiology of *Fmr1*-mediated reproductive disorders.

2.2 Rationale for determining the role of FMR1 gene mutations in female fertility

Mutations in the Fragile X Messenger Ribonucleoprotein 1 (*FMR1*) gene lead to the most common genetic form of intellectual disability and autism, called Fragile X Syndrome (FXS) [57, 58]. In addition to intellectual impairment, *FMR1* gene mutations are also associated with reproductive disorders, such as early menopause in females, and macroorchidism in males [59-62]. The *FMR1* gene encodes FMR protein (FMRP), an mRNA binding protein that regulates the protein levels of its target genes [16, 63]. Target mRNAs bound by FMRP encode a variety of proteins, including transcription factors that regulate other genes [64-66]. Mutation of this gene that causes FXS entails full expansion of the unstable CGG trinucleotide repeats (>200) that leads to hypermethylation, silencing of the gene and the loss of FMRP. Premutation, in a range of 50-200 repeats, causes *Fragile X*-associated Tremor/Ataxia Syndrome (FXTAS) and exhibits reduced FMRP levels. While the mechanisms of intellectual impairments following FMRP loss are beginning to emerge, mechanisms of reproductive disorders are not known. Although FMRP is ubiquitous, it is highly abundant in the nervous system. In the brain, FMRP binds mRNAs that encode synaptic proteins, contributing to cognitive dysfunctions in FXS [64-66]. The effect of *FMR1* mutations on the cortex and hippocampus have been analyzed [67, 68], however, how mutations affect hypothalamic functions has not been examined. Herein, we investigated the effects of FMRP loss in reproduction, specifically

on a population of hypothalamic neurons that regulate the hypothalamus-pituitary-gonadal axis.

Given that *FMRI* gene mutations are also associated with reproductive disorders, [59-62], combined with increasing infertility rates [69, 70], it is critical to examine *FMRI* role in the reproductive axis. Reproduction is controlled by hypothalamic neurons that secrete gonadotropin-releasing hormone (GnRH) neuropeptide [71, 72]. GnRH is secreted in a pulsatile fashion into the hypophysial-portal system, to regulate synthesis and secretion of pituitary gonadotropin hormones, luteinizing hormone (LH) and follicle-stimulating hormone (FSH), which in turn regulate gonadal function [73]. Synchronization of GnRH secretion is determined by an upstream regulatory network. One population of such afferent neurons are GABAergic neurons from the mediobasal hypothalamus [74-80]. Although GABA is the main inhibitory neurotransmitter in the brain, GABA is excitatory for GnRH neurons [75, 81-83]. Changes in GnRH neuron connectivity and its innervation control neuropeptide pulsatile secretion and consequently gonadotropin hormone levels.

Contrary to the hypothalamus, gonadal roles of FMRP have been analyzed in several reports. Macroorchidism in men affected with FXS [61] is caused by increased Sertoli cell proliferation during development [84]. In women, mutations in the *FMRI* gene comprise the largest number of cases with the known genetic causes of early cessation of reproductive function [60, 85, 86]. *FMRI* exhibits X-linked dominant inheritance pattern and associated disorders have a high penetrance [87], which contributes to their high incidence [88]. Premature ovarian failure is an infertility disorder

affecting 1% of reproductive age women that lose ovarian function before the age of 40 [1, 89]. Women with early menopause experience not only early infertility, but increased risk of cardiovascular disease, osteoporosis and depression [90]. Premutations of the *FMRI* gene are primarily associated with the early loss of reproductive function, which may be due to the much higher prevalence of premutations compared to full mutations. Although to a lesser degree, premutation also causes lower levels of FMRP, and thus, lack of FMRP may cause pathologies in both premutation and full mutation [91]. Contrary to men, premature ovarian failure in women with *FMRI* mutations is not a developmental disorder. Previous studies in mice [86] and humans, [19, 62, 92, 93] didn't find differences in primordial follicle numbers, indicating that early follicular development is not affected. Women affected with mutations have elevated FSH [19, 94], which stimulates the cyclic recruitment of a wave of ovarian follicles into the growing pool in each menstrual or estrous cycle [95]. However, it is still not clear how *FRMI* mutations lead to early infertility.

With a high prevalence of *FMRI* mutations in women of child-bearing age, investigating FMRP-mediated effects on reproductive function will help us understand the mechanism of early menopause. Previous studies that examined ovarian hormone levels or follicle development, failed to explain early infertility. In this study, we first examined the reproductive function in female *Fmr1* KO mice and determined that the mouse model lacking the *Fmr1* gene mimics the reproductive deficits observed in women with *FMRI* mutations associated with reduced FMRP levels. We further observed that *Fmr1* KO mice had larger litters and more corpora lutea in the ovaries, but normal

primordial follicle count, indicating increased recruitment. In addition, we found an increase in gonadotropin levels, inhibin B and steroid hormone levels, which indicated that ovarian feedback is present. We further analyzed ovarian vascularization and innervation, and observed changes that may explain increased FSH. Ovariectomy however, revealed a hypothalamic contribution to increased LH. We then analyzed alteration in gene expression and protein levels of critical hypothalamic molecules, and examined the consequence of FMRP loss on hypothalamic GnRH neurons that have been neglected for their potential role in the etiology of early menopause and show changes in GABAergic innervation. We show higher LH pulse frequency, before and after ovariectomy, which indicates higher GnRH neuron activity, correlating with alterations in GnRH neuron connectivity. Therefore, central mechanisms, most likely via alterations in the activity of GnRH neurons, in addition to ovarian effects, can contribute to increased gonadotropins and higher recruitment of follicles leading to reproductive dysfunction in women with *FMRI* mutations.

2.3 Materials and Methods

Animals

All animal procedures were performed with approval from the University of California (Riverside, CA) Animal Care and Use Committee and in accordance with the National Institutes of Health Animal care and Use Guidelines. Breeding pairs of FVB.129P2-Fmr1tm1Cgr/J (*Fmr1* KO) and their congenic controls (WT) mice were obtained from Jackson Laboratories and bred in-house. Mice were maintained under a

12-h light, 12-h dark cycle and received food and water *ad libitum*. Since we were interested in determining the mechanisms of premature ovarian failure in women with mutations in the *FMRI* gene, only female mice were used for our studies. Estrous cycle stage was determined with vaginal smears and females were collected in a specific estrous cycle stage, as indicated for each analysis. For fertility studies, *Fmr1* KO females and WT controls were housed with WT males and their litters and numbers of pups per litter were recorded. Ovariectomy was performed as described before using 8-week-old mice [96]. Animals were allowed to recover and seven days later blood was collected for hormone analyses as described below.

Hormone assay

Previous studies using FXS mouse models demonstrated that these mice have a heightened response to stress and altered levels of glucocorticoids [97], which can lead to a decrease in luteinizing hormone (LH) levels [98, 99]. To reduce stress, animals were acclimated by daily handling and tail massage for two weeks prior to hormone measurements. For LH measurements, blood was collected from the tail and analyzed by an in house ultra-sensitive ELISA. The capture monoclonal antibody (anti-bovine LH beta subunit, 518B7) was provided by Janet Roser, University of California. The detection polyclonal antibody (rabbit LH antiserum, AFP240580Rb) was provided by the National Hormone and Peptide Program (NHPP). HRP-conjugated polyclonal antibody (goat anti-rabbit) was purchased from DakoCytomation (Glostrup, Denmark; D048701-2). Mouse LH reference prep (AFP5306A; NHPP) was used as the assay standard. Assay

sensitivity is 0.016 ng/ml, while intra-assay coefficient of variation is 2.2% and inter-assay coefficient of variation was 7.3% at the low end of the curve. Other hormone assays were performed by the University of Virginia, Ligand Core using serum that was obtained from the inferior *vena cava*. The University of Virginia Center for Research in Reproduction Ligand Assay and Analysis Core is supported by the Eunice Kennedy Shriver NICHD/NIH Grant R24HD102061. The blood was left to coagulate for 15 min at room temperature, and then centrifuged at 2000 RCF for 15 min for serum separation. FSH was assayed by RIA using reagents provided by Dr. A.F. Parlow and the National Hormone and Peptide Program, as previously described [100]. Mouse FSH reference prep AFP5308D was used for assay standards. Inhibin and steroid hormone levels were analyzed using validated commercially available assays, information for which can be found on the core's website: <http://www.medicine.virginia.edu/research/institutes-and-programs/crr/lab-facilities/assay-methods-page> and reported in [101]. Limits of detection were 2.4 ng/ml for FSH, 3 pg/ml for estradiol, and 100 pg/ml for testosterone. Intra- and inter-assay coefficients of variation were 6.9%/7.5%, 6.0%/11.4% and 4.4%/6.4% for FSH, estrogen (E2) and testosterone (T), respectively. Each animal used for each hormone analysis is represented as a dot in the figure.

Pulsatile LH levels

Pulsatile secretion of LH strictly corresponds to GnRH secretion [102, 103]. LH is used as an indicator of GnRH secretion, since GnRH secretion into median eminence cannot be measured in mice. To ascertain if LH or GnRH neuron secretion is affected, we

measured LH pulses and used an ultrasensitive ELISA assay for LH that allows for LH measurement in 5 μ l of whole blood [104]. Mice were acclimated for 2 weeks by daily tail massage. 10 μ L of blood was collected every 8 min for 3 hours from the tail vein [98, 105]. LH levels were analyzed using ELISA described above. LH amplitude was determined by subtracting the LH value at the peak from the basal value prior to the onset of the pulse and averaged for each mouse. Mean LH concentration was calculated by averaging LH values, while pulse frequency was determined using freeware DynPeak algorithm.

Nanostring analysis of hypothalamic gene expression

8-week old female mice were perfused with ice cold PBS, brains rapidly removed and flash frozen in isopentane on dry ice. Coronal brain sections of 500 μ m were obtained using vibratome, the hypothalamus was dissected and analyzed for gene expression changes by Nanostring. RNA was isolated using the RNAqueous[®]-Micro Kit (Ambion) and quantified using Nanodrop. Gene expression in 50 ng RNA per sample was analyzed using the Nanostring instrument, according to manufacturer's instruction, with the nCounter Mouse Neuroinflammation Panel (770 genes, gene list available at the manufacturer's website). The panel was customized with an addition of 30 custom probes for hypothalamic neuropeptides and their receptors. Only samples with an RNA integrity number RIN > 7 were used for Nanostring. All data passed QC, with no imaging, binding, positive control, or CodeSet content normalization flags. Data analysis was performed using nSolver Analysis Software 4.0, including nCounter Advanced Analysis

(version 2.0.115). Genes with an expression lower than the limit of detection after background subtraction, and compared to negative controls included in the panel, were excluded. Seven housekeeping control genes that are included in the panel, were used for normalization. A heatmap of differentially expressed genes (DEG) was created using Heatmapper software from University of Alberta (Edmonton, Canada; [106]). Results are plotted in the Volcano plot as log fold change vs. log p-value, and genes with changes higher than 25% were indicated with colors in the figures: red indicates genes higher in KO compared to WT, while green indicates genes that are higher in the WT compared to KO. Genes with significant changes in expression are indicated above the dashed line. Gene ontology (GO) enrichment analysis of the DEG genes was performed using the ShinyGo 0.76.3 platform (South Dakota State University [107]). False discovery rate (FDR) cutoff was 0.05, with the pathway minimum set to 10.

qPCR Analysis

Total RNA was extracted from ovaries using Trizol (Invitrogen, CA), and from hypothalamus and pituitary using the RNAqueous®-Micro Kit (Ambion), quantified using Nanodrop and the same amount per sample reverse transcribed using Superscript IV (Invitrogen, CA). qPCR was performed using an iQ SYBR Green supermix and an IQ5 real-time PCR machine (Bio-Rad Laboratories, Hercules, CA), with previously characterized specific primers, under the following conditions: 95 °C for 15 min, followed by 40 cycles at 95 °C for 20 s, 56 °C for 30 s, and 72 °C for 30 s. The amount of the gene of interest was calculated by comparing the threshold cycle obtained for each

sample with the standard curve generated in the same run and normalized to the beta-2-microglobulin (B2M) or GAPDH housekeeping genes, as indicated, in the same sample using $\Delta\Delta\text{Ct}$ method. Preliminary experiments analyzed several housekeeping genes and determined that these housekeeping genes do not differ between genotypes. Replicates were averaged. After each run, a melting curve analysis was performed to confirm that a single amplicon was generated in each reaction.

Histological analyses and immunohistochemistry

WT controls and *Fmr1* KO mice were anesthetized, perfused with 20 ml PBS and 20 ml 4% paraformaldehyde; and tissues were collected. Ovaries were fixed in 4% paraformaldehyde, embedded in paraffin, and cut to 20 μm sections. Slides were deparaffinized in xylene, rehydrated and H&E stain was performed to count ovarian follicles. For ovarian vasculature and innervation studies, frozen floating 60 μm sections were stained with antibody to CD31 (1:2000 dilution, 553370, BD Biosciences) or with antibody to tyrosine hydroxylase (TH, 1:5000, ab112, Abcam) for 48 hours at 4°C, followed by overnight incubation with goat anti-rat IgG-Alexa 488 (1:2000, A11006, Vector Laboratories, Burlingame, CA) or goat anti-rabbit IgG-Alexa 488 (1:1000, A11034, Vector Laboratories, Burlingame, CA), respectively. Vascularization of corpora lutea and antral follicles was quantified by the mean fluorescent intensity (MFI) using Fiji ImageJ. Ovarian innervation was quantified by counting the number of neuronal projections in direct contact with follicles or corpora lutea.

Hypothalami were sectioned to 100 μm sections. Sections containing organum vasculosum laminae terminalis (OVLT) where GnRH neurons are located, were blocked and stained for GnRH using rabbit anti-GnRH antibodies (1:10,000 dilution) kindly provided by Greg Anderson (University of Otago; Dunedin, New Zealand [108]), GABA γ 2 receptor subunit (1:10,000 dilution, guinea pig anti-GABA γ 2, Synaptic systems 224 004), VGAT (1:5,000, mouse anti-VGAT, Synaptic systems 131 011) for 72 hours at 4°C. After PBST washes, slides were incubated overnight at 4°C with secondary antibodies goat anti-rabbit IgG-Alexa 488 (1:1000, A11034, Vector Laboratories, Burlingame, CA); anti-mouse IgG-Alexa 594 (1:1000, A11032, Vector Laboratories, Burlingame, CA); anti-guinea pig–biotin (1:1000, BA-7000) followed by streptavidin-Cy5 (1:1000, 434316, Vector Laboratories, Burlingame, CA). Secondary antibody-only controls were performed to determine antibody specificity.

Immunostaining for FMRP was performed using antigen retrieval methods, as previously described [109]. Slices were stained overnight with mouse anti-FMRP (1:1000; Developmental Studies Hybridoma Bank, catalog #2F5-1-s, RRID: AB_10805421). Secondary antibody was donkey anti-mouse Alexa 594 (1:300; Molecular Probes, A-21202). Slices were mounted on slides with Vectashield mounting medium containing DAPI (Vector Laboratories, H-1200).

To determine puncta density, we followed our established protocol as previously published [110-114]. Puncta were counted in the individual neurons where at least 45 μm of the axon proximal to soma can be observed using z-stack acquired by confocal Leica SP2 microscope. Images were encoded for blind analysis. Puncta numbers were

quantified by scrolling through the series of captured images in the z-stack using LAS X software and counted for each GnRH soma and along the 45 μm length of axon, at 15- μm intervals. At least 15-20 individual neurons from 4-5 different sets of mice marked by hand and with the Neurolucida program (MBF Bioscience, Vermont) and counted. 3-D reconstruction was performed by Imaris software (Bitplane, Inc; Concord, MA).

Western blot

Whole cell lysates were obtained from the dissected hypothalami from WT controls and FMR1 knockout mice and after protein determination, the same amount of protein was run on SDS-PAGE, transferred on nitrocellulose membrane and probed for: GABA α 2 receptor subunit (1:1000, 14104-1-AP, Proteintech), NMDAR1 (1:1000, 32-0500 Invitrogen), NMDAR2B (1:1000, 07-632 EMD Millipore), postsynaptic density protein 95 (PSD-95; 1:1000, 3409, Cell Signaling), Synaptophysin (SYPH; 1:1000, 4329, Cell Signaling), neuronal marker, Microtubule-associated protein 2 (MAP2; 1:5000, ab5392, Abcam) or α -tubulin (1:1000, sc-9104, Santa Cruz Biotechnology). Bands were quantified using ChemiDoc imaging system (Bio-Rad, Hercules, CA).

Statistical analyses.

Statistical differences between WT control and *Fmr1* KO mice ($p < 0.05$) were determined by t-test, or ANOVA when appropriate, followed by Tukey's post-hoc test for multiple comparisons using Prism software (GraphPad, CA).

2.4 Results

Fmr1 knockout female mice experience early cessation of reproductive function.

Since women with *FMRI* mutation experience increased risk of early menopause, to begin investigating the role of FMRP in reproductive function, we first determined if the lack of FMRP in female *Fmr1* KO mice can mimic reproductive dysfunctions observed in women with reduced levels of FMRP due to *FMRI* mutation. In affected people, full expansion of the unstable CGG trinucleotide repeats (>200) leads to hypermethylation, silencing of the gene and the loss of FMRP and FXS. CGG expansion in a range of 50-200 repeats, or *FMRI* premutation, exhibit reduced FMRP levels and FXTAS. Due to differential methylation between human and mouse genes, the *Fmr1* KO is a widely used mouse model to study Fragile X Syndrome and is considered a better model than putative mimics of the CGG repeat expansion [115, 116]. Our study showed that *Fmr1* KO female mice experienced early vaginal opening, an external sign of puberty in mice (Fig. 1A, *FMRI*, *Fmr1* knock-out (KO); WT, wild-type control; each point represents a mouse, while bars represent group average). *Fmr1* KO mice demonstrated vaginal opening at postnatal day 29 (p29), compared to p31 in WT controls. At 8 weeks of age, we paired *Fmr1* KO females and control WT females, with control males and recorded birth dates

and number of litters, and the number of pups in each litter, until they stopped reproducing. We determined that *Fmr1* KO female mice exhibited early cessation of reproductive function, which is similar to early menopause in women with *FMRI* mutation or premutation (Fig. 1B, each point represents a mouse) [6, 117]. *Fmr1* KO mice stopped having litters at 5.5 months of age and an average age of the last litter was p163 (FMR1, black squares), compared to p263 for WT control females (WT, open circles). Similar to the penetrance in women with mutations in the *FMRI* gene [87], we observed different degrees of premature cessation of reproductive function. *Fmr1* KO females split into two groups based on the age at last litter: females more severely affected with the mutation that stopped reproducing at p97, and less severely affected females that had the last litter at p221. Nonetheless, the difference between controls (p263) and less affected females (p221) was also statistically significant. There was no difference in the length of time between litters (Fig. 1C) or in the estrous cycle duration (data not shown). We counted the number of pups in the litters and determined that *Fmr1* KO females had larger litters (Fig. 1D). The average litter size of the first two litters was 7.5 pups for controls and 11 pups for *Fmr1* KO. There was no difference in weight at any age between KO and control females (data not shown) and thus, change in reproductive function does not stem from a difference in weight. Therefore, similar to women with a mutation in the *FMRI* gene, *Fmr1* KO female mice experience early cessation of reproductive function.

To examine if early cessation of reproductive function is due to initially diminished ovarian reserve or to an accelerated loss of follicles, we counted the number

of primordial follicles in pre-pubertal females at 3 weeks of age (p21, Fig. 2A count, and Fig. 2D representative images). Three equal size areas of the ovarian cortex were selected per mouse, primordial follicles counted, and the numbers were averaged for each mouse. There was no difference in the number of primordial follicles between *Fmr1* KO and WT females, indicating that development of the initial pool is not affected by the *Fmr1* loss. The analysis of the number of corpora lutea (CL) in the ovaries at 6 weeks of age (p42) showed that *Fmr1* KO females had over 4 times more corpora lutea than WT controls. *Fmr1* KO had 10.2 average number of corpora lutea per ovary compared to 2.2 corpora lutea per ovary in controls (Fig. 2B count, Fig. 2E representative images). Given that *Fmr1* KO females exhibited early vaginal opening, to confirm that the increase in corpora lutea in KO females does not stem from early puberty, we counted the number of corpora lutea at 9 weeks of age (at p63; Fig. 2C). At p63, an average number of corpora lutea per ovary was significantly higher in *Fmr1* KO females (8.6 corpora lutea) compared to control WT mice (5.4 corpora lutea). Together, these results demonstrate that *Fmr1* KO female mice stop reproducing early, have the same primordial follicle pool, but increased number of corpora lutea corresponding to the larger litter size in young animals, indicating potentially higher recruitment to the growing pool in young animals.

Fmr1 KO females exhibit increased gonadotropin and ovarian hormone levels

Given that ovarian function is regulated by gonadotropin hormones from the pituitary, we analyzed the hormone levels in female mice in diestrus at 9 weeks of age (Fig. 3). LH and FSH levels were significantly higher in diestrus *Fmr1* KO. LH doubled

in KO to 0.84 ng/ml from 0.42 ng/ml in controls. Serum FSH was also higher with 4.2 ng/ml in KO, compared to 2.3 ng/ml in diestrus controls (Fig. 3A). Since LH and FSH β -subunit transcription, that is unique for each hormone, precedes changes in hormone concentration in the circulation, and fluctuations in mRNA levels in the gonadotrope correlate with concentration of the hormones [73], we analyzed pituitary mRNA levels (supplemental Fig.1). Both LH β and FSH β expression was increased in *Fmr1* KO mice, while expression of the common α GSU, GnRH receptor or other pituitary hormones was unchanged. Our results may also indicate that high FSH leads to higher recruitment of follicles in the growing pool, which together with high LH results in more corpora lutea.

Previous studies postulated that ovarian impairment contributed to diminished negative feedback, which in turn caused increased FSH observed in affected women [19, 94]. To address this possibility, we analyzed ovarian hormones that provide feedback to the hypothalamus and pituitary in 8-week-old diestrus females before cessation of reproductive function. Steroid hormones primarily provide feedback to the hypothalamus, while inhibin regulates FSH levels [118-123]. Testosterone was significantly increased in *Fmr1* KO female mice, 279 pg/ml in KO compared to 200 pg/ml in controls (Fig. 3B, T). Progesterone was elevated as well to 3 ng/ml in *Fmr1* KO from 1.7 ng/ml in controls (Fig. 3B, P). We also analyzed inhibin B levels in diestrus females in the circulation, and determined that inhibin B was higher in KO mice, 1.9 ng/ml compared to 1.5 ng/ml in controls (Fig. 3B, Inh B). Our results demonstrate that inhibin B is higher in young animals, which may be a result of larger number of follicles, or alternatively that is stimulated by higher FSH levels. This means that inhibin feedback is present, and can not

explain elevated FSH. Increased steroid hormone levels also demonstrate that negative feedback is present and increased LH cannot be explained by reduced negative feedback. This implicates central mechanisms at the level of the hypothalamus, rather than ovarian insufficiency in the reproductive phenotype of *Fmr1* KO mice. Together, our results demonstrate elevated gonadotropin hormone levels, higher testosterone and progesterone, more corpora lutea, larger litters in young animals, and early cessation of reproductive function.

Ovariectomy reveals hypothalamic and ovarian contribution to endocrine changes

To discern ovarian contribution from the hypothalamic origin of the disorders, we ovariectomized (OVX) the mice and a week later analyzed LH and FSH levels. Over 10-fold higher LH and over 20-fold higher FSH confirmed the successful OVX (compare levels in Fig. 3 and Fig. 4). Interestingly, LH remained significantly higher in OVX KO mice (8 ng/ml) compared to OVX WT mice (6 ng/ml), while there was no difference in FSH levels between WT and *Fmr1* KO females after OVX. Therefore, increased LH in unmodified animals likely stems from central dysregulation, while increased FSH is of ovarian origin. However, since inhibin B and steroid hormones are higher in *Fmr1* KO than in WT, contrary to our expectations, it is not clear how ovaries contribute to increased FSH in KO mice.

Increased innervation and vascularization in the ovaries.

To address seemingly discordant results, where ovariectomy revealed that increased FSH has ovarian contribution while ovarian hormones are increased, we analyzed ovarian vascularization and innervation. Using an endothelial cell marker, CD31 we stained ovarian sections and analyzed vascularization around follicles and corpora lutea. Follicles from WT and *Fmr1* KO had the same degree of vascularization (Fig. 5A, representative image; Fig. 5B, quantification). However, corpora lutea (CL) were more highly vascularized in *Fmr1* KO than in WT mice (Fig. 5C low magnification, top). Higher magnification revealed more abundant and thicker vasculature in the *Fmr1* KO CL (Fig. 5C, bottom, Fig. 5D, quantification).

Although FMRP is expressed at high level in neurons, ovarian innervation was not examined to possibly explain ovarian phenotype observed in *Fmr1* KO mice. Using antibodies to tyrosine hydroxylase, the rate-limiting enzyme of catecholamine synthesis, we counted numbers of neuronal projections that reach the theca layer of growing follicles. Secondary follicles in *Fmr1* KO ovaries had significantly more neuronal fibers than WT follicles; 4.8 average fibers per secondary follicle in KO compared to 2.3 average fibers in WT (Fig. 6A, representative images; Fig 6B quantification). Innervation of CLs was very variable within each animal and between animals, and we did not identify significant differences between WT and KO mice (Fig. 6C bottom left quarter of CL with innervation presented, Fig. 6D, quantification). Together, ovarian histology demonstrated increased vascularization of corpora lutea and increased innervation of secondary follicles in *Fmr1* KO mice.

Altered levels of synaptic molecules in the hypothalamus of *Fmr1* KO mice.

Our results demonstrate elevated LH before and after ovariectomy, which is regulated by GnRH secretion. To address the mechanisms of changed LH, we examined changes in the hypothalamus, first focusing on genome-wide gene expression changes caused by the loss of *Fmr1* gene. Although FMRP is an RNA-binding protein that regulates protein levels of its targets, since FMRP regulates expression of several transcription factors, genome-wide changes in the RNA expression signatures can identify pathogenic pathways that may be indirectly regulated by FMRP. Previous analyses of *Fmr1* KO transcriptomes focused on embryonic hippocampus and cortex, and identified overexpression of immune-related genes and downregulation of genes implicated in behavioral phenotype [124]. For that reason, we used Nanostring neuroinflammation panel, which contains 770 genes implicated in neurological disorders, neuronal injury, neurotransmission, neuron-glia interactions, neuroplasticity, cell integrity, neuroinflammation, and metabolism; and added 30 custom probes for hypothalamic neuropeptides and their receptors. The complete list of genes that changed in KO compared to WT is presented by the heatmap (Fig. 7A). There were 59 gene that were upregulated >120% from WT levels, and 39 genes that were downregulated <80% of WT levels, delineated with a dashed line. Significant changes in expression of neuropeptides and other genes of interest were highlighted in the volcano plot (Fig 7B, log fold change vs. log p-value, statistically significant change in expression indicated with a dashed line; red, upregulated genes in KO compared to WT; green, downregulated gene in KO compared to WT). Immediate early gene, *Egr1*, *Fos* and *Jun*, that are used as

markers of neuronal activation, were upregulated in *Fmr1* KO mice. Genes encoding GABA_A receptor γ 2 subunit, (GABAR γ 2, *Gabrg2*) which is the obligatory subunit of the pentameric GABA_A receptor [125]; and PSD-95 (*Dlg4*), a postsynaptic scaffolding protein anchoring glutamate receptors, were upregulated in KO mice. *Ppfia4*, involved in neurotransmitter release, and *Opalin*, important for oligodendrocyte differentiation, were also upregulated. On the other hand, genes correlated with DNA repair, *Ercc2*; neurodegenerative disorders, *Serpina3n*; hypoxia, *Hif1a*; and apoptosis, *Hcar2* and *Bag4*, were downregulated. Importantly, genes encoding GLAST, *Slc1a3*, and VGLUT2, *Slc17a6*, were also downregulated. Of interest, neuropeptide gene encoding GnRH, *Gnrh*, was upregulated, while genes for kisspeptin, *Kiss1*, and neurokinin B, *Nkb*, *Tac3*; and Cocaine and Amphetamine Regulated Transcript, *Cart*, were downregulated. We confirmed changes in GnRH and kisspeptin expression by qPCR of hypothalamic lysates (Fig. 7C). GO pathway analysis indicated that pathways such as AP1 complex, comprised of Fos and Jun, myelin adaxonal regulation, spine and dendrite development were upregulated, while neuropeptide binding, ubiquitin ligase binding, and receptor signaling pathways were downregulated (Fig. 7D).

Considering changes in excitation/inhibition synaptic balance in the cortical neurons of *Fmr1* KO mice [126], we next investigated the levels of several synaptic proteins involved in regulating GnRH neuronal activity in hypothalamus at the protein level. Although previous studies showed changes in neurotransmitter receptor levels, such as GABA_A receptor for GABA, and NMDA receptor for glutamate, in several brain regions of male *Fmr1* KO mice, no studies were done in females or in the hypothalamus.

Hypothalami were dissected from diestrus female brains, and levels of synaptic molecules were measured by western blotting. We analyzed GABAR γ 2 (GABRG2) levels in the hypothalami of KO and control female mice in diestrus, since GABA transmission activates GnRH neurons, via activation of GABA_A receptor [81, 127], and determined that *Fmr1* KO females had significantly higher levels of GABAR γ 2 GABA_A receptor than controls (Fig. 8A, representative western blots; Fig. 8B quantification). Protein levels correlate with gene expression analysis, indicating that GABAR γ 2 may be indirectly regulated by *Fmrp*. We then analyzed levels of the glutamatergic NMDA receptors (NMDARs, or NRs) [128, 129], since 30-50% of GnRH neurons respond to NMDA [130, 131]. NR1 is an obligatory subunit that forms a heterotetramer with either 2A or 2B subunits (other isoforms are less frequent). We determined that NR1 (NMDAR1, GluN1) levels were increased in the hypothalami of KO mice compared to controls (Fig. 8D). Depending on the NR2 isoform, NMDAR is localized at synapses or extrasynaptically with different effects on long-term potentiation or negative feedback, respectively [112, 132]. NR2B is localized extrasynaptically, and we determined that the levels of NR2B are lower in the KO mice compared to controls (Fig. 8E). Genes encoding these proteins did not change at the transcriptional level, which indicates that they may be regulated by *Fmrp* at the protein level. We also analyzed levels of PSD-95, since GnRH neurons express PSD-95 [133], and determined that PSD-95 protein levels were the same in *Fmr1* KO and controls, which is contrary to gene expression studies and again points to direct regulation by *Fmrp* (Fig. 8C). Taken together, an increase in the

synaptic GABA_A and NR1 receptors, and a decrease in extrasynaptic NR2B, likely contributes to altered activity of hypothalamic neurons in *Fmr1* KO female mice.

Lack of FMRP changes GnRH neuron connectivity

To determine if FMRP loss alters neurotransmitter receptor levels specifically in GnRH neurons, we first confirmed that 82% of GnRH neurons express FMRP protein (Fig. 9A, left image, confocal microscopy, right image, 3D reconstruction to demonstrate FMRP inside GnRH neurons). Antibody specificity was determined by staining the hypothalami from *Fmr1* KO mice (not shown). We also analyzed GnRH neuron number in *Fmr1* KO mice to compare to WT to ascertain if increased in GnRH neuron number contributes to higher LH. There was no difference in the number of GnRH neurons in WT and KO mice (not shown).

Since GABA is critical for GnRH function [81, 127], and we determined elevated GABA γ 2 subunit of the GABA_A receptor in the hypothalami of KO mice compared to controls by western blot, we analyzed if GABA_A receptor immunoreactivity is increased specifically in GnRH neurons. To determine GABA_A receptor distribution in GnRH neurons, we immunostained 100 μ m coronal sections of the preoptic area of the hypothalamus for GABA γ 2 and GnRH. After staining, sections were imaged with high-resolution confocal microscopy. GABA γ 2 receptors showed puncta-like distribution in GnRH neurons. GABA γ 2 receptor puncta colocalized with GnRH immunoreactivity were identified by closely apposed puncta when no black pixels were visible between two signals in optical slices, and counted blind to condition by scrolling through the series of

captured z-stack images for each GnRH soma and along the process, at 15- μ m intervals, for each GnRH neuron. At least 15 neurons were counted from each mouse, and the average for each mouse was calculated (represented by a dot in the Fig. 9C with bars representing group average). We determined that GABA α 2 puncta numbers increased significantly in the GnRH neuron soma and in the first 15 μ m of the process proximal to the soma (Fig. 9C quantification, Fig 9B, representative images, top WT, bottom *Fmr1* KO). The increase in GABAergic inputs in this area is significant, since this region of the neuron is the region where action potentials are initiated [134], and it exhibits synaptic plasticity during development and in different hormonal milieu [135-137]. Since GABA is excitatory for GnRH neurons [75, 81-83], the alteration of the receptor levels may enhance GnRH neuron responsiveness and neuropeptide secretion, which in turn would cause changes in gonadotropin secretion.

To determine GnRH innervation, we also analyzed appositions of GABA α 2 subunit of the GABA_A receptor with vesicular GABA transporter (VGAT), presynaptic marker of GABAergic terminals. We performed a triple stain for GnRH, GABA α 2 and VGAT, and as above, counted number of puncta where VGAT was in a close opposition to GABA α 2 in GnRH neurons (Fig. 10A). We counted at least 15-20 neurons from each mouse, 5 pairs of mice; and used Imaris software to perform 3-D modeling of VGAT-GABA_A receptor appositions (Fig. 10B). *Fmr1* KO mice had a higher number of GABAergic appositions in GnRH neuron soma and proximal process, in the segment 1-15 μ m and segment 16-30 μ m from the soma, than WT controls (Fig. 10C). The

increase in synaptic GABA_A receptors in the proximal process indicates higher innervation of GnRH neurons in the area that is plastic and receives synaptic input.

FMRP regulates LH pulsatility

Pulsatile secretion of LH strictly corresponds to GnRH secretion [102, 103]. LH is used as an indicator of GnRH secretion, since GnRH secretion into median eminence cannot be measured in mice. To ascertain whether GnRH neuron secretion was affected, we measured LH pulses and used an ultrasensitive ELISA assay for LH [104] that allows for LH measurement in 5 µl of whole blood. Mice were acclimated for 2 weeks by daily tail massage. Serial sample collection every 8 min for 3 hours from the tail vein was performed [98, 105]. Representative LH pulse profile from unmodified WT and KO mice are presented in Fig 11A, right side (WT control, top; *Fmr1* KO, bottom). Number of LH pulses per 2.5 hours of measurement were determined using DynPeak algorithm and compared between genotypes. LH, and therefore GnRH, pulse frequency was significantly higher in *Fmr1* KO mice compared to WT controls (Fig. 11A, left side). Amplitude was determined by subtracting the highest LH value from the basal value prior to the onset of the pulse and averaged for each mouse (Fig. 11A, middle).

Pulsatile LH analyses were performed using ovariectomized animals as well. Frequency of LH secretion was faster in OVX *Fmr1* KO animals compared to OVX WT mice (Fig. 11B, left; representative profiles right), while pulse amplitude was the same. Representative pulse profiles are shown on the right side. These experiments determined that the lack FMRP increased LH pulse frequency, indicating higher GnRH neuron

activity corresponding to higher GABAergic innervation of GnRH neuron. It is possible the lack of FMRP alters GnRH neuropeptide secretion leading to the faster GnRH pulse frequency and elevated LH, which contributes to ovarian dysregulation in young animals.

2.5 Discussion

We sought out to uncover the effects of FMRP loss on hypothalamic GnRH neurons and ovarian function, which may help elucidate the mechanisms of early cessation of reproductive function in females with a mutation in the *FMRI* gene. Women with *FMRI* mutations comprise the majority of known genetic causes of premature ovarian failure [59, 89, 138]. Premature ovarian failure or primary ovarian insufficiency is the most extreme manifestation of premature ovarian senescence and affects about 1% of women [1]. Premature reproductive senescence affects approximately 10% of women and is characterized by an early depletion of ovarian follicles [1]. Molecular causes of premature cessation of reproductive function in women with *FMRI* mutations and mechanisms underlying reproductive dysfunctions are still unknown. The hypothalamus was especially neglected in previous studies addressing *FMRI* function, or etiology of premature reproductive senescence. Our study is the first to examine the hypothalamic function of the *FMRI* gene. We analyzed mechanisms of reproductive disorders associated with *FMRI* mutations using the *Fmr1* KO female mice, since knockout mice lack Fmrp mimicking the loss of FMRP in humans with *FMRI* mutation. *Fmr1* KO female mice is a useful model to study reproductive disorders in women with a mutation in the *FMRI* gene, as they exhibit early cessation of reproductive function similar to

women with *FMRI* mutations. The main findings of this study implicate central mechanisms and ovarian innervation in reproductive disorders associated with the FMRP loss. We demonstrate that *Fmr1* KO female mice show higher GnRH neuron and ovarian follicle innervation, increased GnRH neuron activity, and augmented gonadotropin levels, all of which may contribute to increased recruitment of ovarian follicles to the growing pool, corresponding to a higher number of corpora lutea and larger litters in young animals. Together, our results point to hypothalamic mechanisms, specifically GnRH neuron connectivity, and ovarian innervation in the reproductive disorders associated with FMRP loss that have not been considered before.

Women with early menopause face not only infertility, but an increased risk of heart disease and osteoporosis [139-143]. Most women are only diagnosed after their ovarian function has ceased, since they seek care due to infertility or amenorrhea. In that case, it is difficult to predict earlier hormonal changes, when ovarian reserves are relatively normal. As of yet, there are no screening strategies to detect women with increased risk before they are symptomatic [144]. Most studies analyzing a role of FMRP have focused on males, while females are rarely included. Furthermore, cortical mechanisms attracted the attention of the investigators, because FXS is the most common monogenic cause of intellectual disability and autism. However, the mechanism underlying the dysregulation of reproductive function in *FMRI* mutations was not extensively studied. Several reports demonstrate elevated FSH in women affected with *FMRI* mutations showing early menopause [19, 94], which are consistent with our observations in mice. Since the primary reproductive defect in females with *FMRI*

mutation is premature ovarian failure, gonadal origin was proposed. We demonstrate that primordial follicle number is unaffected by *Fmr1* loss, which agrees with previous studies that showed that women with *FMRI* mutation and mouse models of premutation have normal pool of primordial follicles [86, 92, 93, 117]. This indicates that early ovarian development is not adversely affected by the loss of FMRP. Our results using complete KO model show larger litters and more corporal lutea, while premutation mouse models have smaller litters [24, 86], but reasons for differences are not clear. Our results do not preclude other intra-ovarian defects that may contribute to the early loss of follicles and early depletion, such as increased atresia as suggested in [24]. Given that there is no difference in primordial follicle development, inappropriate ovarian response to gonadotropin stimulation, compounded by changes in gonadotropin levels, likely contributes to early cessation of reproductive function in *FMRI* mutations.

Removal of ovaries demonstrated that increased FSH depends on ovarian feedback. However, the increase in FSH is not a result of the lack of negative feedback as we show that in females, ovarian hormones, inhibin or steroid hormones, are higher than in controls, indicating that hormonal feedback to the pituitary and hypothalamus was present. Studies in women with *FMR1* mutations are inconclusive, with one study reporting unchanged inhibin [62], while the other found decreased inhibin [19]. The latter study is the only one, to our knowledge, that analyzed steroid hormone levels and found decreased progesterone [19]. The discrepancy may arise due to the age of the subjects, as discussed above. Increase in inhibin B levels in our results, implies that higher FSH

occurs irrespective of inhibin feedback, in fact, may lead to increased inhibin, and thus, may be the cause rather than the consequence of reproductive disorders.

Since ovarian hormones did not provide adequate explanation, we examined ovarian innervation and vascularization, and detected increased vascularization of corpora lutea which may correlate with higher progesterone levels [145]. Increased progesterone may lead to higher FSH [146, 147]. Fluorescent studies with endothelial cells marker reveal that large follicle vascularization is not changed, but corpora lutea exhibit increased vascularization. Developing corpus luteum is a site of rapid angiogenesis, under the influence of the vascular endothelial growth factor (VEGF) [145, 148, 149]. Studies in several species determined that angiogenesis and VEGF induction is stimulated by LH [150-152]. Thus, increased LH in our study likely contributes to increased vascularization of the corpus luteum. Treatment with VEGF antagonist demonstrated decreased progesterone [153]. Therefore, increased progesterone in *Fmr1* KO mice we report here may be due to increased vascularization of corpora lutea. Several studies determined that progesterone could increase FSH at the transcriptional level, which is thought to be important for the specific secondary rise of FSH during luteal phase. Progesterone treatment in combination with estrogen, increased FSH, while antiprogestins blocked FSH secretion and mRNA expression during the preovulatory surge [154] and during the secondary rise [155]. Therefore, our studies postulate that increased LH may cause increased angiogenesis during luteinization, which leads to higher progesterone, which in turn increase FSH, and may explain why increased LH is of hypothalamic origin, while increased FSH requires ovaries.

Ovaries receive sympathetic innervation via two routes [156-158]. The superior ovarian nerve projections innervate the secretory component of the ovary. The fibers surround the developing follicles, but do not penetrate the granulosa layer or the corpus luteum. We determined that innervation of the follicles with fibers that originate from the superior ovarian nerve is increased. This innervation is required for steroidogenesis, since transection of the nerve reduced steroid hormone levels [159-161]. Thus, higher steroid hormone levels may be a result of increased innervation. As discussed above, this may contribute to higher FSH levels in KO animals.

Increased LH likely stems from higher GnRH secretion, via increased GnRH pulse frequency, since GnRH from the hypothalamus strictly regulates LH secretion. We determined that GnRH neurons have increased GABAergic innervation, which is excitatory for GnRH neurons [75, 81-83]. Therefore, it is possible that increased GABA tone leads to altered responsiveness of GnRH neurons to the pulse generator and the upstream regulatory network. Alternatively, constantly increased GABA input may lead to increased activity of GnRH neurons. The idea of enhanced activation of GnRH neurons is also supported by the observed increases in neurotransmitter receptor levels in the hypothalamus and specifically GnRH neurons. FMRP binds mRNAs that encode synaptic proteins [64-66] and previous studies reported altered levels of GABA_A receptors and NMDA receptors in several brain areas. Contrary to the studies in the cortex and hippocampus, we determined that GABA_A receptor levels are increased in the hypothalamus at the mRNA and protein levels. 30%-50% of GnRH neurons respond to NMDA [130, 131], and our studies in the hypothalamus agree with previous studies in

the cortex that demonstrate increased NMDA receptors in *Fmr1* KO mice. Therefore, the increase in NMDA and GABA receptors, that are both excitatory for GnRH neurons, likely changes GnRH neuron function and GnRH neuropeptide secretion.

Therefore, both the hypothalamus and ovaries contribute to endocrine disruption that may lead to larger litters in young animals. Hypothalamic contribution to the etiology of early menopause has been underappreciated. We propose that changes in GnRH neuron and ovarian innervation contribute to changes in gonadotropin hormones, FSH and LH, levels. This may cause early depletion of ovarian follicles and premature cessation of reproductive function, which will be addressed in future studies. Together, our results point to hypothalamic mechanisms and ovarian innervation in the reproductive function disorders associated with FMRP loss that have not been considered before.

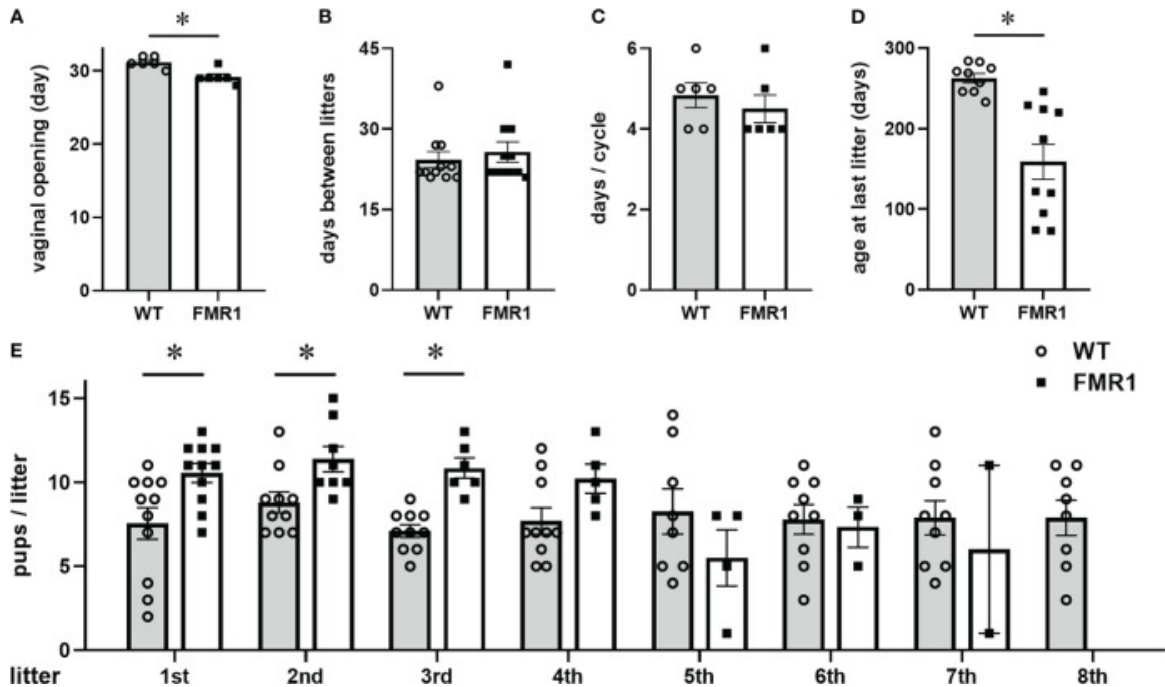


Figure 2.1. *Fmr1* knockout (KO) females stop reproducing early. A, *Fmr1* KO females (*FMR1*, white bars represent group mean \pm standard error, and each black square represents one animal) experience early vaginal opening, an external sign of puberty, at postnatal day (p) 29, compared to wild type controls at p31 (WT, gray bars represent mean \pm standard error, open circles represent each animal); B, *Fmr1* KO females have litters at the same rate as WT controls; C, No difference in the length of the estrous cycle; D, Determined by the age at the last litter, *Fmr1* KO females stop reproducing early at p163, compared to WT controls at p263; Each point represents one animal, and bars represent group means \pm standard error. Statistical significance (*, $p < 0.05$) was determined with t-test followed by Tukey's post hoc test. E, *Fmr1* KO females have more pups per litter in the first 3 litters. Each point represents one litter with number of pups in 1st – 8th litter indicated, and bars represent group means \pm standard error.

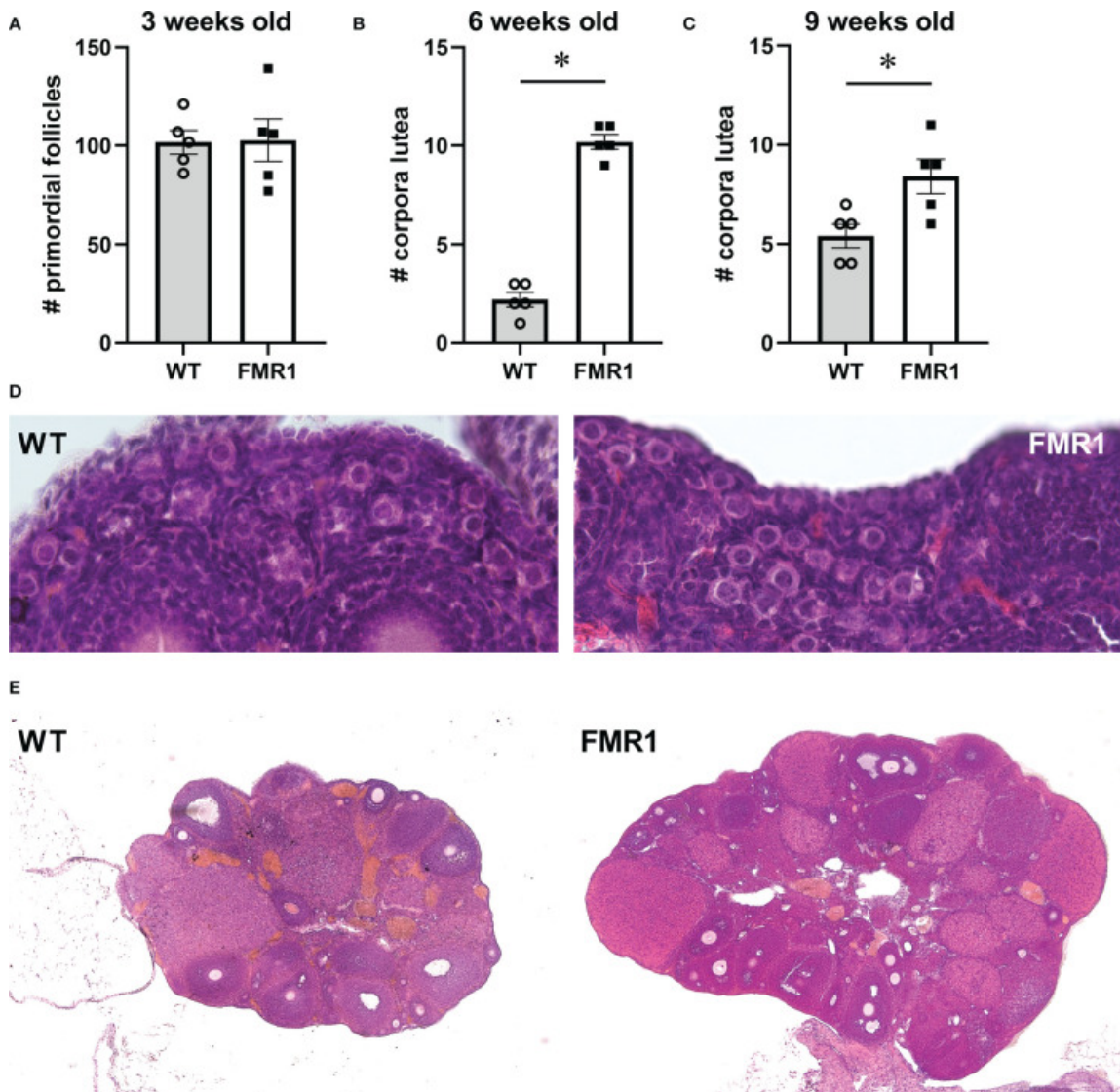


Figure 2.2. Ovarian histology demonstrates more corpora lutea in young *Fmr1* KO mice. *Fmr1* KO females (*FMR1*, white bars represent group mean \pm standard error while each black square represents one animal) were compared to wild type controls (WT, gray bars represent mean \pm standard error, each open circle represents one animal). A, Primordial follicles were counted at 3 weeks of age. Each point represents one mouse, and an average of 4 separate $1 \times 10^{-8} \text{ m}^2$ areas in the ovary cortex of each mouse. B-C, corpora lutea were counted at 6 (B) and 9 weeks of age (C) throughout each ovary. D, representative images of ovaries from 3-week old mice to observe primordial follicles (63x). E, representative images of ovaries at 6 weeks of age to observe numbers of corpora lutea (40x). Statistical significance, indicated with * ($p < 0.05$) was determined with t-test followed by Tukey's post hoc test.

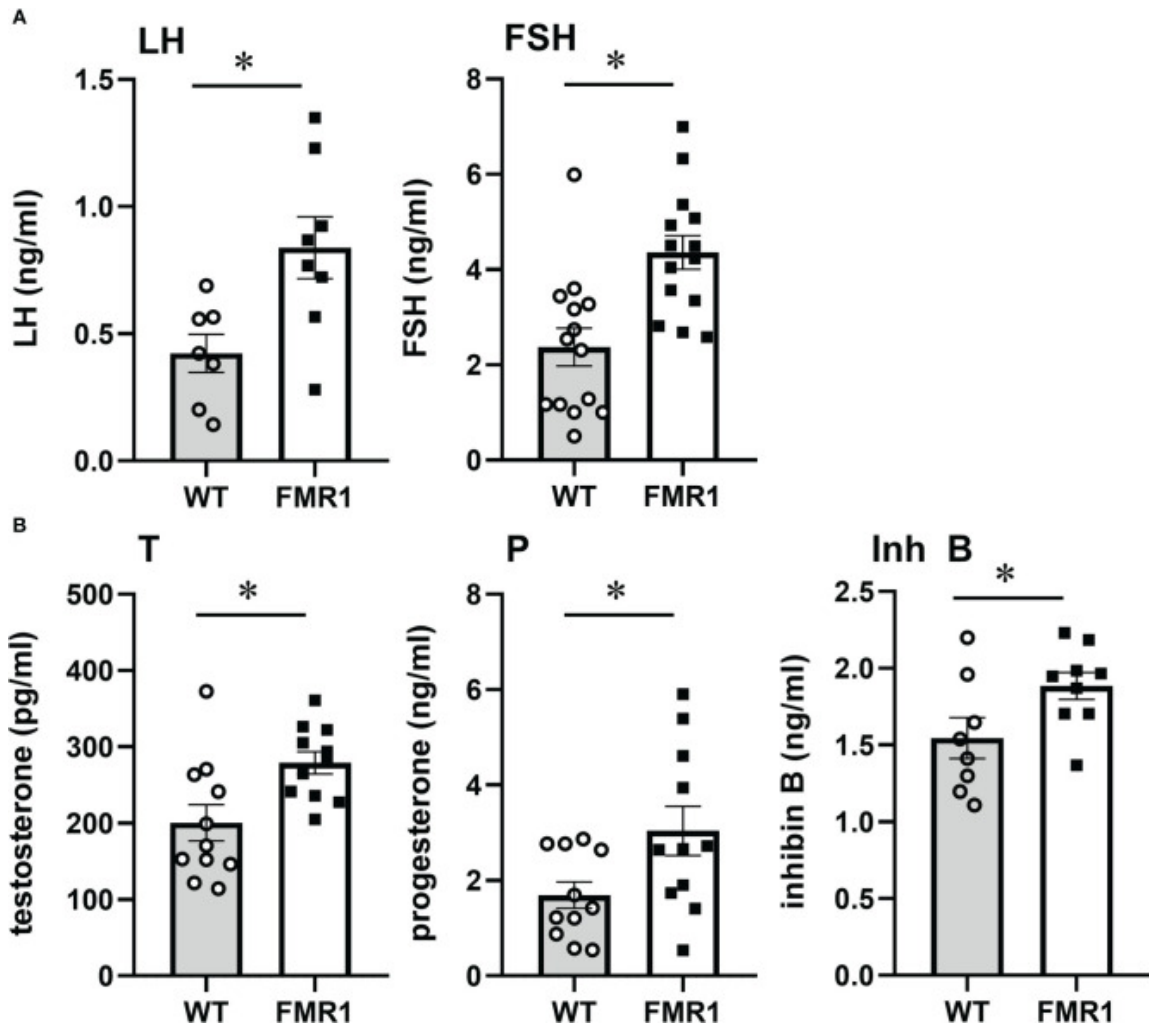


Figure 2.3. *Fmr1* KO mice have higher LH and FSH. Serum levels of LH and FSH, testosterone (T), progesterone (P) and inhibin B (Inh B) in diestrus females in WT controls and *Fmr1* KO. Each point represents one animal, while bars represent group means \pm standard error. LH was sampled from the tail tip after acclimatization to handling, to minimize stress and prevent exposure to isoflurane that may affect LH levels. FSH, T, P, Inh B samples are obtained from inferior vena cava. Statistical significance, indicated with a * ($p < 0.05$) was determined with t-test followed by Tukey's post hoc test.

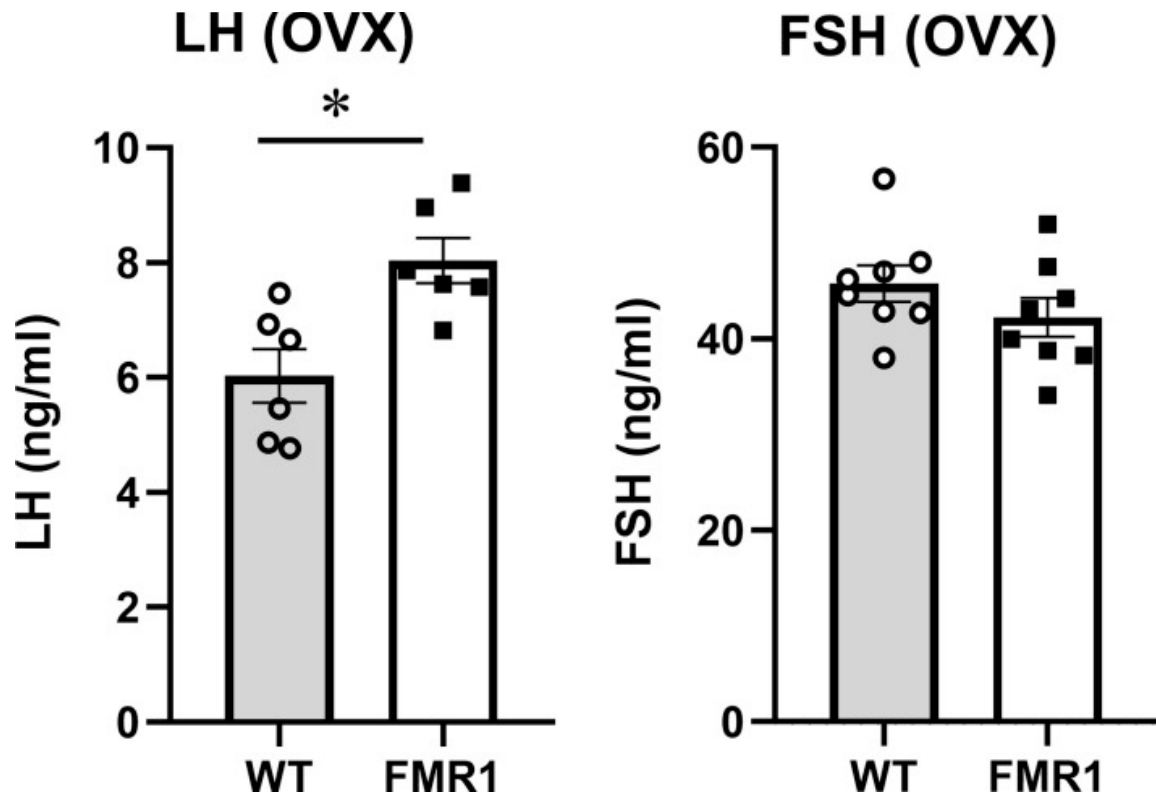


Figure 2.4. Ovariectomized *Fmr1* KO mice have higher LH. One week after ovariectomy, LH and FSH samples were collected as in Fig. 3. Each point represents one animal, while bars represent group means \pm standard error. Statistical significance, indicated with a * ($p < 0.05$) was determined with t-test followed by Tukey's post hoc test.

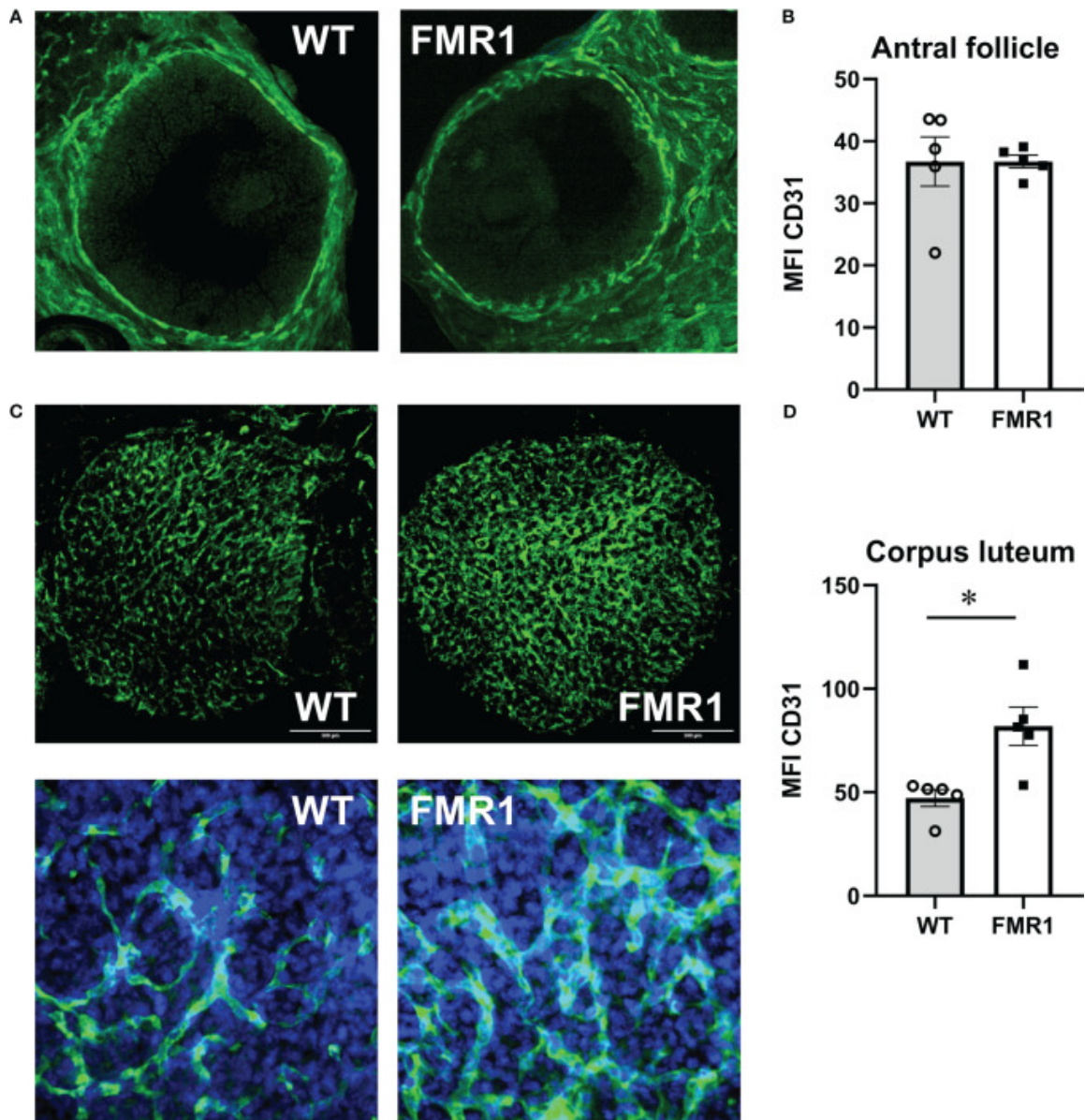


Figure 2.5. *Fmr1* KO have increased corpus luteum vascularization. Ovaries were sectioned and stained with antibodies to CD31 (PECAM-1, Platelet endothelial cell adhesion molecule) to visualize vascularity. Mean fluorescent intensity (MFI) was determined using Fiji imageJ. Consistent areas were used to quantify fluorescence intensity. A, Representative images of antral follicles. B, MFI quantification. C, Corpora lutea representative images; top, 1.6 mm x 1.6 mm area, CD31 green; bottom, 300 μm x 300 μm area, CD31, green, DAPI, blue. D, MFI quantification. Statistical significance, indicated with a * (p < 0.05) was determined with t-test followed by Tukey's post hoc test.

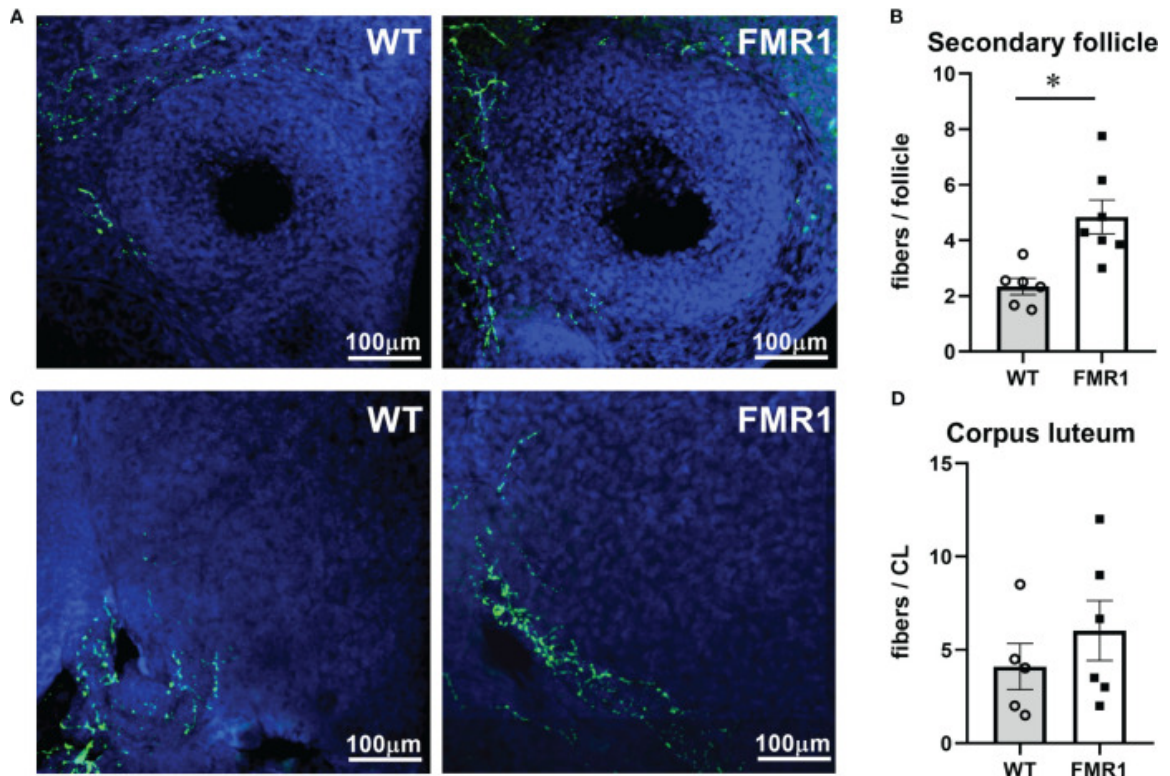


Figure 2.6. *Fmr1* KO have higher innervation of growing follicles. Ovaries were sectioned and stained with antibodies to tyrosine hydroxylase (TH, green) to visualize innervation around secondary follicles (A) and corpora lutea (C). Fibers that surround the follicles and penetrate theca layer were counted (B, D).

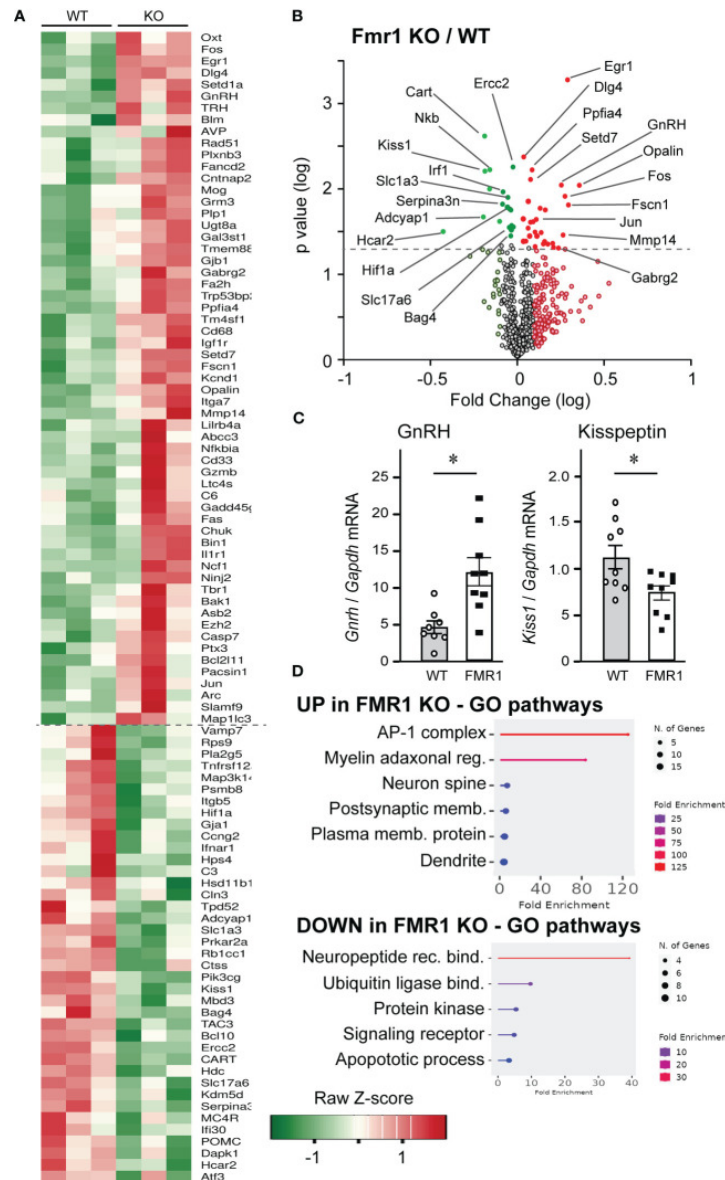


Figure 2.7. Nanostring analysis demonstrates significant changes in hypothalamic gene expression in *Fmr1* KO mice. A, Hypothalami from 3 mice per group were dissected and 50 ng RNA used in Nanostring analysis. Heatmap indicates gene expression changes in *Fmr1* KO hypothalami that are <0.8-fold and >1.2-fold over WT. B, Data were plotted as log fold change on x-axis vs. log p value on y-axis, and dashed line indicates significance. Red indicates genes that are increased in KO compared to WT mice, while green indicates genes that are decreased in KO compared to WT. Genes below the dotted line, light red and light green did not reach significance. C, qPCR of the hypothalamus confirms changes in GnRH and kisspeptin expression. Each point represents one animal and bars represent group average. Statistical significance is indicated with *, determined by t-test followed by Tukey's post hoc test. D, Gene ontology pathway analysis indicates upregulated (top) and downregulated (bottom) pathways in the *Fmr1* KO mice.

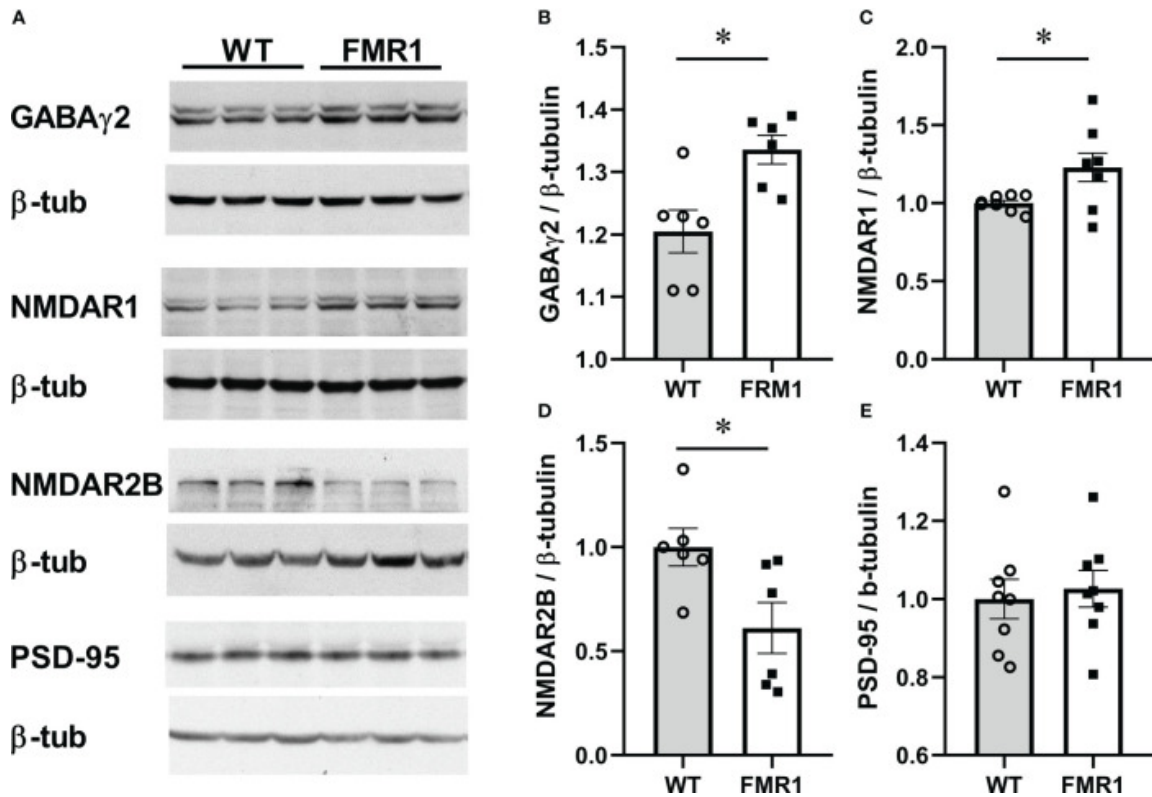


Figure 2.8. *Fmr1* KO females have higher levels of the obligatory GABA_A receptor subunit in hypothalami. Hypothalami were dissected and protein levels analyzed by western blotting. Representative blots are shown in (A). Protein levels from 6 mice per group were quantified using Chemidoc and levels of neuronal proteins normalized to β -tubulin (B). Statistical significance ($p < 0.05$), determined with t-test followed by Tukey's post hoc test, is indicated with a *.

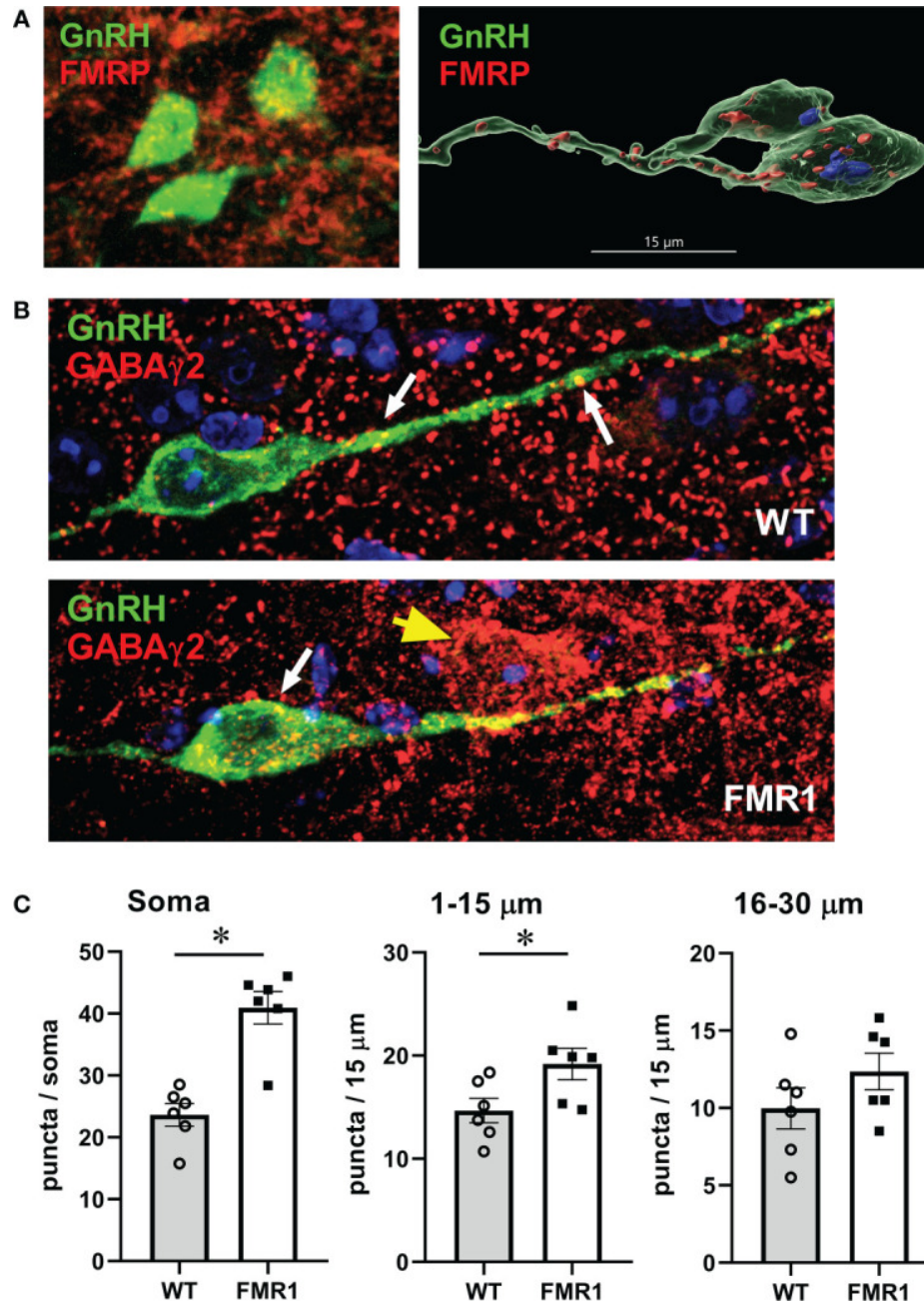


Figure 2.9. GnRH neurons of *Fmr1* KO females have more GABA_A receptors. A, GnRH neurons (green) express *Fmrp* (red, top panels). B, Representative GnRH neurons (green) from WT control (top panel) and *Fmr1* KO mice (bottom panel) co-stained with GABA γ 2 antibody (red). C, Quantification of B. Each point represents one animal and an average of 15-20 neuron per animal, and bars represent group means. Panels represent counts in the whole soma, along the first 15 μ m segment of the process (1-15 μ m) and second 15 μ m segment (16-30 μ m) from the soma, as indicated above. Statistical significance ($p < 0.05$), determined with t-test followed by Tukey's post hoc test, is indicated with a *.

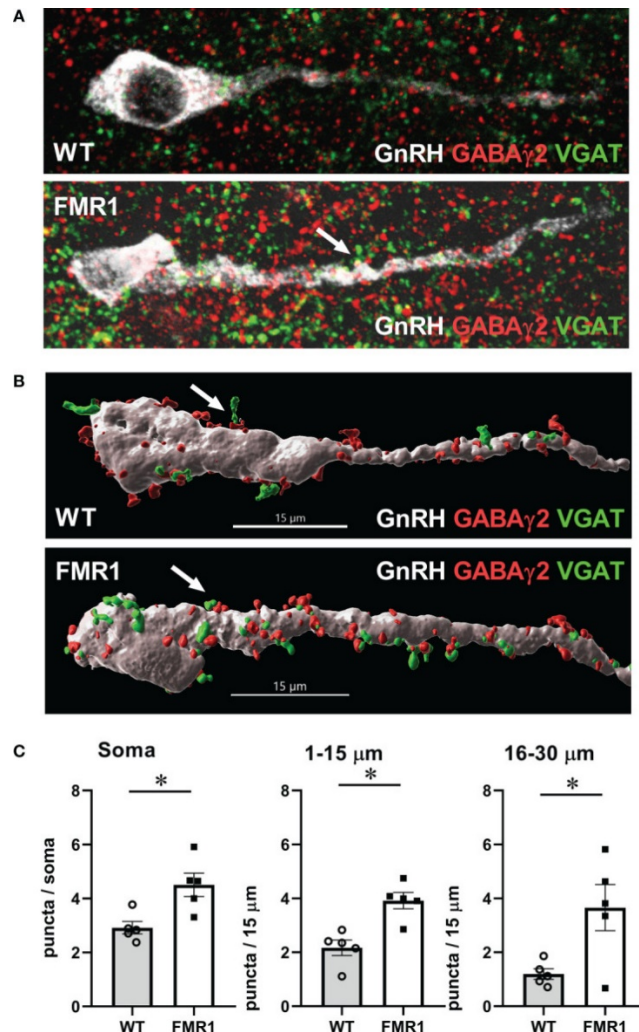


Figure 2.10. GnRH neurons of *Fmr1* KO females have more synaptic GABA_A receptors. A, Representative images of triple stain for presynaptic VGAT (green), GABA γ 2 receptor (red) and GnRH (white); B, 3-D GnRH neuron models using Imaris software. VGAT (green) appositions to GABA γ 2 receptor subunits (red) in GnRH neurons (white) were counted in 15-20 neurons per mouse, five mice from each group. C, Quantification from different regions of the neuron, as above, is presented in panels, and significance indicated with *.

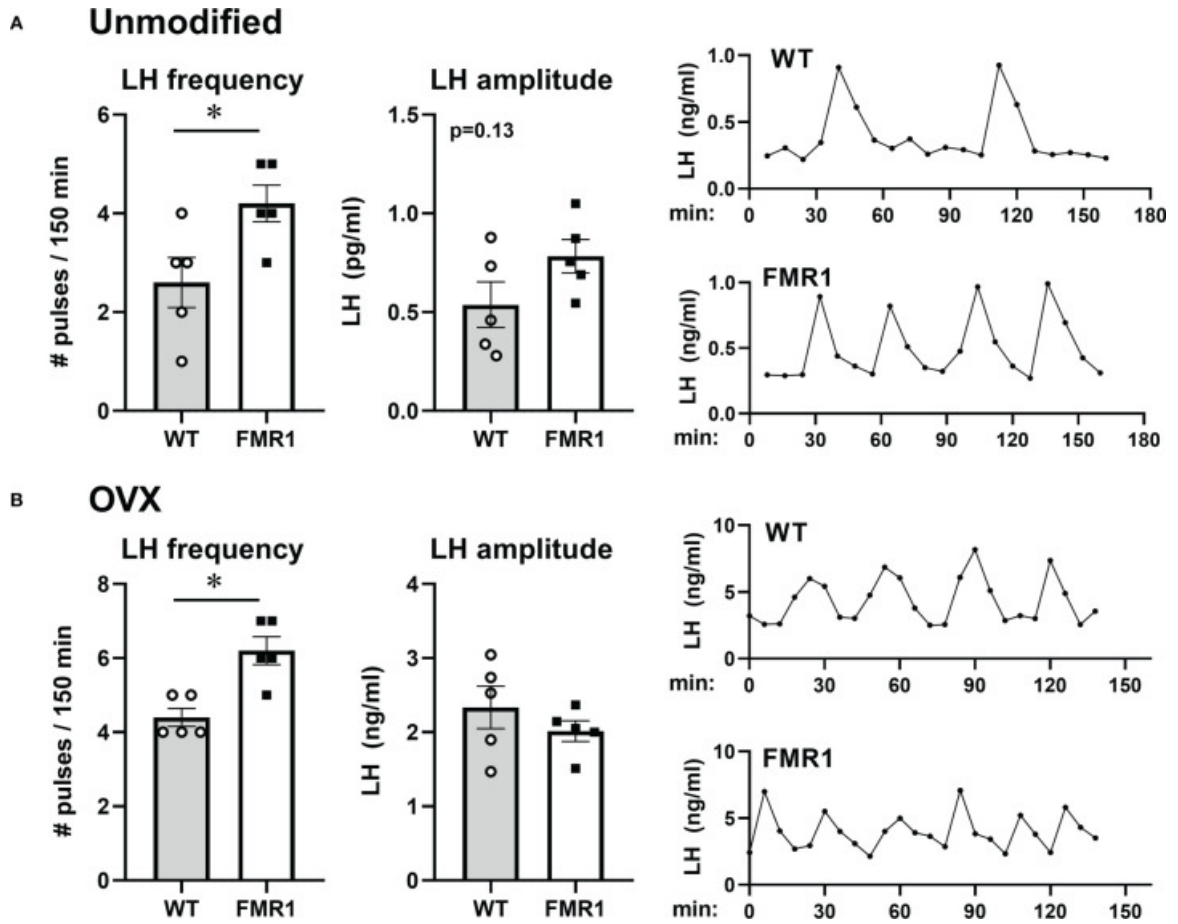


Figure 2.11. Higher LH / GnRH pulse frequency in *Fmr1* KO females before and after ovariectomy. LH pulse frequency reflects GnRH neuron activity. A, Frequent tail-tip whole blood sampling over 3 hours demonstrate higher pulse frequency of LH in *Fmr1* KO female mice in diestrus. Representative profiles from WT control in the top and *Fmr1* KO at the bottom (right side), pulse frequency calculated from pulse profiles using DynPeak (left); amplitude was determined by subtracting the LH value at the peak from the basal value prior to the onset of the pulse and averaged for each mouse (middle). B, LH pulse in ovariectomized (OVX) animals. Statistical significance ($p < 0.05$), determined with t-test followed by Tukey's post hoc test, is indicated with a *.

Supplemental:

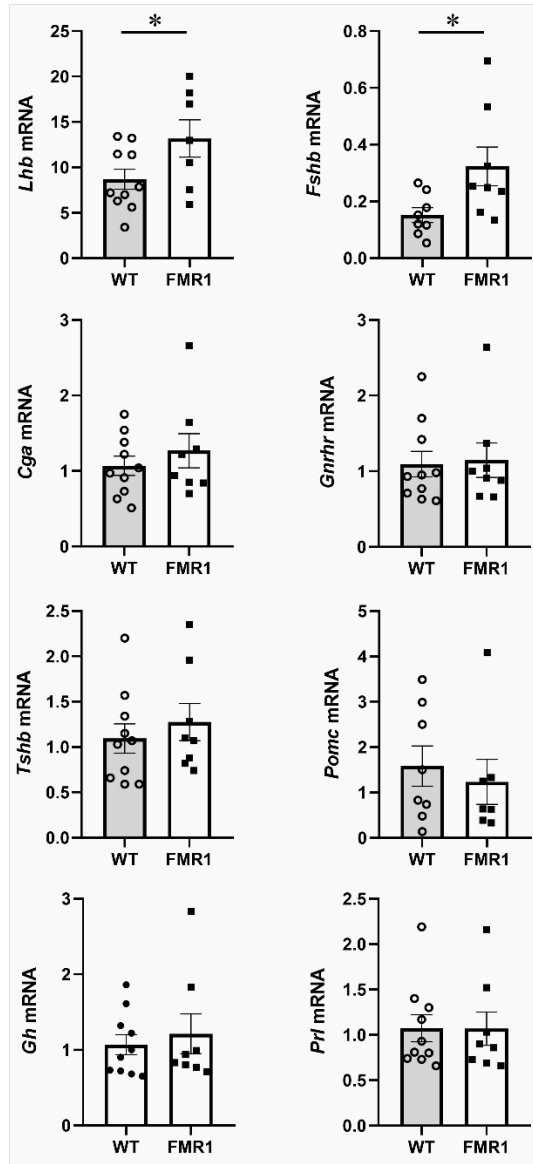


Figure S1. *Fmr1* KO females have higher LHb and FSHb mRNA expression. Pituitary mRNA was analyzed by RT-qPCR to determine the expression of pituitary hormones. LHb and FSHb are increased, while expression of other hormones is unchanged. Each point represents one animal, while bars represent group means. mRNA levels were normalized to B2M mRNA. Statistical significance ($p < 0.05$), determined with t-test followed by Tukey's post hoc test, is indicated with a *.

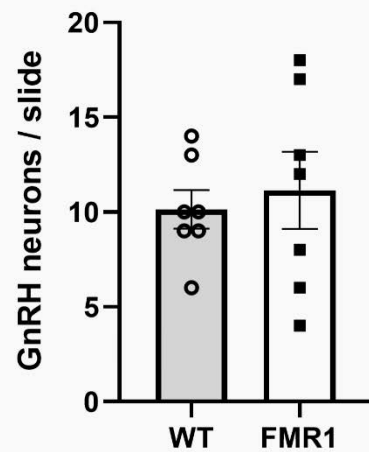
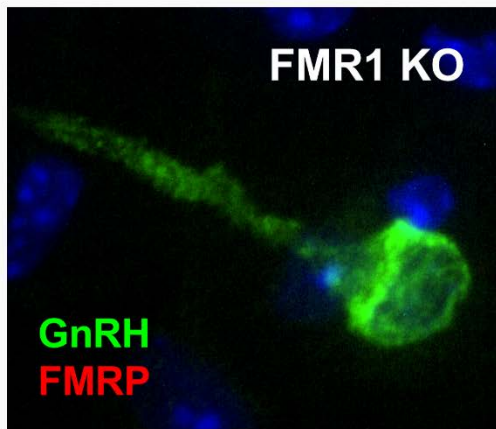


Figure S2. Left, Specificity of antibody to FMRP is determined by staining hypothalamic sections from *Fmr1* KO mice. Right, Every 5th coronal section containing the preoptic area of the hypothalami from WT and *Fmr1* KO female mice were stained with anti-GnRH antibodies and GnRH neurons counted. Each point represents average number of neurons from all counted sections for one animal, while bars represent group means.

References for Chapter Two

1. Kiss, J., et al., *Evidence for vesicular glutamate transporter synapses onto gonadotropin-releasing hormone and other neurons in the rat medial preoptic area*. Eur J Neurosci, 2003. 18(12): p. 3267-78.
2. Bailey, J.D., A. Centers, and L. Jennes, *Expression of AMPA receptor subunits (GluR1-GluR4) in gonadotrophin-releasing hormone neurones of young and middle-aged persistently oestrous rats during the steroid-induced luteinising hormone surge*. J Neuroendocrinol, 2006. 18(1): p. 1-12.
3. Eyigor, O. and L. Jennes, *Kainate receptor subunit-positive gonadotropin-releasing hormone neurons express c-Fos during the steroid-induced luteinizing hormone surge in the female rat*. Endocrinology, 2000. 141(2): p. 779-86.
4. Rula Abbud *'~, M.S.S., *Do GnRH neurons express the gene for the NMDA receptor?* Brain Research, 1995: p. 117-120.
5. Jermes, O.E.L., *Expression of glutamate receptor subunit mRNAs in gonadotropin-releasing hormone neurons during the sexual maturation of the female rat*. Neuroendocrinology, 1997.
6. Smyth, C. and M. Wilkinson, *A critical period for glutamate receptor-mediated induction of precocious puberty in female rats*. J Neuroendocrinol, 1994. 6(3): p. 275-84.
7. Mahachoklertwattana, P., et al., *N-methyl-D-aspartate (NMDA) receptors mediate the release of gonadotropin-releasing hormone (GnRH) by NMDA in a hypothalamic GnRH neuronal cell line (GT1-1)*. Endocrinology, 1994. 134(3): p. 1023-30.
8. Raymond Dingleline, K.B., Derek Bowie and Stephen F. Traynelis, *The Glutamate Receptor Ion Channels*. Pharmacological Reviews, 1999. 51 p. 7-62.
9. Furukawa, H., et al., *Subunit arrangement and function in NMDA receptors*. Nature, 2005. 438(7065): p. 185-92.
10. G.L. Westbrook, J.D.C., *Activation Kinetics Reveal the Number of Glutamate and Glycine Binding Sites on the N-Methyl-BAspartate Receptor*. Neuron, 1991. 7: p. 605-613.
11. Wu, Q.J. and M. Tymianski, *Targeting NMDA receptors in stroke: new hope in neuroprotection*. Mol Brain, 2018. 11(1): p. 15.

12. Frank, R.A., et al., *NMDA receptors are selectively partitioned into complexes and supercomplexes during synapse maturation*. *Nat Commun*, 2016. 7: p. 11264.
13. Kim, E. and M. Sheng, *PDZ domain proteins of synapses*. *Nat Rev Neurosci*, 2004. 5(10): p. 771-81.
14. Lundbye, C.J., A.K.H. Toft, and T.G. Banke, *Inhibition of GluN2A NMDA receptors ameliorates synaptic plasticity deficits in the Fmr1(-/y) mouse model*. *J Physiol*, 2018. 596(20): p. 5017-5031.
15. Eadie, B.D., et al., *NMDA receptor hypofunction in the dentate gyrus and impaired context discrimination in adult Fmr1 knockout mice*. *Hippocampus*, 2012. 22(2): p. 241-54.
16. Whiting, P.J., *GABA-A receptor subtypes in the brain: a paradigm for CNS drug discovery?* *Drug Discovery Today*, 2003. 8(10): p. 445-450.
17. David Nutt, D.M., *GABAA Receptors- Subtypes, Regional Distribution, and Function*. *Journal of clinical sleep medicine*, 2006. 2.
18. Christopher N. Connolly, B.J.K., Bernard J. McDonald, Trevor G. Smart‡, and Stephen J. Moss, *Assembly and Cell Surface Expression of Heteromeric and Homomeric γ -Aminobutyric Acid Type A Receptors*. *Journal of Biological Chemistry*, 1995. 271(1): p. 89-96.
19. NISTR1, L.S.a.A., *GABA RECEPTOR MECHANISMS IN THE CENTRAL NERVOUS SYSTEM*. *Progress in Neurobiology*, 1991. 36: p. 35-92.
20. Chen, K., et al., *Role of GABAB receptors in GABA and baclofen-induced inhibition of adult rat cerebellar interpositus nucleus neurons in vitro*. *Brain Res Bull*, 2005. 67(4): p. 310-8.
21. Messenger, S., et al., *Kisspeptin directly stimulates gonadotropin-releasing hormone release via G protein-coupled receptor 54*. *Proc Natl Acad Sci U S A*, 2005. 102(5): p. 1761-6.
22. d'Anglemont de Tassigny, X. and W.H. Colledge, *The role of kisspeptin signaling in reproduction*. *Physiology (Bethesda)*, 2010. 25(4): p. 207-17.
23. Moenter, J.P.-F.a.S.M., *Kisspeptin Increases γ -Aminobutyric Acidergic and Glutamatergic Transmission Directly to Gonadotropi*. *Endocrinology*, 2010.
24. Franceschini, I., et al., *Kisspeptin immunoreactive cells of the ovine preoptic area and arcuate nucleus co-express estrogen receptor alpha*. *Neurosci Lett*, 2006. 401(3): p. 225-30.

25. Foradori, C.D., et al., *Colocalization of progesterone receptors in parvicellular dynorphin neurons of the ovine preoptic area and hypothalamus*. *Endocrinology*, 2002. 143(11): p. 4366-74.
26. I. Kallo, E.H.P.C.B.V.M.C.H.E.K.A.C.S.R.B.M.A.G.W.S.D.Z.L., *The kisspeptin system of the human hypothalamus: sexual dimorphism and relationship with gonadotropin releasing hormone and neurokinin B neurons*. *European Journal of Neuroscience*, 2010. 31(11).
27. Dahl, S.K., et al., *Dynorphin immunoreactive fibers contact GnRH neurons in the human hypothalamus*. *Reprod Sci*, 2009. 16(8): p. 781-7.
28. Michael N. Lehman, L.M.C., and Robert L. Goodman, *Minireview: Kisspeptin:Neurokinin B: Dynorphin (KNDy) Cells of the Arcuate Nucleus: A Central Node in*. *Endocrinology*, 2010.
29. Shelling, A.N., *Premature ovarian failure*. *Reproduction*, 2010. 140(5): p. 633-41.
30. Diane J. Allingham-Hawkins¹, Riyana Babul-Hirji¹, David Chitayat¹, Jeanette J.A. Holden², et al., *Fragile X Premutation Is a Significant Risk Factor for Premature Ovarian Failure*. 1999.
31. Eastell, R., *Management of osteoporosis due to ovarian failure*. *Med Pediatr Oncol*, 2003. 41(3): p. 222-7.
32. Bretherick, K.L., M.R. Fluker, and W.P. Robinson, *FMRI repeat sizes in the gray zone and high end of the normal range are associated with premature ovarian failure*. *Hum Genet*, 2005. 117(4): p. 376-82.
33. Ying-Hul Fu, D.P.A.K., Antonio Pizzutl, Maura Piereti, James S.Sutcliffe, Stephen Richards, Annemieke J. M. H. Verkerk, Jeanette J. A. Holden, Raymond G. Fenwick, Jr., Stephen T. Warren, Ben A. Oostra, David L. Nelson, and C. Thomas Caskey*, *Variation of the CGG Repeat at the Fragile X Site Results in Genetic Instability*. *Cell*, 1991. 67: p. 1047-1058.
34. Sullivan, A.K., et al., *Association of FMRI repeat size with ovarian dysfunction*. *Hum Reprod*, 2005. 20(2): p. 402-12.
35. Anna Murray, *Premature Ovarian Failure and the FMRI Gene*. *SEMINARS IN REPRODUCTIVE MEDICINE*, 2000. 18.
36. D'Hulst, C., et al., *Decreased expression of the GABAA receptor in fragile X syndrome*. *Brain Res*, 2006. 1121(1): p. 238-45.

37. Curia, G., et al., *Downregulation of tonic GABAergic inhibition in a mouse model of fragile X syndrome*. Cereb Cortex, 2009. 19(7): p. 1515-20.
38. Wu, X., et al., *Estrous cycle regulation of extrasynaptic delta-containing GABA(A) receptor-mediated tonic inhibition and limbic epileptogenesis*. J Pharmacol Exp Ther, 2013. 346(1): p. 146-60.
39. Lieb-Lundell, C.C.E., *Three Faces of Fragile X*. Physical Therapy, 2016. 96(11): p. 1782-1790.
40. Lozano, R., et al., *Fragile X syndrome: A review of clinical management*. Intractable & rare diseases research, 2016. 5(3): p. 145-157.
41. Allingham-Hawkins, D.J., et al., *Fragile X premutation is a significant risk factor for premature ovarian failure: the International Collaborative POF in Fragile X study--preliminary data*. Am J Med Genet, 1999. 83(4): p. 322-5.
42. Wheeler, A.C., et al., *Health and reproductive experiences of women with an FMR1 premutation with and without fragile X premature ovarian insufficiency*. Frontiers in genetics, 2014. 5: p. 300-300.
43. Berkovitz, G.D., et al., *Gonadal function in men with the Martin-Bell (fragile-X) syndrome*. Am J Med Genet, 1986. 23(1-2): p. 227-39.
44. Murray, A., et al., *Reproductive and menstrual history of females with fragile X expansions*. Eur J Hum Genet, 2000. 8(4): p. 247-52.
45. Edbauer, D., et al., *Regulation of synaptic structure and function by FMRP-associated microRNAs miR-125b and miR-132*. Neuron, 2010. 65(3): p. 373-84.
46. Feng, Y., et al., *Translational suppression by trinucleotide repeat expansion at FMR1*. Science, 1995. 268(5211): p. 731-4.
47. Ascano, M., et al., *FMRP targets distinct mRNA sequence elements to regulate protein expression*. Nature, 2012. 492: p. 382.
48. Darnell, J.C., O. Mostovetsky, and R.B. Darnell, *FMRP RNA targets: identification and validation*. Genes Brain Behav, 2005. 4(6): p. 341-9.
49. Darnell, J.C., et al., *FMRP stalls ribosomal translocation on mRNAs linked to synaptic function and autism*. Cell, 2011. 146(2): p. 247-61.
50. Rais, M., et al., *Sensory Processing Phenotypes in Fragile X Syndrome*. ASN Neuro, 2018. 10: p. 1759091418801092.

51. Booker, S.A. and P.C. Kind, *Mechanisms regulating input-output function and plasticity of neurons in the absence of FMRP*. Brain Res Bull, 2021. 175: p. 69-80.
52. Kelley, A.S., et al., *Disparities in accessing infertility care in the United States: results from the National Health and Nutrition Examination Survey, 2013–16*. Fertility and Sterility, 2019. 112(3): p. 562-568.
53. Petraglia, F., G.I. Serour, and C. Chapron, *The changing prevalence of infertility*. International Journal of Gynecology & Obstetrics, 2013. 123: p. S4-S8.
54. Forni, P.E. and S. Wray, *GnRH, anosmia and hypogonadotropic hypogonadism--where are we?* Front Neuroendocrinol, 2015. 36: p. 165-77.
55. Bliss, S.P., et al., *GnRH signaling, the gonadotrope and endocrine control of fertility*. Front Neuroendocrinol, 2010. 31(3): p. 322-40.
56. Coss, D., *Regulation of reproduction via tight control of gonadotropin hormone levels*. Molecular and Cellular Endocrinology, 2018. 463: p. 116-130.
57. Wang, L. and S.M. Moenter, *Differential Roles of Hypothalamic AVPV and Arcuate Kisspeptin Neurons in Estradiol Feedback Regulation of Female Reproduction*. Neuroendocrinology, 2020. 110(3-4): p. 172-184.
58. Herbison, A.E. and S.M. Moenter, *Depolarising and hyperpolarising actions of GABA(A) receptor activation on gonadotrophin-releasing hormone neurones: towards an emerging consensus*. J Neuroendocrinol, 2011. 23(7): p. 557-69.
59. Pielecka-Fortuna, J., Z. Chu, and S.M. Moenter, *Kisspeptin acts directly and indirectly to increase gonadotropin-releasing hormone neuron activity and its effects are modulated by estradiol*. Endocrinology, 2008. 149(4): p. 1979-86.
60. George, J.T. and S.B. Seminara, *Kisspeptin and the hypothalamic control of reproduction: lessons from the human*. Endocrinology, 2012. 153(11): p. 5130-6.
61. Seminara, S.B., *Kisspeptin in reproduction*. Semin. Reprod. Med., 2007. 25(5): p. 337-343.
62. Novaira, H.J., et al., *Genetic mechanisms mediating kisspeptin regulation of GnRH gene expression*. J Neurosci, 2012. 32(48): p. 17391-400.
63. Novaira, H.J., et al., *Disrupted kisspeptin signaling in GnRH neurons leads to hypogonadotropic hypogonadism*. Mol Endocrinol, 2014. 28(2): p. 225-38.

64. Sullivan, S.D. and S.M. Moenter, *Gamma-aminobutyric acid neurons integrate and rapidly transmit permissive and inhibitory metabolic cues to gonadotropin-releasing hormone neurons*. *Endocrinology*, 2004. 145(3): p. 1194-202.
65. Sullivan, S.D. and S.M. Moenter, *Neurosteroids alter gamma-aminobutyric acid postsynaptic currents in gonadotropin-releasing hormone neurons: a possible mechanism for direct steroidal control*. *Endocrinology*, 2003. 144(10): p. 4366-4375.
66. DeFazio, R.A., et al., *Activation of A-type gamma-aminobutyric acid receptors excites gonadotropin-releasing hormone neurons*. *Mol. Endocrinol.*, 2002. 16(12): p. 2872-2891.
67. Slegtenhorst-Eegdeman, K.E., et al., *Macroorchidism in FMR1 knockout mice is caused by increased Sertoli cell proliferation during testicular development*. *Endocrinology*, 1998. 139(1): p. 156-62.
68. Sherman, S.L., et al., *Use of model systems to understand the etiology of fragile X-associated primary ovarian insufficiency (FXPOI)*. *J Neurodev Disord*, 2014. 6(1): p. 26.
69. Lu, C., et al., *Fragile X premutation RNA is sufficient to cause primary ovarian insufficiency in mice*. *Human Molecular Genetics*, 2012. 21(23): p. 5039-5047.
70. Rodriguez-Revenge, L., et al., *Penetrance of FMR1 premutation associated pathologies in fragile X syndrome families*. *European journal of human genetics : EJHG*, 2009. 17(10): p. 1359-1362.
71. Macpherson, J.N. and A. Murray, *Development of Genetic Testing for Fragile X Syndrome and Associated Disorders, and Estimates of the Prevalence of FMR1 Expansion Mutations*. *Genes (Basel)*, 2016. 7(12): p. pii: E110.
72. Chapman, C., L. Cree, and A.N. Shelling, *The genetics of premature ovarian failure: current perspectives*. *International journal of women's health*, 2015. 7: p. 799-810.
73. Shuster, L.T., et al., *Premature menopause or early menopause: long-term health consequences*. *Maturitas*, 2010. 65(2): p. 161-166.
74. Kenneson, A., et al., *Reduced FMRP and increased FMR1 transcription is proportionally associated with CGG repeat number in intermediate-length and premutation carriers*. *Hum Mol Genet*, 2001. 10(14): p. 1449-54.

75. Hoffman, G.E., et al., *Ovarian Abnormalities in a Mouse Model of Fragile X Primary Ovarian Insufficiency*. Journal of Histochemistry & Cytochemistry, 2012. 60(6): p. 439-456.
76. Conca Dioguardi, C., et al., *Granulosa cell and oocyte mitochondrial abnormalities in a mouse model of fragile X primary ovarian insufficiency*. Mol Hum Reprod, 2016. 22(6): p. 384-96.
77. Welt, C.K., P.C. Smith, and A.E. Taylor, *Evidence of early ovarian aging in fragile X premutation carriers*. J Clin Endocrinol Metab, 2004. 89(9): p. 4569-74.
78. Pastore, L.M. and J. Johnson, *The FMR1 gene, infertility, and reproductive decision-making: a review*. Frontiers in Genetics, 2014. 5: p. 195.
79. Gougeon, A., *Regulation of ovarian follicular development in primates: facts and hypotheses*. Endocr. Rev., 1996. 17(2): p. 121-155.
80. Kreisman, M.J., et al., *Estradiol Enables Chronic Corticosterone to Inhibit Pulsatile Luteinizing Hormone Secretion and Suppress Kiss1 Neuronal Activation in Female Mice*. Neuroendocrinology, 2020. 110(6): p. 501-516.
81. Hardiman, R.L. and A. Bratt, *Hypothalamic-pituitary-adrenal axis function in Fragile X Syndrome and its relationship to behaviour: A systematic review*. Physiol Behav, 2016. 167: p. 341-353.
82. Yang, J.A., et al., *Acute Psychosocial Stress Inhibits LH Pulsatility and Kiss1 Neuronal Activation in Female Mice*. Endocrinology, 2017. 158(11): p. 3716-3723.
83. Breen, K.M., et al., *Stress levels of glucocorticoids inhibit LHbeta-subunit gene expression in gonadotrope cells*. Mol Endocrinol, 2012. 26(10): p. 1716-31.
84. Gay, V.L., A.R. Midgley, Jr., and G.D. Niswender, *Patterns of gonadotrophin secretion associated with ovulation*. Fed. Proc., 1970. 29(6): p. 1880-1887.
85. Haisenleder, D.J., et al., *Estimation of estradiol in mouse serum samples: evaluation of commercial estradiol immunoassays*. Endocrinology, 2011. 152(11): p. 4443-7.
86. Wilson, R.C., et al., *Central electrophysiologic correlates of pulsatile luteinizing hormone secretion in the rhesus monkey*. Neuroendocrinology, 1984. 39(3): p. 256-60.
87. Moenter, S.M., et al., *Dynamics of gonadotropin-releasing hormone release during a pulse*. Endocrinology, 1992. 130(1): p. 503-510.

88. Steyn, F.J., et al., *Development of a methodology for and assessment of pulsatile luteinizing hormone secretion in juvenile and adult male mice*. *Endocrinology*, 2013. 154(12): p. 4939-45.
89. McCosh, R.B., M.J. Kreisman, and K.M. Breen, *Frequent Tail-tip Blood Sampling in Mice for the Assessment of Pulsatile Luteinizing Hormone Secretion*. *J Vis Exp*, 2018. 137(137): p. 57894.
90. Babicki, S., et al., *Heatmapper: web-enabled heat mapping for all*. *Nucleic Acids Res*, 2016. 44(W1): p. W147-53.
91. Ge, S.X., D. Jung, and R. Yao, *ShinyGO: a graphical gene-set enrichment tool for animals and plants*. *Bioinformatics*, 2020. 36(8): p. 2628-2629.
92. Evans, M.C., et al., *Evidence that insulin signalling in gonadotrophin-releasing hormone and kisspeptin neurones does not play an essential role in metabolic regulation of fertility in mice*. *J Neuroendocrinol*, 2014. 26(7): p. 468-79.
93. Lovelace, J.W., et al., *Deletion of Fmr1 from Forebrain Excitatory Neurons Triggers Abnormal Cellular, EEG, and Behavioral Phenotypes in the Auditory Cortex of a Mouse Model of Fragile X Syndrome*. *Cereb Cortex*, 2020. 30(3): p. 969-988.
94. Lainez, N.M., et al., *Diet-Induced Obesity Elicits Macrophage Infiltration and Reduction in Spine Density in the Hypothalamus of Male but Not Female Mice*. *Frontiers in Immunology*, 2018. 9(1992): p. 1992.
95. Shi, Y., et al., *Focal adhesion kinase acts downstream of EphB receptors to maintain mature dendritic spines by regulating cofilin activity*. *J Neurosci*, 2009. 29(25): p. 8129-42.
96. Pontrello, C.G., et al., *Cofilin under control of beta-arrestin-2 in NMDA-dependent dendritic spine plasticity, long-term depression (LTD), and learning*. *Proc Natl Acad Sci U S A*, 2012. 109(7): p. E442-51.
97. Sidhu, H., et al., *Genetic removal of matrix metalloproteinase 9 rescues the symptoms of fragile X syndrome in a mouse model*. *J Neurosci*, 2014. 34(30): p. 9867-79.
98. Koeppen, J., et al., *Functional Consequences of Synapse Remodeling Following Astrocyte-Specific Regulation of Ephrin-B1 in the Adult Hippocampus*. *J Neurosci*, 2018. 38(25): p. 5710-5726.
99. Berman, R.F., et al., *Mouse models of the fragile X premutation and fragile X-associated tremor/ataxia syndrome*. *J Neurodev Disord*, 2014. 6(1): p. 25.

100. Mientjes, E.J., et al., *The generation of a conditional Fmr1 knock out mouse model to study Fmrp function in vivo*. *Neurobiol Dis*, 2006. 21(3): p. 549-55.
101. Noto, V., et al., *The impact of FMRI gene mutations on human reproduction and development: a systematic review*. *J Assist Reprod Genet*, 2016. 33(9): p. 1135-47.
102. Terasawa, E., *Neuroestradiol in regulation of GnRH release*. *Horm Behav*, 2018. 104: p. 138-145.
103. Radovick, S., J.E. Levine, and A. Wolfe, *Estrogenic regulation of the GnRH neuron*. *Front Endocrinol (Lausanne)*, 2012. 3: p. 52.
104. Herbison, A.E., *The Gonadotropin-Releasing Hormone Pulse Generator*. *Endocrinology*, 2018. 159(11): p. 3723-3736.
105. Goodman, R.L. and M.N. Lehman, *Kisspeptin neurons from mice to men: similarities and differences*. *Endocrinology*, 2012. 153(11): p. 5105-18.
106. Makanji, Y., et al., *Inhibin at 90: From Discovery to Clinical Application, a Historical Review*. *Endocrine Reviews*, 2014. 35(5): p. 747-794.
107. Bernard, D.J., et al., *Mechanisms of FSH synthesis: what we know, what we don't, and why you should care*. *Fertil. Steril.*, 2010. 93(8): p. 2465-85.
108. Prilutsky, D., et al., *Gene expression analysis in Fmr1KO mice identifies an immunological signature in brain tissue and mGluR5-related signaling in primary neuronal cultures*. *Molecular Autism*, 2015. 6(1): p. 66.
109. Spergel, D.J., *Modulation of Gonadotropin-Releasing Hormone Neuron Activity and Secretion in Mice by Non-peptide Neurotransmitters, Gasotransmitters, and Gliotransmitters*. *Front Endocrinol (Lausanne)*, 2019. 10: p. 329.
110. Antoine, M.W., et al., *Increased Excitation-Inhibition Ratio Stabilizes Synapse and Circuit Excitability in Four Autism Mouse Models*. *Neuron*, 2019. 101(4): p. 648-661.e4.
111. Sullivan, S.D., R.A. DeFazio, and S.M. Moenter, *Metabolic regulation of fertility through presynaptic and postsynaptic signaling to gonadotropin-releasing hormone neurons*. *J Neurosci*, 2003. 23(24): p. 8578-85.
112. Yin, W., et al., *Novel localization of NMDA receptors within neuroendocrine gonadotropin-releasing hormone terminals*. *Exp Biol Med (Maywood)*, 2007. 232(5): p. 662-73.

113. Urbanski, H.F. and S.R. Ojeda, *A role for n-methyl-D-aspartate (NMDA) receptors in the control of LH secretion and initiation of female puberty.* Endocrinology, 1990. 126: p. 1774-1776.
114. Iremonger, K.J., et al., *Glutamate regulation of GnRH neuron excitability.* Brain Res, 2010. 1364: p. 35-43.
115. Christian, C.A. and S.M. Moenter, *The neurobiology of preovulatory and estradiol-induced gonadotropin-releasing hormone surges.* Endocr Rev, 2010. 31(4): p. 544-77.
116. Seeburg, P.H., et al., *The NMDA receptor channel: molecular design of a coincidence detector.* Recent Prog. Horm. Res., 1995. 50: p. 19-34.
117. Lim, W.L., et al., *Maternal Dexamethasone Exposure Alters Synaptic Inputs to Gonadotropin-Releasing Hormone Neurons in the Early Postnatal Rat.* Front Endocrinol (Lausanne), 2016. 7: p. 117.
118. Herde, M.K. and A.E. Herbison, *Morphological Characterization of the Action Potential Initiation Segment in GnRH Neuron Dendrites and Axons of Male Mice.* Endocrinology, 2015. 156(11): p. 4174-86.
119. Chan, H., et al., *Dendritic spine plasticity in gonadotropin-releasing hormone (GnRH) neurons activated at the time of the preovulatory surge.* Endocrinology, 2011. 152(12): p. 4906-14.
120. Cottrell, E.C., et al., *Postnatal remodeling of dendritic structure and spine density in gonadotropin-releasing hormone neurons.* Endocrinology, 2006. 147(8): p. 3652-3661.
121. Li, S., et al., *The increase in the number of spines on the gonadotropin-releasing hormone neuron across pubertal development in rats.* Cell Tissue Res, 2016. 364(2): p. 405-14.
122. Murray, A., *Premature ovarian failure and the FMR1 gene.* Semin Reprod Med, 2000. 18(1): p. 59-66.
123. Robinson, L.J., et al., *FSH-receptor isoforms and FSH-dependent gene transcription in human monocytes and osteoclasts.* Biochem Biophys Res Commun, 2010. 394(1): p. 12-7.
124. Iqbal, J., et al., *Follicle-stimulating hormone stimulates TNF production from immune cells to enhance osteoblast and osteoclast formation.* Proc Natl Acad Sci U S A, 2006. 103(40): p. 14925-30.

125. Sun, L., et al., *FSH directly regulates bone mass*. Cell, 2006. 125(2): p. 247-60.
126. Zaidi, M., et al., *New insights: elevated follicle-stimulating hormone and bone loss during the menopausal transition*. Curr Rheumatol Rep, 2009. 11(3): p. 191-5.
127. Zhu, L.L., et al., *Blocking FSH action attenuates osteoclastogenesis*. Biochem Biophys Res Commun, 2012. 422(1): p. 54-8.
128. Hale, G.E., D.M. Robertson, and H.G. Burger, *The perimenopausal woman: Endocrinology and management*. The Journal of Steroid Biochemistry and Molecular Biology, 2014. 142: p. 121-131.
129. Hoffman, G.E., et al., *Ovarian abnormalities in a mouse model of fragile X primary ovarian insufficiency*. J Histochem Cytochem, 2012. 60(6): p. 439-56.
130. Fraser, H.M. and C. Wulff, *Angiogenesis in the corpus luteum*. Reprod Biol Endocrinol, 2003. 1: p. 88.
131. Thackray, V.G., P.L. Mellon, and D. Coss, *Hormones in synergy: Regulation of the pituitary gonadotropin genes*. Mol. Cell. Endocrinol., 2010. 314(2): p. 192-203.
132. Thackray, V.G., S.M. McGillivray, and P.L. Mellon, *Androgens, progestins and glucocorticoids induce follicle-stimulating hormone β -subunit gene expression at the level of the gonadotrope*. Mol. Endocrinol., 2006. 20(9): p. 2062-2079.
133. Stouffer, R.L., et al., *Endocrine and local control of the primate corpus luteum*. Reprod Biol, 2013. 13(4): p. 259-71.
134. Stouffer, R.L., F. Xu, and D.M. Duffy, *Molecular control of ovulation and luteinization in the primate follicle*. Front Biosci, 2007. 12: p. 297-307.
135. Trau, H.A., J.S. Davis, and D.M. Duffy, *Angiogenesis in the primate ovulatory follicle is stimulated by luteinizing hormone via prostaglandin E2*. Biol Reprod, 2015. 92(1): p. 15.
136. Robker, R.L., J.D. Hennebold, and D.L. Russell, *Coordination of Ovulation and Oocyte Maturation: A Good Egg at the Right Time*. Endocrinology, 2018. 159(9): p. 3209-3218.
137. Stocco, C., C. Telleria, and G. Gibori, *The molecular control of corpus luteum formation, function, and regression*. Endocr Rev, 2007. 28(1): p. 117-49.

138. Fraser, H.M., et al., *Suppression of luteal angiogenesis in the primate after neutralization of vascular endothelial growth factor*. *Endocrinology*, 2000. 141(3): p. 995-1000.
139. Ringstrom, S.J., et al., *The antiprogestins RU486 and ZK98299 affect follicle-stimulating hormone secretion differentially on estrus, but not on proestrus*. *Endocrinology*, 1997. 138(6): p. 2286-90.
140. Knox, K.L. and N.B. Schwartz, *RU486 blocks the secondary surge of follicle-stimulating hormone in the rat without blocking the drop in serum inhibin*. *Biol Reprod*, 1992. 46(2): p. 220-5.
141. Riquelme, R., et al., *Role of ovarian sympathetic nerves and cholinergic local system during cold stress*. *Journal of Endocrinology*, 2019. 242(2): p. 115-124.
142. Lara, H.E., et al., *Changes in sympathetic nerve activity of the mammalian ovary during a normal estrous cycle and in polycystic ovary syndrome: Studies on norepinephrine release*. *Microsc Res Tech*, 2002. 59(6): p. 495-502.
143. Uchida, S., *Sympathetic regulation of estradiol secretion from the ovary*. *Auton Neurosci*, 2015. 187: p. 27-35.
144. Mayerhofer, A., et al., *A role for neurotransmitters in early follicular development: induction of functional follicle-stimulating hormone receptors in newly formed follicles of the rat ovary*. *Endocrinology*, 1997. 138(8): p. 3320-9.
145. Aguado, L.I. and S.R. Ojeda, *Ovarian adrenergic nerves play a role in maintaining preovulatory steroid secretion*. *Endocrinology*, 1984. 114(5): p. 1944-6.
146. Ramírez Hernández, D.A., et al., *Role of the superior ovarian nerve in the regulation of follicular development and steroidogenesis in the morning of diestrus I*. *J Assist Reprod Genet*, 2020. 37(6): p. 1477-1488.

CHAPTER THREE

Obesity Alters POMC and Kisspeptin Neuron Crosstalk Leading to Reduced Luteinizing Hormone in Male Mice

A version of this paper was submitted for publication Pedro et al., Journal of
Neuroscience 2024

3.1 Abstract

Obesity is a significant public health concern due to its high prevalence and numerous comorbidities. Obesity is associated with hypogonadism in males, characterized by low testosterone and sperm number. Previous studies determined that these stem from dysregulation of central regulators of reproduction, but different experimental paradigms prevented clear understanding of mechanisms. Herein, we used mice exposed to chronic high fat diet, that mimics human obesity, to determine mechanisms of obesity-mediated impairment. Consistent with obese humans, we demonstrated lower luteinizing hormone (LH), and lower pulse frequency of LH secretion, but unchanged pituitary responsiveness to GnRH. Peripheral and central kisspeptin injections, and DREADD-mediated activation of kisspeptin neurons, demonstrated that kisspeptin neurons were suppressed in chronically obese mice. This prompted us to investigate regulators of kisspeptin secretion. We determined that LH response to NMDA stimulation was lower in obese mice, which corresponded to reduced levels of glutamate receptor in kisspeptin neurons that may be critical for kisspeptin synchronization. Given that kisspeptin neurons also interact with POMC neurons, which regulate satiety and are particularly affected by obesity, we examined their crosstalk and determined that LH response to either DREADD-mediated activation of POMC neurons or central injection of aMSH, a product of POMC, is abolished in obese mice. This was accompanied by diminished levels of aMSH receptor, MC4R, in kisspeptin neurons. Together, our studies determined that chronic obesity leads to downregulation of

receptors that regulate kisspeptin neurons, which is associated with lower LH pulse frequency leading to lower LH and hypogonadism.

3.2 Rational

Reproduction is an energy demanding process and proper regulation relies on the intricate interplay between the reproductive and feeding circuits in the hypothalamus. Obesity has been increasing in incidence [1], and is one of the most prevailing endocrine disorders affecting fertility in men [2, 3]. Obese men experience hypogonadism, a decrease in testosterone, sperm count, and sperm quality [4, 5]. Our group and others determined that obese males experience decreased luteinizing hormone (LH) and testosterone levels, which points to a central dysregulation [6-9]. However, clear consensus in understanding of underlying mechanisms was confounded by different models: genetic or diet induced obesity (DIO), length of diet exposure, diet composition, or whether leptin resistance was established. Here, we analyzed changes in reproductive circuitry in the hypothalamus, during chronic diet-induced obesity, to mimic human condition.

LH levels, and fertility in general, rely on the tight regulation of pulsatile gonadotropin releasing hormone (GnRH) release from neurons that are scattered in the rostral forebrain and extend long processes to the median eminence [10]. The GnRH decapeptide stimulates the synthesis and secretion of LH and follicle-stimulating hormone (FSH) from the anterior pituitary, that in turn regulate gametogenesis and steroidogenesis [11, 12]. Pulsatile GnRH secretion is regulated by afferent neurons,

primarily kisspeptin neurons located in the arcuate nucleus (ARC) [13-15]. Recent findings revealed that kisspeptin neurons may synchronize their own pulse initiation via glutamate signaling [16, 17]. Dysregulation of kisspeptin function can significantly impact fertility, however, the role of kisspeptin neurons in obesity-mediated reproductive disorders is currently unknown [18-20]. Kisspeptin neurons integrate inputs from the feeding circuitry, comprised of several populations in the hypothalamus. One such population is pro-opiomelanocortin (POMC) that receives information on energy stores via leptin from the adipose tissue. The activity of POMC neurons increases in obesity, in the presence of elevated leptin, which then stimulates satiety and energy expenditure [21]. POMC neurons secrete alpha melanocyte stimulating hormone (α MSH) that acts on the melanocortin 4 receptors (MC4R) in target neurons, including kisspeptin [22-24]. Central injection of α MSH or an MC4R agonist stimulates LH secretion, through kisspeptin neurons [25-27]. In agreement, optogenetic activation of POMC neurons activates ARC kisspeptin neurons [28]. Although our understanding of this interplay between POMC and kisspeptin neurons is beginning to emerge, whether this is altered in chronic conditions such as obesity, is unknown.

Chronic obesity leads to adaptations in the POMC network, which in turn can negatively impact reproductive circuitry. Obesity leads to a reduced number of synaptic contacts to POMC neurons [29]. High fat diet increases POMC mRNA expression and increases POMC neuron excitability [30, 31]. These findings suggest a complex relationship between the regulation of POMC neurons and obesity, wherein changes can impact the ability of POMC neurons to regulate energy homeostasis. Given the

interconnectedness of the reproductive and feeding circuits, dysregulation of POMC neurons may have deleterious effects on reproductive health. This knowledge gap underscores the need for further research to elucidate the underlying mechanisms of obesity-mediated reproductive dysfunction.

In this study, we employed a high fat-diet (HFD) mouse model to investigate the effects of obesity on reproductive function. Our previous publications analyzed mechanisms of impaired reproductive function in obesity and determined lower luteinizing hormone (LH) specifically in males, but not in females [6]. We further determined changes in the pituitary transcriptomes using scRNA-sequencing [32] and changes in neuropeptide and synaptic molecule gene expression in the hypothalamus, using a custom Nanostring probe panel [6, 33]. These were more pronounced in males than females [6, 33]. We also reported neuroinflammatory changes that were specific for males [6, 33-35]. Here, we identified that HFD led to a remarkable increase in LH responsiveness to kisspeptin, accompanied by unchanged pituitary responsiveness, in obese male mice, suggesting dysregulation of kisspeptin neurons. Chemogenetic activation of kisspeptin and POMC neurons, along with investigation of innervation, revealed downregulation of several receptors in kisspeptin neurons that are important for kisspeptin synchronization. This change in connectivity is associated with alteration in the interaction between POMC and kisspeptin neurons in HFD. The disruption in the crosstalk between the feeding and reproductive circuitry may provide a mechanistic link between HFD-induced obesity and reproductive dysfunction in obese men.

3.3 Material and Methods

Animals

All animal procedures were performed with the approval of the University of California, Riverside, Institutional Animal Care and Use Committee under the National Institute of Health Animal Care and Use Guidelines. Three-week-old male C57BL/6J mice were obtained from Jackson Laboratory, acclimated for 1 week in our facility and randomly assigned to the high fat diet group (HFD, catalog number D12492, 60% kcal from fat; 5.21 kcal/g; carbohydrate 20% kcal, protein 20% kcal, fat 60% kcal (lard 0.32 g/g diet, soybean oil 0.03 g/g); Research Diet, New Brunswick, NJ) or the control diet group (CTR, D12450J, 10% kcal from fat; matching sucrose levels to HFD; 3.82 kcal/g; carbohydrate 70% kcal, protein 20% kcal, fat 10% kcal (lard 0.02 g/g diet, soybean oil 0.025 g/g); Research Diet, New Brunswick, NJ) for 12 weeks before experimentation. Mice were maintained on a 12-hour light, 12-hour dark cycle and received food and water ad libitum. All mice were handled daily for two weeks prior to experiments by experienced lab personnel to habituate them to handling and reduce stress.

To visualize GnRH neurons, *Gnrh1*-GFP mice were kindly provided by Suzanne Moenter [36]. To target fluorescence to kisspeptin neurons, *Kiss1*-Cre^{+/-} mice were obtained from Jackson Laboratory (strain 023426) and crossed with *ROSA26*-EGFP mice, also from Jackson Laboratory (strain 004077) [24, 37]. *POMC1*-Cre^{+/-} mice were obtained from Jackson Laboratory (strain 005965) [38]. All were randomly placed on CTR or HFD at four weeks of age for 12 weeks.

LH Secretion

LH pulsatile secretion was measured by tail-tip blood sampling. Two weeks prior to sampling, mice were acclimated to handling by daily tail massage. For the experiment, a small nick was made at the tip of the tail, and 10 μ l of blood was sampled every 8 minutes for 180 minutes [39-41]. An ultrasensitive ELISA [42] was used to detect LH levels, in 10 μ l of blood diluted with 40 μ l of 0.1M PBS, 0.05% tween-20, 0.2% BSA. The capture antibody was obtained from Janet Roser, University of California, Davis (anti-bovine LH beta subunit, 518B7), the detection polyclonal antibody (rabbit LH antiserum, AFP240580Rb) was obtained from the National Hormone and Peptide Program (NHPP), and HRP-conjugated polyclonal antibody (goat anti-rabbit) was purchased from DakoCytomation (Glostrup, Denmark; D048701-2). Mouse LH reference (AFP5306A; NHPP) was used as the assay standard. Assay sensitivity was 0.016 ng/ml, the intra-assay coefficient of variation 2.2%, and the inter-assay coefficient of variation 7.3% at the low end of the curve. LH amplitude was determined by subtracting the basal LH value before the onset of the pulse from the peak level. LH pulse frequency was determined using the freeware DynPeak algorithm [43].

Stereotaxic Injections

Adeno-associated virus AAV9 driving the hM3D(Gq)-mCherry (hM3Dq) under the human synapsin promoter (AAV9-hSyn-DiO-hM3D(Gq)-mCherry, 44361-AAV9, Addgene) was used to express designer receptors activated only by designer drugs (DREADDs) specifically in kisspeptin or POMC neurons. Kiss1-Cre+/-EGFP or

POMC-Cre^{+/-} mice (n=6-8 per group) were fed CTR or HFD for 12 weeks as indicated above. After 12 weeks of diet exposure, mice were anesthetized with isoflurane and placed in a stereotaxic apparatus (Digital stereotaxic instrument, SGL M, Model: 68803, RWD) with head and nose fixed. The arcuate nucleus of the hypothalamus was targeted bilaterally using coordinates from bregma: ML: \pm 0.25 mm; AP: -1.32 mm; DV: -5.85 mm from the dura). 200 nl of hM3Dq (5.4×10^{12} GC/mL;) or control virus (AAV9-hSyn-DIO-mCherry, 50459-AAV9, Addgene) was injected to each side at a rate of 50 nl per minute with a 1 μ l 26-gauge Hamilton syringe. After injection, the syringe was left in situ for another 5 minutes, and then, slowly over a minute, removed. Mice were placed on their respective diets for additional two weeks. To analyze LH secretion in response to kisspeptin and POMC activation, three baseline LH measurements were collected prior to clozapine-n-oxide (CNO; 34233-69-7, MedChemExpress) injection. CNO doses of 0.3mg/kg or 1mg/kg CNO, or saline as control, were injected intraperitoneally (i.p.) and tail-tip blood collected at times indicated in the figures. One week later, treatments with CNO or saline were switched while mice were fed their respective diets.

Intraperitoneal (i.p.) injections

To determine pituitary or GnRH neuron responsiveness of CTR and HFD fed mice, 16-week old animals were injected intraperitoneally (i.p.) with 1 μ g/kg GnRH (L7134-5MG, Sigma-Aldrich), 1 mg/kg kisspeptin (445888-1MG, Millipore Sigma) or saline. Two blood samples were taken 10 minutes apart prior to injection to obtain basal

levels of LH. After injection, 10 μ l of tail-tip blood was sampled every 10 minutes at time points indicated in each figure. Samples were assayed for LH using the ultra-sensitive ELISA as described above.

Intracerebroventricular (icv) injections

14-week-old C57B/J6 male mice fed CTR or HFD for 10 weeks (n=6-7 per treatment group) were secured in a stereotaxic frame (Digital stereotaxic instrument, SGL M, Model: 68803, RWD), placed on 37 C heat pad, and anesthetized with isoflurane. Stereotaxic coordinates to target the lateral ventricle ML: 1mm; AP: -0.5mm; DV: -2.5 mm, according to the Paxinos and George mouse brain atlas, were used for guide cannula implantation (Cannula kit#3 26G 5MM, 126GA5MMKTT, Plastics 1 Technologies, Roanoke, VA). The guide cannula was secured with dental cement and then fitted with a dummy cannula. After a two-week recovery period on respective diets, mice received a single 2 μ l icv injection of one of the following: 3 nmol α MSH (M4135, Sigma Aldrich), 7 nmol NMDA (HY-17551, MedChemExpress), 1 nmol kisspeptin (445888-1MG, Millipore), or sterile saline (concentrations based on previous publications: [27, 44-46]. As above, 10 μ l of blood was taken three times, 10 minutes apart, before injection to measure basal levels, after which an internal cannula attached to a Hamilton syringe was used to inject the above-described compounds. The cannula was left in place for 10 minutes. Blood sampling continued every 10 minutes for times indicated in the figure legends. Mice were allowed to roam freely in their respective cages during the procedure to reduce stress. Blood was assayed for LH, as described above. Accurate cannula

placement to the lateral ventricle was determined by Cresyl violet dye injection and confirmed after dissection.

Immunohistochemistry

GnRH neuron innervation. 4-week-old *Gnrh1*-GFP male mice were fed CTR or HFD for 12 weeks, after which mice were perfused transcardially with 20 ml 0.1M PBS and with 20 ml 4% paraformaldehyde (PFA). Brains were dissected and post-fixed in 4% PFA for 1 hour on ice, then cryoprotected with 30% sucrose in 0.1M PBS for 48 hours. 100 μ m coronal sections containing the organum vasculosum laminae terminalis (OVLT), the medial septum, the rostral preoptic area, and the anterior hypothalamic area were blocked with 10% goat serum and, if necessary with M.O.M kit (mouse on mouse immunodetection kit, BMK-2202, Vector Laboratories, Burlingame, CA); then stained for GFP (1:10,000, chicken anti-GFP, AB13970, Abcam), anti-GABA γ 2 (1:10,000, guinea pig anti-GABA γ 2, 224 004, Synaptic systems), and VGAT (1:5,000, mouse anti-VGAT, 131 011, Synaptic systems) for 72 hours at 4 C. After PBST washes, slides were incubated overnight at 4 C with secondary antibodies: anti-rabbit IgG-Alexa 488 (1:1000, A11034, Invitrogen); anti-mouse IgG-Alexa 594 (1:1000, A11032, Invitrogen); anti-guinea pig-biotin (1:1000, BA-7000, Vector Laboratories, Burlingame, CA) followed by streptavidin-Cy5 (1:1000, 434316, Vector Laboratories, Burlingame, CA). Secondary antibody-only controls were performed to determine antibody specificity. We followed our established protocol for determining puncta density [6, 47, 48]. Puncta in a close contact, where no black pixels were visible in between, were

counted in the individual neurons by an investigator blinded to the group; in section where at least 45 μm of the neuronal projection proximal to soma could be observed using a z-stack, acquired with a Zeiss 880 confocal laser scanning inverted microscope. At least 15-20 neurons from 4-5 mice from each group were counted and averaged. 3D reconstruction was performed using Imaris software (Bitplane, Inc; Concord, MA).

Kisspeptin neuron innervation. To investigate the effects of diet-induced obesity on kisspeptin neuron innervation, Kiss1-Cre^{+/-}-EGFP male mice were placed on either a CTR or HFD for 12 weeks. Brains were collected as described above, and the arcuate nucleus of the hypothalamus was sectioned at 55 μm . After blocking as above, sections were incubated with primary antibodies for GFP (1:10,000, chicken anti-GFP, AB13970, Abcam), rabbit anti-NR2A (1:5000, 07-632, EMD Millipore), mouse anti-GluR2 (1:5000, MAB397, EMD Millipore), guinea pig anti-VGLUT2 (1:5000, 135 404, Synaptic systems), or rabbit anti-MC4R (1:5000, AMR-024, Alomone labs) for 72 hours at 4 C. Primary antibodies made in mouse were blocked additionally with M.O.M kit (mouse on mouse immunodetection kit, BMK-2202 Vector Laboratories, Burlingame, CA). NR2A, GluR2, and MC4R were amplified with a biotinylated antibody (1:5000, anti-rabbit biotinylated, BA-1000, or 1:5000, anti-mouse biotinylated, BA-9200; both from Vector Laboratories, Burlingame, CA), overnight at 4 C followed by streptavidin-Cy5 (1:2000, 434316, Invitrogen) overnight at 4 C. For anti-GFP and anti-VGLUT2 secondary antibodies anti-chicken IgG-Alexa 488 (1:2000, A11039, Invitrogen) and anti-guinea pig IgG-Alexa 594 (1:2000, A11076, Invitrogen) were used, respectively and incubated overnight at 4 C. Sections were then mounted on slides, and cover slipped with

VECTASHIELD Vibrance containing DAPI (H-1800, Vector Laboratories, Burlingame, CA). Puncta colocalized to the soma or within 15 μm of the proximal process in 15-40 neurons were counted from four-five mice in each group. Z-stack images were acquired by Zeiss 880 confocal laser scanning inverted microscope, and 3D reconstruction was performed as described above.

cFOS-positive kisspeptin and POMC neurons. Kiss1-Cre^{+/-}-EGFP and POMC neuronal activity was analyzed by determining cFOS expression. Coronal sections containing the arcuate nucleus were stained with anti-GFP (1:5000, chicken anti-GFP, AB13970, Abcam) to visualize kisspeptin neurons, or anti- β -endorphin (1:5000, rabbit anti- β -endorphin, H-022-33, Phoenix Pharmaceuticals) to visualize POMC neurons, and anti-cFOS (1:10,000, guinea pig anti-cFOS, 226 308, Synaptic systems) for 72 hours at 4°C. Secondary antibodies: anti-chicken IgG-Alexa 488 (1:2000, A11039, Invitrogen); anti-rabbit IgG-Alexa 488 (1:2000, A11034, Invitrogen); biotinylated anti-guinea pig (1:5000, BA-7000 Vector Laboratories, Burlingame, CA) followed by streptavidin-Cy5 (1:2000, 434316, Invitrogen) were incubated overnight at 4 C. 10 to 15 sections, containing over 300 neurons per animal, were quantified using Fiji ImageJ version 1.45f, and data was presented as a percent of co-labeled neurons.

Viral targeting of kisspeptin and POMC. To determine the percent targeting of DREADDs in kisspeptin neurons and POMC neurons, sections from Kiss1-Cre^{+/-}-EGFP or POMC-Cre^{+/-} mice containing the arcuate nucleus of the hypothalamus were stained using primary antibodies for GFP (1:5000, chicken anti-GFP, AB13970, Abcam) to visualize kisspeptin neurons, or β -endorphin (1:5000, rabbit anti- β -endorphin, H-022-33,

Phoenix Pharmaceuticals) to visualize POMC, and mCherry (1:5000, anti-mCherry, M11217, Invitrogen) to visualize neurons with viral expression. Secondary antibodies were anti-chicken IgG-Alexa 488 (1:2000, A11039, Invitrogen), anti-rabbit IgG-Alexa 488 (1:2000, A11034, Invitrogen), and anti-rat IgG-Alexa 594 (1:2000, A11007, Invitrogen). Sections were mounted on charged slides, and then cover slipped with VECTASHIELD vibrance with DAPI (H-1800, Vector Laboratories, Burlingame, CA). Percent targeting was determined by dividing the number of colocalized GFP and mCherry positive kisspeptin neurons by the total number of kisspeptin neurons, and dividing the number of colocalized β -endorphin and mCherry positive POMC neurons by the total number of POMC neurons.

Statistical analyses

Normal distribution was determined by Shapiro-Wilk test. Statistical differences between measurements in CTR and HFD groups ($p < 0.05$) were determined by t-test or ANOVA as appropriate, followed by Tukey's post-hoc test for multiple comparisons, using Prism software (GraphPad, CA).

3.4 Results

Male mice on a high-fat diet experience lower LH pulse frequency

To investigate the mechanisms driving reproductive dysfunction in obese males, we utilized the diet-induced obesity (DIO) model. A week after weaning, mice were randomly placed on CTR or HFD for 12 weeks. We previously reported that HFD mice experience hyperleptinemia, reduced testosterone levels, and lower sperm count [6, 32, 35]. Consistent with our previous reports, mice on HFD gained significantly more weight than mice on CTR (final weights after 12 weeks: CTR 27.5g and HFD 46.88g) and demonstrated a 170% higher weight than CTR (Fig. 1A; each point represents a mouse, and the bar represents the group average \pm SEM). HFD mice had significantly lower LH levels than CTR (Fig 1B; CTR, 0.35 ng/ml compared to HFD, 0.18 ng/ml). To determine if lower LH levels stem from lower pulse frequency of LH secretion, we analyzed LH pulsatility by frequent blood sampling (Fig. 1C, representative pulse profiles). We determined a decrease in LH pulsatile secretion in HFD males. CTR males had 3 pulses in 3 hours, while HFD males had 1.6 pulses during the sampling period (Fig. 1D). On the other hand, LH amplitude was not significantly affected by HFD (Fig. 1E; 0.22 ng/ml in CTR compared to 0.12 ng/ml in HFD). Given that a pulse of LH directly corresponds to a pulse of GnRH [49], these results suggest a dysregulation of GnRH pulsatile activity in obesity.

Since the pituitary secretes LH in response to GnRH, and we observed lower LH in HFD males, we investigated whether HFD exposure modified pituitary responsiveness to GnRH stimulation. Two samples taken before GnRH injection determined lower basal

LH in HFD males, consistent with previous results. GnRH injection resulted in rapid LH secretion with peak levels after 10 minutes in both groups. LH increased from 0.11 ng/ml to 3.7 ng/ml in CTR (n=5), and from 0.063 ng/ml to 2.58 ng/ml in HFD (n=5) (Fig. 1F). Since the basal LH levels differed in CTR and HFD animals, to determine pituitary responsiveness to exogenous GnRH, we normalized LH values to the basal LH level, as in previous publications analyzing gonadotropin induction is response to GnRH [50-54]. Fold change from basal LH was calculated and determined that in CTR, GnRH injection resulted in 33.9-fold increase in LH, while in HFD, GnRH injection resulted in 41-fold induction in LH levels (Fig 1G). Fold change of LH in response to GnRH was not statistically different between CTR and HFD, implying that pituitary responsiveness was unaffected by HFD. Given that pituitary responsiveness to exogenous GnRH is not affected by HFD, the lower LH pulse frequency and lower basal LH in HFD suggests the dysregulation of the GnRH pulse generator, prompting us to investigate kisspeptin.

Peripheral and central response to kisspeptin suggests kisspeptin neurons are suppressed by HFD

Since our data revealed decreased LH pulse frequency and kisspeptin neurons are a key population that regulates GnRH neuron pulsatility, we investigated the response to exogenous kisspeptin in HFD. CTR and HFD male mice were injected intraperitoneally (i.p.) with 1 μ g/g kisspeptin (kiss, Fig. 2A), and LH levels were analyzed as above. Kisspeptin injection in CTR mice caused a rapid LH secretion from 0.24 ng/ml before injection to 2.4 ng/ml after 10 minutes and a peak of 3.50 ng/ml after 40 minutes; while

in HFD, LH levels increased from 0.07 ng/ml to 2.3 ng/ml at 10 minutes and a peak of 2.50 ng/ml at 40 minutes (Fig. 2A, left). Area under the curve (AUC) was greater in CTR compared to HFD (Fig. 2A, right), which is consistent with previous studies [8]. Due to the differences in basal LH levels, we analyzed LH fold change as above and determined that in CTR, LH increased 10-fold at 10 minutes and 14.6-fold after 40 minutes; while in HFD, LH increased 33-fold after 10 minutes and 35.7-fold after 40 minutes (Fig. 2B, left). AUC determined that kisspeptin injection results in a remarkably higher fold induction of LH secretion in HFD compared to CTR (Fig. 2B, right).

Given these unexpected results, we investigated the effects of central injection of kisspeptin to circumvent peripheral influences. A cannula was placed in the lateral ventricle of CTR and HFD males, and 1 nmol kisspeptin was injected. Central injections of kisspeptin elicited a robust LH secretion, similarly to previous studies [55-57]. LH secretion demonstrated no differences in LH levels achieved by central kisspeptin injection at 10 and 40 minutes between CTR and HFD (CTR, from 0.24 ng/ml to 2.77 ng/ml at 10 minutes; HFD from 0.13 ng/ml to 2.75 ng/ml at 10 minutes) (Fig. 2C). However, at 90 minutes, we observed a significantly higher LH levels in CTR of 4.2 ng/ml compared to 3.78 ng/ml in HFD (Fig. 2C). The AUC revealed no significant difference between CTR and HFD (Fig. 2C, right). As above, due to differences in basal LH levels, we calculated fold changes and determined that CTR mice had 11.5-fold increase in LH response at 10 minutes, and 17.5-fold increase at 90 minutes. HFD mice again had a higher fold change of 21.1-fold at 10 minutes and 29.10-fold change at 90 minutes (Fig. 2D, left). The significant increase in LH fold change observed in HFD was

consistent when AUC was calculated (Fig. 2D, right). Together, lack of differences in LH levels after kisspeptin treatment demonstrate that GnRH neurons and the pituitary gonadotropes in HFD respond normally to exogenous kisspeptin, to either central or peripheral kisspeptin injection, implicating reduced kisspeptin signaling as a cause of lower LH in obesity. Fold change calculations result in higher LH induction in HFD males imply that endogenous kisspeptin neurons are suppressed in obesity.

To further investigate this hypothesis, we used chemogenetics to activate endogenous kisspeptin neurons and analyze LH response. Kiss1-Cre-EGFP mice were used to express hM3Dq in kisspeptin neurons, after AAV virus was stereotactically injected in the ARC. Bilateral stereotaxic injection of 5.4×10^{12} GC/ml AAV9-hSyn-DiO-hM3D(Gq)-mCherry (hM3Dq) resulted in infection of 76% of kisspeptin neurons, as determined by colocalization of EGFP reporter with mCherry, after Cre-mediated recombination in kisspeptin neurons (Fig. 3A). To ensure that DREADD activation with CNO did not maximize the response that would prevent us to observe differences in HFD compared to control, we performed a dose response analyses and injected 0.3 mg/kg and 1 mg/kg CNO i.p.. A robust dose-dependent secretion of LH occurred in response to CNO. 0.3 mg/kg CNO resulted in 6.9-fold increase in LH at the peak after 20 minutes (from 0.21 ng/ml at time 0, to 1.44 ng/ml at 20 minutes), while 1 mg/kg CNO resulted in 10.7-fold induction at the peak after 30 minutes (from 0.18 ng/ml to 1.92 ng/ml; Fig. 3B). To control for CNO off-target responses, Kiss-Cre- mice were also bilaterally injected with hM3Dq and treated with 0.3 mg/kg CNO, which did not result in increased LH secretion (Fig. 3C). In addition, Kiss-Cre+ mice, that were bilaterally injected with

hM3Dq, were treated with sterile saline, which confirmed absence of increased LH secretion without CNO (Fig. 3C). These data support specific activation of Kiss1-Cre neurons expressing hM3Dq after CNO injections. Then, mice with Kiss1-Cre⁺ neurons expressing hM3Dq were injected i.p. with 0.3 mg/kg CNO and LH measured. Activation of kisspeptin neurons resulted in an increase of LH from 0.23 ng/ml to 1.40 ng/ml at 20 minutes post CNO in CTR mice, compared to an increase from 0.07 ng/ml to 1.01 ng/ml in HFD males. The difference at peak levels 20 minutes after CNO injection between CTR and HFD was not significant (Fig. 3D). Due to the difference in basal level before CNO induction, fold change was analyzed and determined that CNO injection resulted in 6.1 fold increase in LH in CTR mice, and 14.4-fold increase in LH secretion in HFD mice (Fig. 3E). These results determined that HFD male mice responded more robustly to kisspeptin than CTR male mice, in all treatments: to peripheral and central injection and DREADD-mediated neuron activation. Together, our data suggest that the ability of ARC kisspeptin neurons to regulate GnRH neurons and LH secretion is not affected by HFD, and that in fact, kisspeptin neurons are likely suppressed in obesity.

Glutamatergic regulation of kisspeptin neurons is suppressed in HFD

Several studies demonstrated that glutamatergic stimulation, specifically N-methyl-D-aspartate (NMDA) treatment, increases LH secretion, without increased expression of cFOS in GnRH neurons [44, 58], while recent evidence suggested that kisspeptin neuron synchronization and pulse initiation is dependent on glutamate [16, 17]. Since our result above indicated kisspeptin neurons were impaired in obesity, we

then investigated glutamatergic innervation of kisspeptin neurons and LH secretion in response to NMDA in HFD. To investigate LH response to NMDA in CTR and HFD, we implanted a cannula into the lateral ventricle and centrally injected 7 nmol NMDA. LH levels increased from 0.15 ng/ml before treatment to 2.16 ng/ml 10 minutes after injection in CTR, while in HFD LH levels increased from 0.1 ng/ml to 0.59 ng/ml (Fig. 4A). For consistency, fold change was calculated, and CTR mice exhibited a 14.4-fold increase in LH 10 minutes post injection, while HFD mice had a 5.9-fold increase in LH (Fig. 4B). Our results revealed that LH secretion in response to NMDA was diminished in HFD male mice. It is possible that kisspeptin neuron synchronization and pulse initiation are dysregulated in HFD due to a decrease in glutamatergic innervation at the level of the kisspeptin neuron.

To examine glutamatergic innervation of kisspeptin neurons, CTR and HFD brains were sectioned, and sections were triple stained for GFP to visualize kisspeptin neurons and either AMPA receptors containing the GluR2 subunit and presynaptic vesicular glutamate transporter 2 (VGLUT2); or NMDA receptors containing the NR2A subunit and VGLUT2, to visualize glutamatergic innervation. GluR2 is an obligatory subunit for synaptic AMPA receptors impermeable to Ca^{2+} [59], and NR2A is an obligatory subunit of synaptic NMDA receptors [60]. Representative images show relative levels of AMPA receptors (Fig. 5A, top) or NMDA receptor (Fig. 5C, top) on kisspeptin neurons in CTR and HFD, and 3D reconstruction to facilitate counting of direct contacts only with kisspeptin neurons (Fig. 5A, 5C, bottom). The relative numbers were quantified and revealed no difference in GluR2-containing AMPA receptor

immunoreactivity (Fig. 5B, top); but a significant decrease in VGLUT2 puncta in HFD kisspeptin neurons compared to CTR. VGLUT2 levels were decreased by 55% at the soma and by 68% in 1-15 μ m segment from the soma (Fig. 5B, bottom). Quantification of NMDA receptors revealed a decrease in NR2A levels in HFD animals compared to CTR; CTR had 23.7 NMDA puncta at the soma, while HFD had 16.3 puncta at the soma (Fig. 5D). More importantly, there was a significant decrease in GluR2 and VGLUT2 colocalization in kisspeptin neurons, which decreased by 67% at the soma, and by 83% at the proximal process (Fig. 5E). There was also a significant decrease in NR2A and VGLUT2 colocalizations in kisspeptin neurons, from 7.4 colocalized puncta in CTR to 2.5 puncta in HFD at the soma, and from 1.7 in CTR to 0.4 in HFD in the proximal process (Fig. 5F). This decrease in glutamatergic innervation can lead to diminished kisspeptin neuron pulse initiation and synchronization.

Lack of LH response to α MSH injection and POMC chemogenetic activation in HFD

Since reproduction is a very energy-demanding process, reproductive circuitry and feeding circuitry neurons in the hypothalamus interact to integrate their functions [20, 61]. Specifically, kisspeptin neurons interact with POMC neurons, a population of neurons that sense energy stores through leptin secreted from fat [22, 62, 63]. POMC neurons regulate satiety and energy expenditure by secreting α MSH that binds MC4R receptors [64]. Given that 1) α MSH injection can stimulate LH secretion, which is dependent on kisspeptin [27] 2) kisspeptin neurons express MC4R [24], and 3) POMC neurons respond to obesity [30], POMC neurons are a good candidate to affect kisspeptin

neuron changes observed here. First, to determine if POMC neurons are affected by HFD, CTR and HFD sections were stained for β -endorphin to visualize POMC neurons, and cFOS, a marker of neuronal activity. CTR mice had 25.5% cFOS-positive POMC neurons, while HFD mice had 36% cFOS-positive POMC neurons, suggesting that excess adiposity leads to more active POMC neurons in HFD (Fig. 6A). This increase in active POMC neurons is attributed to higher leptin levels, since leptin signaling leads to activation of POMC neurons [21].

To further determine LH response to POMC regulation in CTR and HFD, we chemogenetically activated POMC neurons using DREADDs. POMC-Cre⁺ were placed on CTR or HFD for 12 weeks and then POMC-Cre⁺ mice were injected bilaterally with 200 nl of hM3Dq and allowed to recover for two weeks for optimal transduction, on their respective diets. Validation of proper targeting was performed after experiments were completed and determined that 73% of POMC neurons expressed mCherry (Fig. 6B). Controls lacked the response to saline injection (Fig. 6C). After CNO injection LH increased from 0.3 ng/ml to 3.96 ng/ml in CTR mice, while LH secretion did not increase in HFD (Fig. 6D). CNO injection of POMC-Cre⁺ - hM3Dq mice resulted in 13.2-fold increase in LH secretion 120 minutes after injection in CTR males; however, there was no response in HFD males.

To investigate if LH response to POMC neuron product was altered in HFD, we centrally injected α MSH and analyzed LH secretion. We determined that after α MSH treatment LH increased from 0.41 ng/ml to 2.83 ng/ml at 10 minutes post injection in CTR mice, while in the HFD mice this response was abolished (Fig. 6E). We postulate

that the difference in the timing of LH secretion following CNO injection versus α MSH injection may be due to the time required to synthesize and process POMC to α MSH. α MSH stimulated a 6.9-fold increase in LH secretion 10 minutes after injection in CTR; however, there was no response in HFD. Lack of LH response in HFD mice to α MSH treatment and chemogenetic POMC neuron activation supports that POMC - kisspeptin interaction is dysregulated in obesity.

To investigate POMC – kisspeptin interaction in CTR and HFD, we analyzed levels of MC4R in kisspeptin neurons by immunohistochemistry. Kiss1-Cre⁺-EGFP mice on CTR and HFD were stained for GFP and MC4R. (Fig 7A, top, confocal images; Fig 7A, bottom, 3D reconstruction). Kisspeptin neurons in HFD males had significantly fewer MC4R. HFD resulted in a 47% decrease in the immunoreactivity of receptors at the soma and 52% decrease in the proximal process (Fig. 7A, right).

We then quantified the percent of cFOS-positive kisspeptin neurons, as an indication of their activity. We determined CTR mice had 11.1% cFOS-positive kisspeptin neurons, compared to 2.9% in HFD (Fig. 7B). Therefore, HFD resulted in 74% decrease in active kisspeptin neurons, consistent with our previous hypothesis that kisspeptin neurons are suppressed in HFD. Together, our results revealed a decrease in kisspeptin neuron activity, impaired LH secretion in response to NMDA, α MSH, and POMC neuron activation in HFD, likely stemming from overactive POMC neurons that dysregulate the communication between the feeding and reproductive circuit.

3.5 Discussion

Mechanisms that underlie negative effects of obesity on reproductive function are not clear, despite clinical findings that obesity causes decreased testosterone, lowered sperm numbers, and impaired sperm quality [4, 5]. Studies in animal models by us and others confirm clinical findings in humans [6, 8, 65-69]. Males are more prone to obesity-mediated pathologies, while females may be protected [70, 71] and our previous studies focused on delineating mechanisms of sex differences in response to obesity [6, 33-35]. Herein, we focus on understanding mechanisms of reproductive impairment in males. Several studies, including ours, determined that primary effects of diet-induced obesity are central, at the level of the hypothalamus, resulting in lower basal LH [6, 20, 72, 73]. Obesity-associated reduction in testosterone is accompanied by lower LH, compared to the age-related lower testosterone, which is correlated with higher LH, due to a lack of negative feedback [7], again indicating central effects in obesity. However, mechanisms whereby obesity affects reproductive circuitry in the hypothalamus are not clear. Herein, we report several novel findings that contribute to our understanding of obesity-mediated hypogonadism: 1) we determined lower LH pulse frequency in obese animals, implying dysregulation of GnRH pulse generator; 2) we determined that kisspeptin neurons are suppressed in obesity and exogenous kisspeptin results in higher LH response in obese animals; and 3) cross-talk of POMC neurons, that comprise the feeding circuitry and are particularly affected by high fat diet, with kisspeptin neurons is altered due to diminished receptor levels. We postulate that changes in receptor levels may stem from chronically higher activity of POMC neurons, because of increased leptin, that leads to

downregulation of MC4R and glutamate receptors on target neurons. New results presented here expand our understanding of obesity-mediated hypothalamic impairment.

Whether pituitary responsiveness is altered in obesity, in addition to the hypothalamus, has also been investigated. Our results here indicate that pituitary responsiveness, more specifically, gonadotrope response to GnRH injection, is unaltered in obese animals. Our recent study analyzed the pituitary changes in obesity, and demonstrated that somatotrope and lactotrope populations exhibit plasticity, however changes in the gonadotrope may result from either hypothalamic effects or direct impact [32]. One study postulated direct effects on the pituitary, since LH pulses showed lower amplitude but unaltered frequency, during overnight sampling [74]. A more recent study by the same group determined that pituitary responsiveness to GnRH is unchanged, that in both obese and lean individuals GnRH injection caused the same fold increase of LH [75], which agrees with our results presented here. Lower basal LH in our experiments here in mice, above-mentioned study in humans [75], and rats [8], may obscure LH induction in response to treatment, a reason we analyzed LH secretion as the fold change from basal, to determine the level of response after normalizing basal levels. This allowed us to uncover that pituitary responsiveness to GnRH is unchanged, while kisspeptin treatment caused higher LH secretion in HFD.

We demonstrated that in obesity kisspeptin neurons are suppressed, and that exogenous kisspeptin, administered via peripheral or central injection, or by chemogenetic kisspeptin neuron activation, results in higher LH fold response in obese animals than in controls. We also showed that kisspeptin neurons are less active since in

obese mice, a lower percentage of kisspeptin neurons express cFOS, a marker of neuronal activation. They may be suppressed because they exhibit fewer glutamate receptors, and glutamate may play a role in kisspeptin pulse generation [16]. Kisspeptin neurons in obesity also have lower levels of MC4R, an aMSH receptor that allows stimulation by POMC neurons that produce aMSH. Bidirectional communication between POMC and kisspeptin neurons has been demonstrated, indicating close integration of feeding and reproductive circuits [22]. Kisspeptin excites POMC neurons, via kisspeptin neuropeptide and glutamate release [23, 63, 76], while POMC neurons project to ARC kisspeptin neurons [24] and POMC product, aMSH stimulates LH secretion via kisspeptin [27]. It is not clear how is this interaction altered during chronic obesity, that we examined here, since long-lasting obesity may lead to receptor downregulation, leptin resistance [77], biphasic changes in aMSH levels [78], and endoplasmic reticulum stress that modulates neuropeptide processing [79], all of which may exert different effects on POMC – kisspeptin crosstalk. Due to its chronic nature, it is also difficult to distinguish cause and effect, or pinpoint timing of each change. Nonetheless, we determined changes in kisspeptin neuron activity and postulate that these changes are caused by alterations in neuropeptide receptors and/or synaptic, neurotransmitter receptor levels.

Several studies determined that aMSH treatment causes LH secretion in humans [80, 81] and rodents, in the cycle stage dependent manner [72, 82]. MC4R receptor agonist also stimulates LH in sheep [25, 83] and rodents [27]. In this study, we also show that aMSH icv treatment causes rapid LH secretion. Although aMSH elicited ~7-fold change in LH levels, response was more variable than response to kisspeptin or NMDA,

and we postulate that variability may stem from the timing of food intake prior to injection. Consistent with a response to aMSH, here we show for the first time that chemogenetic activation of POMC neurons stimulates LH release. LH secretion following POMC neuron activation with CNO occurred after 2 hours, compared to 20 minutes after kisspeptin neuron activation. This may imply indirect effects of POMC neuron activation, likely via kisspeptin neurons. Additionally, this timing may reflect the need to synthesize and process POMC to aMSH. Previous studies using DREADD-mediated approaches to regulate POMC neuron activity, demonstrated cFOS induction in POMC neurons 90 minutes after CNO injection, a timeframe close to LH secretion [88; 89]. The physiological effects on food intake, that reflect the function of POMC neurons, required 3 days of CNO treatment [88]. To our knowledge, the shortest time frame to observe effects of POMC neuron activation via DREADDs was 8 hours [90]. Considering these, the time frame in our studies may not be unexpected. Surprisingly, HFD-mediated obesity completely abolished LH response to aMSH injection and to POMC neuron activation. We postulate this is due to the MC4R receptor downregulation by chronically active POMC neurons. MC4R levels are 50% lower in kisspeptin neurons of HFD mice. As mentioned above, we hypothesize that changes in MC4R levels may stem from increased leptin-mediated chronic activation of POMC neurons [84]. This implies regulation of POMC – kisspeptin interaction by tightly controlled receptor levels.

In addition to changes in neuropeptide receptor levels, we also observed changes in neurotransmitter receptor levels. Synaptic changes in obesity have been an area of intense investigation and may occur due to receptor downregulation after prolonged

stimulation, alterations in neuron activity, or neuroinflammation-mediated synaptic remodeling by activated astrocyte and microglia. We postulated in our previous studies that neuroinflammation leads to synaptic remodeling [6, 12]. A decrease in a number of synapses following HFD was reported previously in the arcuate nucleus, specifically fewer inhibitory synapses on POMC neurons, which was postulated to cause increased POMC expression and higher POMC neuron activity [85]. Reduced levels of synaptic proteins, synapses, and fewer dendritic spines in HFD, were observed in hippocampal neurons [86], and in prefrontal cortex [87], in addition to our studies in the hypothalamus [6]. We also reported decreased synapses in GnRH neurons in our previous study [6] and in kisspeptin neurons in the current. Future studies will determine mechanisms of synaptic changes that alter POMC-kisspeptin crosstalk in obesity.

In summary, studies presented here demonstrate impaired POMC-kisspeptin crosstalk in obesity, resulting from lower neuropeptide receptor levels and fewer innervations, that lead to suppression of kisspeptin neurons and lower pulse frequency of LH, which results in lower basal LH, and ultimately hypogonadisms.

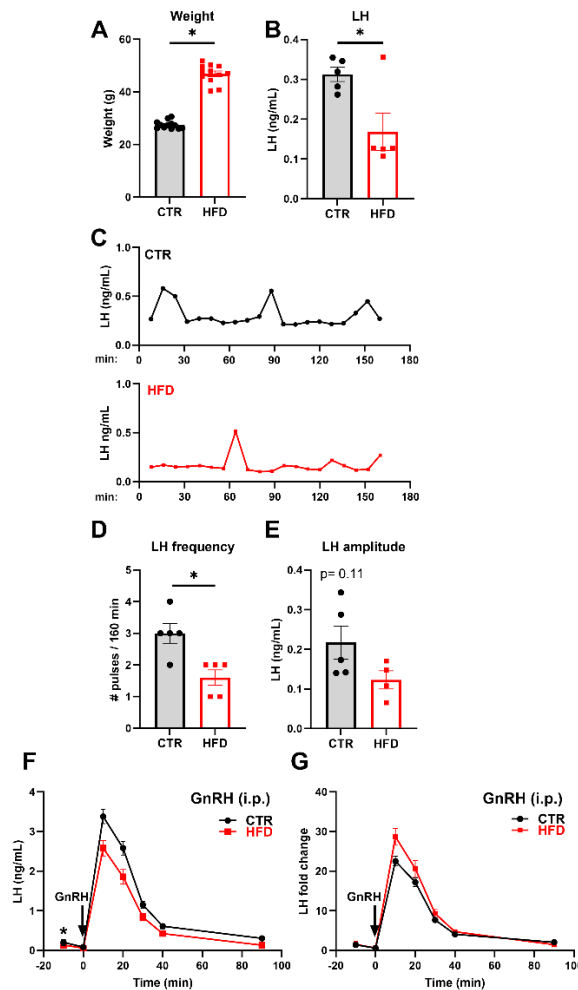


Figure 3.1. Male mice on a high fat diet experience lower LH pulse frequency. A, Weights of male mice after 12-week control (CTR) or high fat diet (HFD) exposure (CTR, gray bars; HFD, red bars; each dot represents one animal, bars represent group mean \pm standard error); B, HFD males have lower LH than CTR; C, Representative LH pulse profile from CTR (top) and HFD (bottom) male mice. D, LH pulse frequency, calculated using DynPeak freeware; E, pulse amplitude was determined by subtracting the basal value from the LH value at the peak and averaged for each mouse. Statistically significant difference between CTR and HFD (indicated with a *, $p < 0.05$), was determined with t-test followed by Tukey's post hoc test. F, Intraperitoneal (i.p.) injection of 1 μ g/kg GnRH in CTR ($n=5$) and HFD ($n=5$) mice was performed and LH levels in the circulation at times indicated in the graphs analyzed by ELISA. The arrow represents timepoint 0, when GnRH was administered; each dot represents the group mean \pm standard error. G, Since basal levels of LH, prior to injection, differ between CTR and HFD, LH fold change was determined by normalizing all points to the basal level.

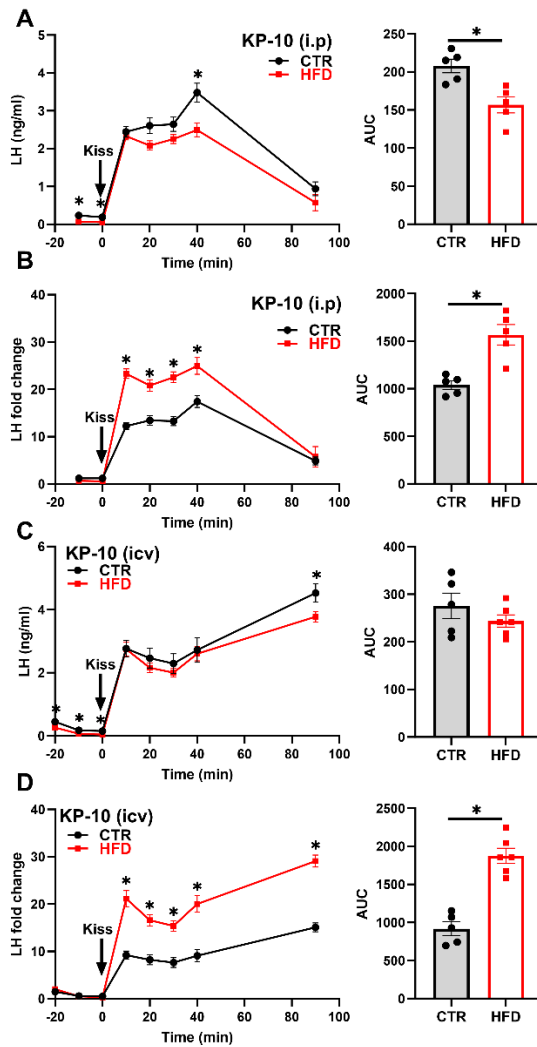


Figure 3.2. Kisspeptin treatment produces higher LH response in HFD mice than CTR. A, C, Left, CTR (n=5) and HFD (n=5 in A, n=6 in C) mice were injected i.p. with 1 mg/kg kisspeptin (A) or intracerebroventricularly (icv, C) with 1 nmol kisspeptin; and LH measured at times indicated in the graph. * indicates statistical difference between CTR and HFD at the same time point. Right, area under the curve (AUC) was calculated and statistically significant difference (*, $p < 0.05$) between CTR and HFD determined by t-test. Each dot represents one animal, bars represent group average. B, D, Left, Due to the difference in basal LH levels, fold change from basal levels was calculated. * indicates statistical difference between CTR and HFD at the same time point. Right, area under the curve (AUC) was calculated and statistically significant difference (*, $p < 0.05$) between CTR and HFD determined by t-test.

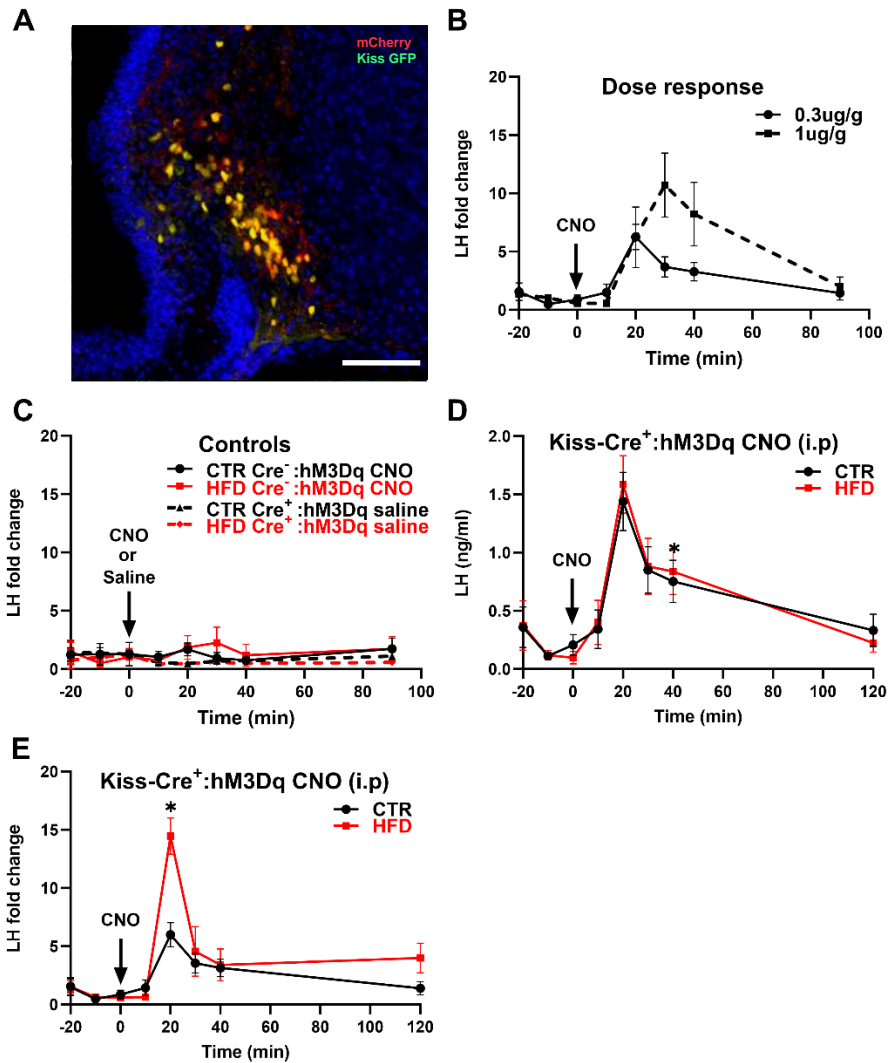


Figure 3.3. Chemogenetic activation of kisspeptin neurons also resulted in higher LH induction in HFD mice. A, Kiss1-Cre⁺-EGFP colocalization with virally transduced hM3Dq-mCherry (red) two weeks after bilateral injection, demonstrates DREADDs targeting to kisspeptin neurons. B, Fold induction of LH secretion after i.p. injection of 0.3 mg/kg (n=6) or 1 mg/kg (n=4) CNO demonstrates dose dependent effects. * indicates statistical difference in response to different CNO concentration at the same time point. C, LH secretion in response to i.p. injection 0.3 mg/kg CNO in Kiss1-Cre⁻ animals injected bilaterally with AAV9 hM3Dq-mCherry (CTR n=4, HFD n=4) and in Kiss-Cre⁺ injected with AAV9 hM3Dq-mCherry (CTR n=7, HFD n=8) injected with saline demonstrate specificity of response. D, LH levels in response to 0.3 mg/kg CNO injection (CTR, n=6; HFD, n=5). * indicates statistically significant difference (p < 0.05) between CTR and HFD at the same time point. E, Fold change of LH from basal levels in response to 0.3 mg/kg CNO injection.

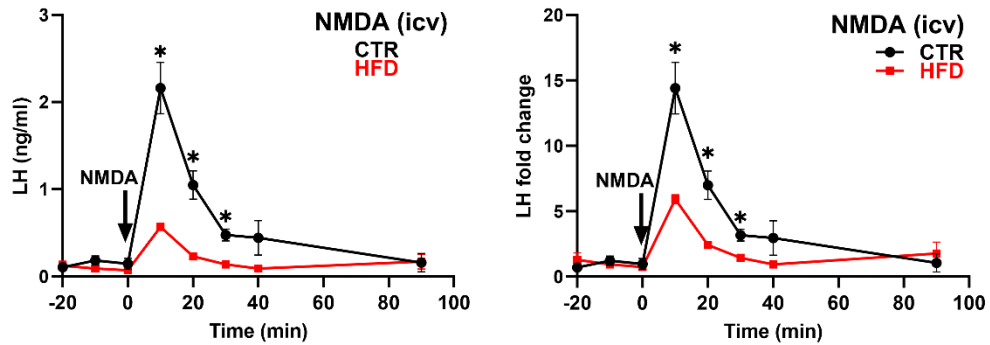


Figure 3.4. LH induction by NMDA is decreased in HFD mice compared to CTR. Left, LH secretion in response to icv injection of 7 nmol NMDA was lower in HFD mice. Right, Fold change from basal of LH response to icv NMDA injection was lower in HFD mice. Each dot represents the group mean \pm standard error (n=4). Statistical significance between CTR compared to HFD at the same time point is indicated with a * ($p < 0.05$).

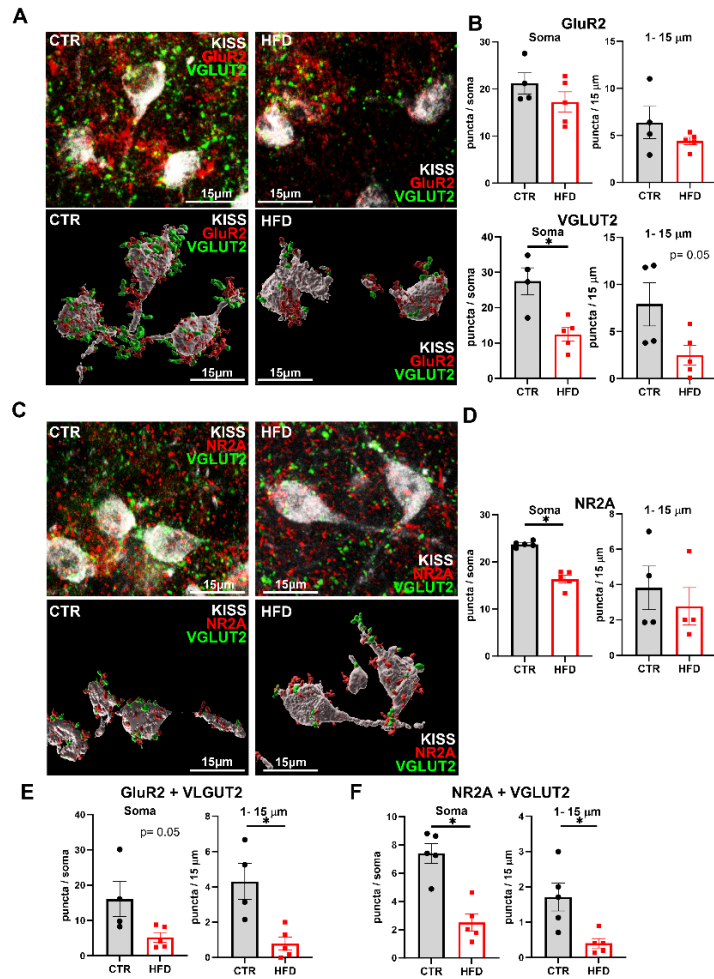


Figure 3.5. Reduced glutamatergic innervation of kisspeptin neurons by HFD. A, AMPA receptors were quantified in kisspeptin neurons in CTR and HFD. Top, representative images of GluR2 (red) and VGLUT2 (green) colocalized to kisspeptin neurons (white, 630x magnification). Bottom, 3D reconstruction using Imaris to assure counting of direct contacts with kisspeptin neurons. B, Quantification of GluR2 (top) and VGLUT2 (bottom) in kisspeptin neuron soma (left) and proximal 15 μm of the process (right). Each dot represents an average for one mouse (15 - 40 neurons counted per animal), and bars represent the group average for CTR (gray) and HFD (red). C, Fewer NMDA receptors on kisspeptin neurons in HFD mice. Top, confocal and bottom, 3D reconstructed representative images of postsynaptic NR2A (red) and presynaptic VGLUT2 (green) on kisspeptin neurons (white). D, Quantification of NR2A numbers in CTR and HFD at the soma and 1-15 μm proximal process. E, Quantification of GluR2 and VGLUT2 colocalization at the kisspeptin neuron soma and proximal 1-15 μm process in CTR (n=5) or HFD (n=5). F, Quantification of NR2A and VGLUT2 colocalization at the kisspeptin neuron soma and proximal 1-15 μm process in CTR (n=5) or HFD (n=5).

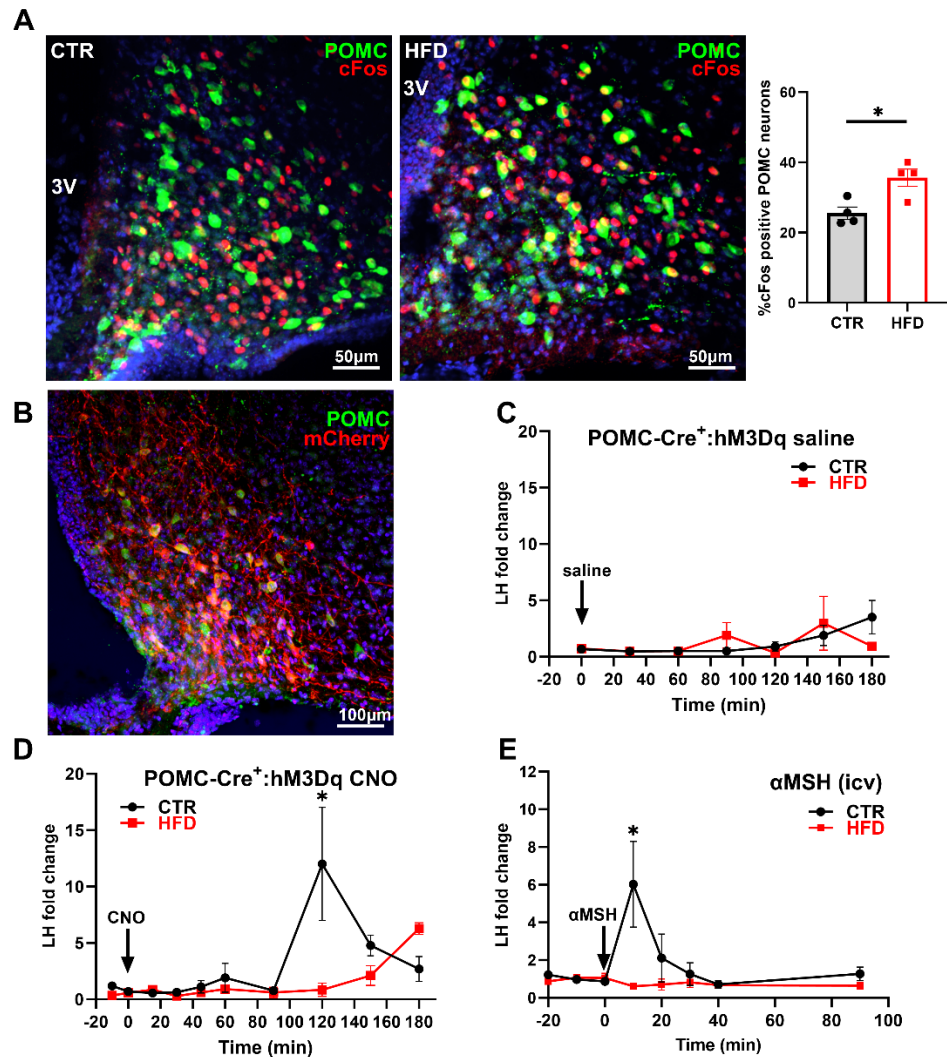


Figure 3.6. HFD diminishes LH response to exogenous POMC activation and α MSH injection. A, Increased numbers of cFOS positive POMC neurons in HFD. Left, images of cFOS (red) colocalization with β -endorphin in POMC (green) neuron in CTR and HFD mice. Right, quantification of c-FOS positive POMC neurons, presented as percent of all POMC neurons. Each dot represents one animal and bars represent group average. * indicates significant difference determined by t-test. B, Representative image of viral DREADD targeting (mCherry) in POMC neurons (green) to demonstrate 74% infection. C, LH levels in CTR (n=5) or HFD (n=7) POMC-Cre⁺ mice expressing hM3Dq DREADDs injected i.p. with saline (n=4). D, LH levels in CTR (n=5) or HFD (n=7) POMC-Cre⁺ positive mice expressing hM3Dq DREADDs injected after 1mg/kg CNO i.p. injection. E, LH levels in response to icv injection of 3 nmol α MSH (CTR, black line n= 5; HFD, red line n=5). Significant difference between CTR and HFD at the same time point is indicated with a * ($p < 0.05$).

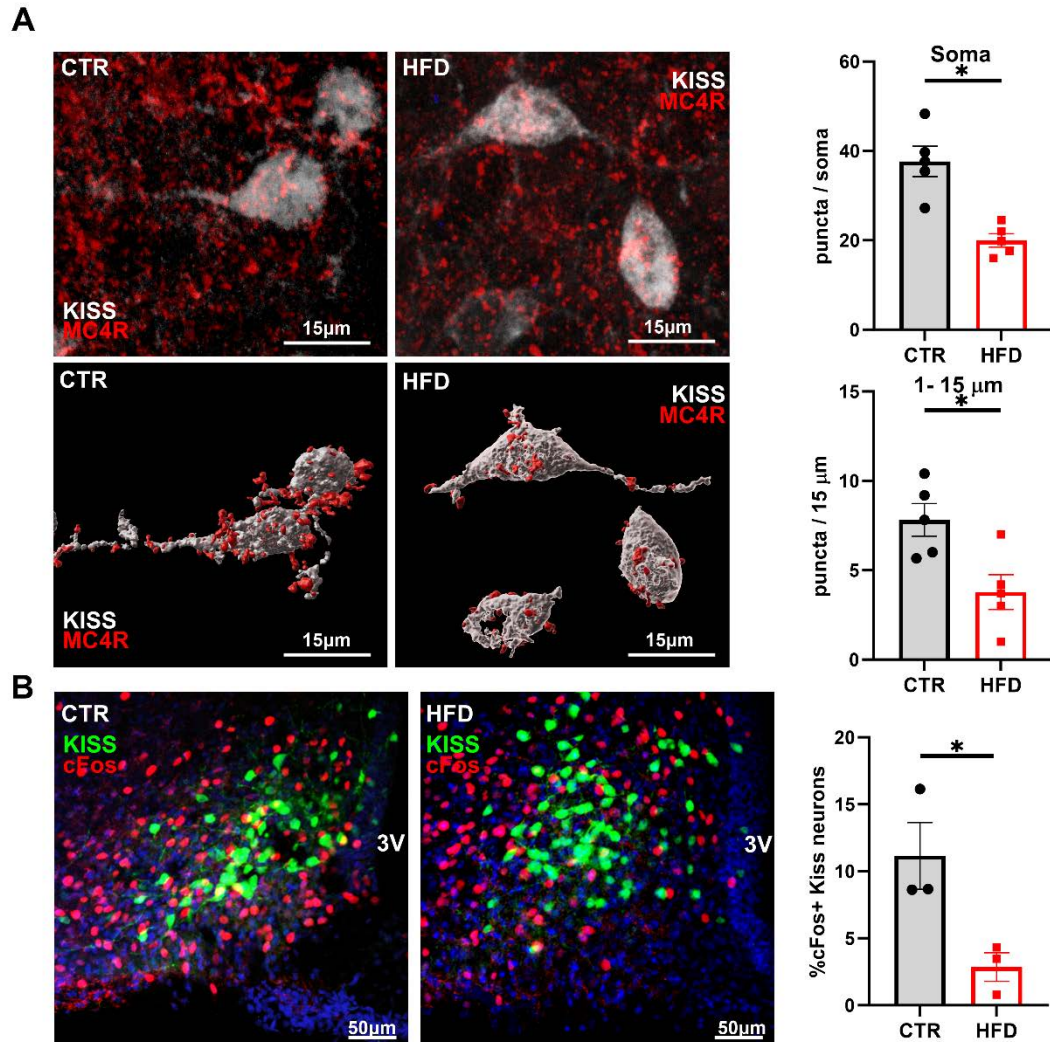


Figure 3.7. Fewer active kisspeptin neurons in HFD mice compared to CTR. A, Kiss-EGFP (n=5) mice were fed CTR or HFD for 12 weeks, after which immunohistochemistry was performed to analyze MC4R and cFOS levels. Top, MC4R receptor (red) colocalized to kisspeptin neurons, identified by GFP (white); Bottom, 3D reconstruction; Right, MC4R puncta in 15-25 neurons per mouse were counted and averaged. B, Left, images of Kiss-GFP and cFOS after CTR and HFD; Right, percent of cFOS positive kisspeptin neurons determined through colocalization of cFOS (red) and kisspeptin neurons (green). Each dot represents one animal, bars represent group average, * indicates statistical difference between CTR and HFD ($p < 0.05$).

References for Chapter Three

1. The Lancet Public, H., *Tackling obesity seriously: the time has come*. Lancet Public Health, 2018. **3**(4): p. e153.
2. Sermondade, N., et al., *BMI in relation to sperm count: an updated systematic review and collaborative meta-analysis*. Hum Reprod Update, 2013. **19**(3): p. 221-31.
3. Santi, D., et al., *Does an increase in adipose tissue 'weight' affect male fertility? A systematic review and meta-analysis based on semen analysis performed using the WHO 2010 criteria*. Andrology, 2023.
4. Du Plessis, S.S., et al., *The effect of obesity on sperm disorders and male infertility*. Nat Rev Urol, 2010. **7**(3): p. 153-61.
5. Hammoud, A.O., et al., *Male obesity and alteration in sperm parameters*. Fertil Steril, 2008. **90**(6): p. 2222-5.
6. Lainez, N.M., et al., *Diet-Induced Obesity Elicits Macrophage Infiltration and Reduction in Spine Density in the Hypothalami of Male but Not Female Mice*. Frontiers in Immunology, 2018. **9**(1992): p. 1992.
7. Wu, F.C., et al., *Hypothalamic-pituitary-testicular axis disruptions in older men are differentially linked to age and modifiable risk factors: the European Male Aging Study*. J Clin Endocrinol Metab, 2008. **93**(7): p. 2737-45.
8. Sanchez-Garrido, M.A., et al., *Obesity-induced hypogonadism in the male: premature reproductive neuroendocrine senescence and contribution of Kiss1-mediated mechanisms*. Endocrinology, 2014. **155**(3): p. 1067-79.
9. Jensen, T.K., et al., *Body mass index in relation to semen quality and reproductive hormones among 1,558 Danish men*. Fertil Steril, 2004. **82**(4): p. 863-70.
10. Goodman, R.L., et al., *Neuroendocrine control of gonadotropin-releasing hormone: Pulsatile and surge modes of secretion*. J Neuroendocrinol, 2022: p. e13094.
11. Coss, D., *Regulation of reproduction via tight control of gonadotropin hormone levels*. Molecular and Cellular Endocrinology, 2018. **463**: p. 116-130.
12. Lainez, N.M. and D. Coss, *Obesity, Neuroinflammation, and Reproductive Function*. Endocrinology, 2019. **160**(11): p. 2719-2736.

13. Novaira, H.J., et al., *Disrupted kisspeptin signaling in GnRH neurons leads to hypogonadotrophic hypogonadism*. Mol Endocrinol, 2014. **28**(2): p. 225-38.
14. Pielecka-Fortuna, J., Z. Chu, and S.M. Moenter, *Kisspeptin acts directly and indirectly to increase gonadotropin-releasing hormone neuron activity and its effects are modulated by estradiol*. Endocrinology, 2008. **149**(4): p. 1979-86.
15. Herbison, A.E., *The Gonadotropin-Releasing Hormone Pulse Generator*. Endocrinology, 2018. **159**(11): p. 3723-3736.
16. Han, S.Y., et al., *Mechanism of kisspeptin neuron synchronization for pulsatile hormone secretion in male mice*. Cell Rep, 2023. **42**(1): p. 111914.
17. Voliotis, M., et al., *Modulation of pulsatile GnRH dynamics across the ovarian cycle via changes in the network excitability and basal activity of the arcuate kisspeptin network*. Elife, 2021. **10**.
18. Ronnekleiv, O.K. and M.J. Kelly, *Kisspeptin excitation of GnRH neurons*. Adv Exp Med Biol, 2013. **784**: p. 113-31.
19. Gottsch, M.L., et al., *Molecular properties of Kiss1 neurons in the arcuate nucleus of the mouse*. Endocrinology, 2011. **152**(11): p. 4298-309.
20. Manfredi-Lozano, M., J. Roa, and M. Tena-Sempere, *Connecting metabolism and gonadal function: Novel central neuropeptide pathways involved in the metabolic control of puberty and fertility*. Front Neuroendocrinol, 2018. **48**: p. 37-49.
21. Cowley, M.A., et al., *Leptin activates anorexigenic POMC neurons through a neural network in the arcuate nucleus*. Nature, 2001. **411**(6836): p. 480-4.
22. Stincic, T.L. and M.J. Kelly, *Estrogenic regulation of reproduction and energy homeostasis by a triumvirate of hypothalamic arcuate neurons*. J Neuroendocrinol, 2022. **34**(6): p. e13145.
23. Fu, L.Y. and A.N. van den Pol, *Kisspeptin directly excites anorexigenic proopiomelanocortin neurons but inhibits orexigenic neuropeptide Y cells by an indirect synaptic mechanism*. J Neurosci, 2010. **30**(30): p. 10205-19.
24. Cravo, R.M., et al., *Characterization of Kiss1 neurons using transgenic mouse models*. Neuroscience, 2011. **173**: p. 37-56.
25. Backholer, K., et al., *Melanocortins mimic the effects of leptin to restore reproductive function in lean hypogonadotropic ewes*. Neuroendocrinology, 2010. **91**(1): p. 27-40.

26. Celis, M.E., *Release of LH in response to alpha-MSH administration*. Acta Physiol Pharmacol Latinoam, 1985. **35**(3): p. 281-90.
27. Manfredi-Lozano, M., et al., *Defining a novel leptin-melanocortin-kisspeptin pathway involved in the metabolic control of puberty*. Mol Metab, 2016. **5**(10): p. 844-857.
28. Stincic, T.L., et al., *Estradiol Drives the Anorexigenic Activity of Proopiomelanocortin Neurons in Female Mice*. eNeuro, 2018. **5**(4).
29. Paeger, L., et al., *Energy imbalance alters Ca(2+) handling and excitability of POMC neurons*. Elife, 2017. **6**.
30. Ziotopoulou, M., et al., *Differential expression of hypothalamic neuropeptides in the early phase of diet-induced obesity in mice*. Am J Physiol Endocrinol Metab, 2000. **279**(4): p. E838-45.
31. Benani, A., et al., *Food intake adaptation to dietary fat involves PSA-dependent rewiring of the arcuate melanocortin system in mice*. J Neurosci, 2012. **32**(35): p. 11970-9.
32. Ruggiero-Ruff, R.E., et al., *Single-Cell Transcriptomics Identifies Pituitary Gland Changes in Diet-Induced Obesity in Male Mice*. Endocrinology, 2023.
33. Chen, K.E., et al., *Visceral adipose tissue imparts peripheral macrophage influx into the hypothalamus*. J Neuroinflammation, 2021. **18**(1): p. 140.
34. Li, J., et al., *Sexual dimorphism in obesity is governed by RELM α regulation of adipose macrophages and eosinophils*. Elife, 2023. **12**.
35. Chen, K.E., N.M. Lainez, and D. Coss, *Sex Differences in Macrophage Responses to Obesity-Mediated Changes Determine Migratory and Inflammatory Traits*. J Immunol, 2021. **206**(1): p. 141-153.
36. Suter, K.J., et al., *Genetic targeting of green fluorescent protein to gonadotropin-releasing hormone neurons: characterization of whole-cell electrophysiological properties and morphology*. Endocrinology, 2000. **141**(1): p. 412-419.
37. Mao, X., et al., *Activation of EGFP expression by Cre-mediated excision in a new ROSA26 reporter mouse strain*. Blood, 2001. **97**(1): p. 324-6.
38. Balthasar, N., et al., *Leptin receptor signaling in POMC neurons is required for normal body weight homeostasis*. Neuron, 2004. **42**(6): p. 983-91.
39. Czieselsky, K., et al., *Pulse and Surge Profiles of Luteinizing Hormone Secretion in the Mouse*. Endocrinology, 2016. **157**(12): p. 4794-4802.

40. McCosh, R.B., M.J. Kreisman, and K.M. Breen, *Frequent Tail-tip Blood Sampling in Mice for the Assessment of Pulsatile Luteinizing Hormone Secretion*. *J Vis Exp*, 2018. **137**(137): p. 57894.
41. Kreisman, M.J., et al., *Estradiol Enables Chronic Corticosterone to Inhibit Pulsatile Luteinizing Hormone Secretion and Suppress Kiss1 Neuronal Activation in Female Mice*. *Neuroendocrinology*, 2020. **110**(6): p. 501-516.
42. Steyn, F.J., et al., *Development of a methodology for and assessment of pulsatile luteinizing hormone secretion in juvenile and adult male mice*. *Endocrinology*, 2013. **154**(12): p. 4939-45.
43. Vidal, A., et al., *DynPeak: an algorithm for pulse detection and frequency analysis in hormonal time series*. *PloS one*, 2012. **7**(7): p. e39001-e39001.
44. d'Anglemont de Tassigny, X., et al., *Kisspeptin signaling is required for peripheral but not central stimulation of gonadotropin-releasing hormone neurons by NMDA*. *J Neurosci*, 2010. **30**(25): p. 8581-90.
45. D'Aniello, A., et al., *Occurrence of D-aspartic acid and N-methyl-D-aspartic acid in rat neuroendocrine tissues and their role in the modulation of luteinizing hormone and growth hormone release*. *Faseb j*, 2000. **14**(5): p. 699-714.
46. Stengel, A., et al., *Centrally injected kisspeptin reduces food intake by increasing meal intervals in mice*. *Neuroreport*, 2011. **22**(5): p. 253-7.
47. Villa, P.A., et al., *Altered GnRH neuron and ovarian innervation characterize reproductive dysfunction linked to the Fragile X messenger ribonucleoprotein (Fmr1) gene mutation*. *Front Endocrinol (Lausanne)*, 2023. **14**: p. 1129534.
48. Ruggiero-Ruff, R.E., et al., *Increased body weight in mice with fragile X messenger ribonucleoprotein 1 (Fmr1) gene mutation is associated with hypothalamic dysfunction*. *Sci Rep*, 2023. **13**(1): p. 12666.
49. Urbanski, H.F., R.L. Pickle, and V.D. Ramirez, *Simultaneous measurement of gonadotropin-releasing hormone, luteinizing hormone, and follicle-stimulating hormone in the orchidectomized rat*. *Endocrinology*, 1988. **123**(1): p. 413-419.
50. Lindaman, L.L., et al., *Phosphorylation of ATF2 and interaction with NFY induces c-Jun in the gonadotrope*. *Mol Cell Endocrinol*, 2013. **365**(2): p. 316-26.
51. Reddy, G.R., et al., *GnRH increases c-Fos half-life contributing to higher FSHbeta induction*. *Mol Endocrinol*, 2013. **27**(2): p. 253-65.

52. Ely, H.A., P.L. Mellon, and D. Coss, *GnRH Induces the c-Fos gene via phosphorylation of SRF by the calcium/calmodulin kinase II pathway*. Mol. Endocrinol., 2011. **25**(4): p. 669-80.
53. Coss, D., et al., *p38 mitogen-activated kinase is critical for synergistic induction of the FSH beta gene by gonadotropin-releasing hormone and activin through augmentation of c-Fos induction and Smad phosphorylation*. Mol. Endocrinol., 2007. **21**(12): p. 3071-3086.
54. Coss, D., et al., *A novel AP-1 site is critical for maximal induction of the follicle-stimulating hormone beta gene by gonadotropin-releasing hormone*. J. Biol. Chem., 2004. **279**: p. 152-162.
55. Gottsch, M.L., et al., *A role for kisspeptins in the regulation of gonadotropin secretion in the mouse*. Endocrinology, 2004. **145**(9): p. 4073-4077.
56. Tonsfeldt, K.J., et al., *The Contribution of the Circadian Gene Bmal1 to Female Fertility and the Generation of the Preovulatory Luteinizing Hormone Surge*. J Endocr Soc, 2019. **3**(4): p. 716-733.
57. Roseweir, A.K., et al., *Discovery of potent kisspeptin antagonists delineate physiological mechanisms of gonadotropin regulation*. J Neurosci, 2009. **29**(12): p. 3920-9.
58. Lee, W.S., et al., *Effects of N-methyl-D-aspartate receptor activation on cFos expression in luteinizing hormone-releasing hormone neurons in female rats*. Endocrinology, 1993. **133**(5): p. 2248-54.
59. Isaac, J.T., M.C. Ashby, and C.J. McBain, *The role of the GluR2 subunit in AMPA receptor function and synaptic plasticity*. Neuron, 2007. **54**(6): p. 859-71.
60. Thomas, C.G., A.J. Miller, and G.L. Westbrook, *Synaptic and extrasynaptic NMDA receptor NR2 subunits in cultured hippocampal neurons*. J Neurophysiol, 2006. **95**(3): p. 1727-34.
61. Rønnekleiv, O.K., J. Qiu, and M.J. Kelly, *Arcuate Kisspeptin Neurons Coordinate Reproductive Activities with Metabolism*. Semin Reprod Med, 2019. **37**(3): p. 131-140.
62. Quarta, C., et al., *POMC neuronal heterogeneity in energy balance and beyond: an integrated view*. Nat Metab, 2021. **3**(3): p. 299-308.
63. Nestor, C.C., et al., *Optogenetic Stimulation of Arcuate Nucleus Kiss1 Neurons Reveals a Steroid-Dependent Glutamatergic Input to POMC and AgRP Neurons in Male Mice*. Mol Endocrinol, 2016. **30**(6): p. 630-44.

64. Andermann, M.L. and B.B. Lowell, *Toward a Wiring Diagram Understanding of Appetite Control*. *Neuron*, 2017. **95**(4): p. 757-778.
65. Bakos, H.W., et al., *The effect of paternal diet-induced obesity on sperm function and fertilization in a mouse model*. *Int J Androl*, 2011. **34**(5 Pt 1): p. 402-10.
66. Vendramini, V., et al., *Reproductive function of the male obese Zucker rats: alteration in sperm production and sperm DNA damage*. *Reprod Sci*, 2014. **21**(2): p. 221-9.
67. DiVall, S.A., et al., *Insulin receptor signaling in the GnRH neuron plays a role in the abnormal GnRH pulsatility of obese female mice*. *PLoS One*, 2015. **10**(3): p. e0119995.
68. Fernandez, M.O., et al., *Obese Neuronal PPARgamma Knockout Mice Are Leptin Sensitive but Show Impaired Glucose Tolerance and Fertility*. *Endocrinology*, 2017. **158**(1): p. 121-133.
69. McGee, W.K., et al., *Effects of hyperandrogenemia and increased adiposity on reproductive and metabolic parameters in young adult female monkeys*. *Am J Physiol Endocrinol Metab*, 2014. **306**(11): p. E1292-304.
70. Gerdts, E. and V. Regitz-Zagrosek, *Sex differences in cardiometabolic disorders*. *Nat Med*, 2019. **25**(11): p. 1657-1666.
71. Parks, B.W., et al., *Genetic architecture of insulin resistance in the mouse*. *Cell Metab*, 2015. **21**(2): p. 334-347.
72. Evans, M.C. and G.M. Anderson, *Neuroendocrine integration of nutritional signals on reproduction*. *J Mol Endocrinol*, 2017. **58**(2): p. R107-r128.
73. Hill, J.W., J.K. Elmquist, and C.F. Elias, *Hypothalamic pathways linking energy balance and reproduction*. *Am J Physiol Endocrinol Metab*, 2008. **294**(5): p. E827-32.
74. Jain, A., et al., *Pulsatile luteinizing hormone amplitude and progesterone metabolite excretion are reduced in obese women*. *J Clin Endocrinol Metab*, 2007. **92**(7): p. 2468-73.
75. Jones, K., et al., *Aromatase Inhibition Ameliorates Decreased LH Output Found in Obese Women*. *Reprod Sci*, 2020. **27**(4): p. 1018-1023.
76. Qiu, J., et al., *Estrogenic-dependent glutamatergic neurotransmission from kisspeptin neurons governs feeding circuits in females*. *Elife*, 2018. **7**.

77. Myers, M.G., Jr., et al., *Obesity and leptin resistance: distinguishing cause from effect*. Trends in endocrinology and metabolism: TEM, 2010. **21**(11): p. 643-651.
78. Wu, Q., et al., *Alpha-Melanocyte-Stimulating Hormone-Mediated Appetite Regulation in the Central Nervous System*. Neuroendocrinology, 2023. **113**(9): p. 885-904.
79. Çakir, I., et al., *Obesity Induces Hypothalamic Endoplasmic Reticulum Stress and Impairs Proopiomelanocortin (POMC) Post-translational Processing**. Journal of Biological Chemistry, 2013. **288**(24): p. 17675-17688.
80. Limone, P., et al., *Evidence for an interaction between alpha-MSH and opioids in the regulation of gonadotropin secretion in man*. J Endocrinol Invest, 1997. **20**(4): p. 207-10.
81. Reid, R.L., N. Ling, and S.S.C. Yen, *Gonadotropin-Releasing Activity of of α -Melanocyte-Stimulating Hormone in Normal Subjects and in Subjects with Hypothalamic-Pituitary Dysfunction**. The Journal of Clinical Endocrinology & Metabolism, 1984. **58**(5): p. 773-777.
82. Alde, S. and M.E. Celis, *Influence of alpha-melanotropin on LH release in the rat*. Neuroendocrinology, 1980. **31**(2): p. 116-20.
83. Backholer, K., J. Smith, and I.J. Clarke, *Melanocortins may stimulate reproduction by activating orexin neurons in the dorsomedial hypothalamus and kisspeptin neurons in the preoptic area of the ewe*. Endocrinology, 2009. **150**(12): p. 5488-97.
84. Pinto, S., et al., *Rapid Rewiring of Arcuate Nucleus Feeding Circuits by Leptin*. Science, 2004. **304**(5667): p. 110-115.
85. Horvath, T.L., et al., *Synaptic input organization of the melanocortin system predicts diet-induced hypothalamic reactive gliosis and obesity*. Proc Natl Acad Sci U S A, 2010. **107**(33): p. 14875-80.
86. Hao, S., et al., *Dietary obesity reversibly induces synaptic stripping by microglia and impairs hippocampal plasticity*. Brain Behav Immun, 2016. **51**: p. 230-9.
87. Bocarsly, M.E., et al., *Obesity diminishes synaptic markers, alters microglial morphology, and impairs cognitive function*. Proc Natl Acad Sci U S A, 2015. **112**(51): p. 15731-6.
88. Jiang, J., et al., *Activation of hypothalamic AgRP and POMC neurons evokes disparate sympathetic and cardiovascular responses*. Am J Physiol Heart Circ Physiol, 2020. 319(5): p. H1069-h1077.

89. Zhan, C., et al., Acute and long-term suppression of feeding behavior by POMC neurons in the brainstem and hypothalamus, respectively. *J Neurosci*, 2013. 33(8): p. 3624-32.
90. Koch, M., et al., Hypothalamic POMC neurons promote cannabinoid-induced feeding. *Nature*, 2015. 519(7541): p. 45-50.

CONCLUSION

My findings provide direct evidence of GnRH network dysregulation due to diet induced obesity and *Fmr1* mutations. *Fmr1* mutations lead to central dysregulation at the level of the GnRH neuron, where a lack of FMRP promotes an increase in excitatory GABAergic innervation. The increase in innervation may promote an increase in GnRH pulsatility, driving high LH levels in females, which affects ovarian function. Young females affected by *Fmr1* mutation with high LH ovulated more oocytes driving the premature exhaustion of ovarian reserve [1].

Obesity due to high fat diet promoted a decrease in GnRH neuron GABAergic innervation and a decrease in kisspeptin neuron glutamatergic innervation. This is significant because kisspeptin pulse initiation is synchronized by glutamate and GABA is excitatory to GnRH neurons. This obesity induced synaptic change suppressed neuron function leading to central reproductive dysregulation. Further probing the potential suppression of kisspeptin neurons, chemogenetic activation of kisspeptin neurons revealed an enhanced LH response in obese mice, indicating suppressed kisspeptin neurons rather than disrupted GnRH regulation. Immunohistochemical assessment of cFos-positive kisspeptin neurons supported this hypothesis, indicating reduced activation in obese males. In addition, we determined that kisspeptin regulation by POMC neurons was significantly diminished due to a decrease in MC4R in kisspeptin neurons. Correspondingly, chemogenetic activation of POMC neurons caused LH secretion in controls but not in HFD males. These findings provide insight into the mechanisms affecting reproductive function due to *FMRI* mutations and diet induced obesity.

In summary, these studies provide insight into the reproductive phenotypes of Fragile X mutation carriers and obesity-mediated hypogonadism in males. Mechanisms identified include dysregulation in GnRH neuron synchronization, elevated GABAergic innervation, and suppressed kisspeptin neurons in response to obesity-induced changes in the crosstalk between feeding and reproductive circuits. Understanding these complexities contributes to addressing infertility challenges and developing targeted interventions for affected individuals.

References for Conclusion

1. Villa, P.A., et al., *Altered GnRH neuron and ovarian innervation characterize reproductive dysfunction linked to the Fragile X messenger ribonucleoprotein (Fmr1) gene mutation*. Front Endocrinol (Lausanne), 2023. **14**: p. 1129534.